



Optimal RWIS Sensor Density and Location – Phase II

<http://aurora-program.org>

Aurora Project 2016-03

**Final Report
February 2020**

About Aurora

Aurora is an international program of collaborative research, development, and deployment in the field of road and weather information systems (RWIS), serving the interests and needs of public agencies. The Aurora vision is to deploy RWIS to integrate state-of-the-art road and weather forecasting technologies with coordinated, multi-agency weather monitoring infrastructures. It is hoped this will facilitate advanced road condition and weather monitoring and forecasting capabilities for efficient highway maintenance and real-time information to travelers.

Iowa State University Nondiscrimination Statement

Iowa State University does not discriminate on the basis of race, color, age, ethnicity, religion, national origin, pregnancy, sexual orientation, gender identity, genetic information, sex, marital status, disability, or status as a US veteran. Inquiries regarding nondiscrimination policies may be directed to the Office of Equal Opportunity, 3410 Beardshear Hall, 515 Morrill Road, Ames, Iowa 50011, telephone: 515-294-7612, hotline: 515-294-1222, email: eooffice@iastate.edu.

Disclaimer Notice

The contents of this report reflect the views of the authors, who are responsible for the facts and the accuracy of the information presented herein. The opinions, findings and conclusions expressed in this publication are those of the authors and not necessarily those of the sponsors.

This document is disseminated under the sponsorship of the U.S. Department of Transportation in the interest of information exchange. The U.S. Government assumes no liability for the use of the information contained in this document. This report does not constitute a standard, specification, or regulation.

The U.S. Government does not endorse products or manufacturers. If trademarks or manufacturers' names appear in this report, it is only because they are considered essential to the objective of the document.

Quality Assurance Statement

The Federal Highway Administration (FHWA) provides high-quality information to serve Government, industry, and the public in a manner that promotes public understanding. Standards and policies are used to ensure and maximize the quality, objectivity, utility, and integrity of its information. The FHWA periodically reviews quality issues and adjusts its programs and processes to ensure continuous quality improvement.

Iowa DOT Statements

Federal and state laws prohibit employment and/or public accommodation discrimination on the basis of age, color, creed, disability, gender identity, national origin, pregnancy, race, religion, sex, sexual orientation or veteran's status. If you believe you have been discriminated against, please contact the Iowa Civil Rights Commission at 800-457-4416 or the Iowa Department of Transportation affirmative action officer. If you need accommodations because of a disability to access the Iowa Department of Transportation's services, contact the agency's affirmative action officer at 800-262-0003.

The preparation of this report was financed in part through funds provided by the Iowa Department of Transportation through its "Second Revised Agreement for the Management of Research Conducted by Iowa State University for the Iowa Department of Transportation" and its amendments.

The opinions, findings, and conclusions expressed in this publication are those of the authors and not necessarily those of the Iowa Department of Transportation or the U.S. Department of Transportation Federal Highway Administration.

Technical Report Documentation Page

1. Report No. Part of TPF-5(290)	2. Government Accession No.	3. Recipient's Catalog No.	
4. Title and Subtitle Optimal RWIS Sensor Density and Location – Phase II		5. Report Date February 2020	
		6. Performing Organization Code	
7. Author(s) Simita Biswas, Tae J. Kwon, Shuoyan Xu, and Liping Fu		8. Performing Organization Report No. Aurora Project 2016-03	
9. Performing Organization Name and Address Department of Civil & Environmental Engineering, University of Alberta 9211-116 Street NW Edmonton, Alberta, Canada T6G 1H9		10. Work Unit No. (TRAIS)	
		11. Contract or Grant No.	
12. Sponsoring Organization Name and Address Aurora Program Federal Highway Administration Iowa Department of Transportation U.S. Department of Transportation 800 Lincoln Way 1200 New Jersey Avenue, SE Ames, Iowa 50010 Washington, DC 20590		13. Type of Report and Period Covered Final Report	
		14. Sponsoring Agency Code SPR-3(042)	
15. Supplementary Notes Visit https://aurora-program.org/ and https://intrans.iastate.edu/ for color pdfs of this and other research reports.			
16. Abstract <p>Preventing weather-related crashes is a significant part of maintaining the safety and mobility of the travelling public during winter months. A road weather information system (RWIS) is a combination of advanced technologies that collect, process, and disseminate road weather and condition information. This information is used by road maintenance authorities to make operative decisions that improve safety and mobility during inclement weather events. Many North American transportation agencies have invested millions of dollars to deploy RWIS stations to improve the monitoring coverage of winter road surface conditions. However, the significant costs of these systems motivate governments to develop a framework to optimize the spatial design of the RWIS network. The design of these networks often varies by region, and it remains an unresolved question what should be the optimal density and location of an RWIS network to provide adequate monitoring coverage of a given region.</p> <p>To fill this gap, this project aimed to develop a methodology for optimizing the density and location of an RWIS network for a given region based on its topographic and weather characteristics. A series of geostatistical spatiotemporal semivariogram models were constructed and compared using topographic position index (TPI) and weather severity index (WSI) to measure relative topographic variation and weather severity, respectively. Specifically, this project considered the nature of spatiotemporally varying RWIS measurements by integrating larger case studies and examining two analysis domains: space and time. The study area captured varying environmental characteristics, including regions with flatland or varied terrain and different severities of winter weather. The optimal RWIS density and location for different topographic and weather severity regions were determined using spatiotemporal semivariogram parameters. Output of this study revealed a strong dependency of optimal RWIS density on topographic and weather characteristics of a region. Moreover, this study suggests that RWIS data collected from a specific region can be used to estimate the number of stations required for regions with similar zonal characteristics. The proposed method will provide decision-makers with a tool they need to develop a long-term RWIS implementation plan.</p>			
17. Key Words density optimization— geostatistics—location allocation—road weather information systems—RWIS—space time kriging		18. Distribution Statement No restrictions.	
19. Security Classification (of this report) Unclassified.	20. Security Classification (of this page) Unclassified.	21. No. of Pages 96	22. Price NA

OPTIMAL RWIS SENSOR DENSITY AND LOCATION – PHASE II

**Final Report
February 2020**

Principal Investigator
Tae J. Kwon, Assistant Professor
University of Alberta

Authors
Simita Biswas, Tae J. Kwon, Shuoyan Xu, and Liping Fu

Sponsored by
Federal Highway Administration Aurora Program
Transportation Pooled Fund
(TPF-5(290))

Preparation of this report was financed in part
through funds provided by the Iowa Department of Transportation
through its Research Management Agreement with the
Institute for Transportation
(Aurora Project 2016-03)

A report from
Aurora Program
Institute for Transportation
Iowa State University
2711 South Loop Drive, Suite 4700
Ames, IA 50010-8664
Phone: 515-294-8103 / Fax: 515-294-0467
<https://aurora-program.org/> and <https://intrans.iastate.edu/>

TABLE OF CONTENTS

ACKNOWLEDGMENTS	ix
LIST OF ABBREVIATIONS AND ACRONYMS	xi
EXECUTIVE SUMMARY	xiii
Topographic Position Index	xiii
Weather Severity Index.....	xiii
Investigation of Spatiotemporal Characteristics of Road Weather and Topographic Factors	xiv
Development of Region-wide RWIS Deployment Strategies	xiv
Evaluation of the Leveraging Effect of Existing RWIS Stations in Neighboring Regions	xiv
RWIS Density Guidelines and Their Statewide Applications	xv
Development of a Web-Based Visualization Tool	xv
1. INTRODUCTION	1
Background	1
Road Weather Information Systems (RWIS)	2
Current Practice of RWIS Network Planning	4
Motivation of the Study	5
Objectives	5
2. PROPOSED METHODOLOGY	7
Characterizations of Topography and Weather	8
Spatial Variogram Modeling.....	10
Spatiotemporal Semivariogram Modeling.....	13
Covariance Models	14
Location Optimization via SSA	15
Density Optimization via PSO.....	18
3. STUDY AREAS AND DATA DETAILS.....	21
Study Areas and RWIS Network	21
Data Description	22
Data Processing.....	23
4. RESULTS AND DISCUSSION	26
TPI and WSI Classes	26
Spatial Semivariogram Modeling Results	27
Spatiotemporal Semivariogram Modeling Results	28
Statewide RWIS Implementation Strategies.....	31
RWIS Density Guidelines and Their Statewide Applications	33
5. CONCLUSION AND RECOMMENDATIONS	40
REFERENCES	43

APPENDIX A. PLOTS OF EXISTING AND OPTIMIZED RWIS LOCATIONS FOR THE ALL-NEW STRATEGY	47
APPENDIX B. LOCATIONS OF THE ALL-NEW OPTIMIZED RWIS NETWORK.....	51
APPENDIX C. PLOTS OF EXISTING AND EXPANDED RWIS LOCATIONS FOR THE EXPANSION STRATEGY	63
APPENDIX D. LOCATION PLAN FOR ADDING NEW STATIONS TO EXISTING RWIS NETWORK.....	67

LIST OF FIGURES

Figure 1. Major components of an RWIS station	3
Figure 2. Overview of the proposed methodology	7
Figure 3. Example of positive and negative TPI values for a typical land surface.....	9
Figure 4. Typical semivariogram with parameters	11
Figure 5. Typical spatiotemporal semivariogram	14
Figure 6. Workflow of spatial simulated annealing.....	17
Figure 7. Distribution of RWIS stations for eight US states.....	21
Figure 8. Study area for location optimization	22
Figure 9. Seasonal road surface temperature details for eight states	25
Figure 10. TPI map of the 14 US states of the study area	26
Figure 11. WSI map of the 14 US states of the study area	27
Figure 12. Comparison of spatial range for TPI classes (left) and WSI classes (right).....	28
Figure 13. Sample spatiotemporal semivariogram of TPI and WSI classes for November 2016 RWIS data	29
Figure 14. Spatial semivariogram ranges for TPI classes (top) and WSI classes (bottom).....	29
Figure 15. Temporal semivariogram ranges for TPI classes (top) and WSI classes (bottom)	30
Figure 16. Spatial and temporal range for flatland area (TPI-1) with different weather severity	31
Figure 17. RWIS optimization for Iowa	32
Figure 18. F-statistic distribution.....	33
Figure 19. Normalized prediction error as a function of RWIS density for TPI classes (top) and WSI classes (bottom).....	34
Figure 20. Number of RWIS stations for benefit increment of 0.1 unit for TPI classes (top) and WSI classes (bottom).....	35
Figure 21. Added number of RWIS stations for marginal benefit increment of 0.1 unit for (a) TPI classes and (b) WSI classes	36
Figure 22. RWIS density comparison for TPI classes (top) and WSI classes (bottom)	37
Figure 23. Optimal RWIS density map.....	38

LIST OF TABLES

Table 1. Descriptive statistics of RST for the calibration states	24
Table 2. RWIS density for TPI-WSI zones for unit area (1/10000 km ²).....	38
Table 3. Suggested RWIS density for the 14 states	39
Table B.1. Optimized new locations for RWIS stations in California.....	51
Table B.2. Optimized new locations for RWIS stations in Colorado	51
Table B.3. Optimized new locations for RWIS stations in Delaware	52
Table B.4. Optimized new locations for RWIS stations in Iowa.....	53
Table B.5. Optimized new locations for RWIS stations in Illinois	54
Table B.6. Optimized new locations for RWIS stations in Kansas	55
Table B.7. Optimized new locations for RWIS stations in Michigan	56
Table B.8. Optimized new locations for RWIS stations in Minnesota.....	57
Table B.9. Optimized new locations for RWIS stations in North Dakota.....	58
Table B.10. Optimized new locations for RWIS stations in Ohio.....	58
Table B.11. Optimized new locations for RWIS stations in Pennsylvania	60
Table B.12. Optimized new locations for RWIS stations in Utah.....	60
Table B.13. Optimized new locations for RWIS stations in Virginia	61
Table B.14. Optimized new locations for RWIS stations in Wisconsin.....	62
Table D.1. Potential additional locations for RWIS stations in California.....	67
Table D.2. Potential additional locations for RWIS stations in Colorado	68
Table D.3. Potential additional locations for RWIS stations in Delaware.....	69
Table D.4. Potential additional locations for RWIS stations in Iowa.....	70
Table D.5. Potential additional locations for RWIS stations in Illinois.....	71
Table D.6. Potential additional locations for RWIS stations in Kansas	72
Table D.7. Potential additional locations for RWIS stations in Michigan.....	73
Table D.8. Potential additional locations for RWIS stations in Minnesota.....	74
Table D.9. Potential additional locations for RWIS stations in North Dakota	75
Table D.10. Potential additional locations for RWIS stations in Ohio	76
Table D.11. Potential additional locations for RWIS stations in Pennsylvania.....	77
Table D.12. Potential additional locations for RWIS stations in Utah	78
Table D.13. Potential additional locations for RWIS stations in Virginia.....	79
Table D.14. Potential additional locations for RWIS stations in Wisconsin.....	80

ACKNOWLEDGMENTS

This research was conducted under the Federal Highway Administration (FHWA) Transportation Pooled Fund Aurora Program using Federal SPR Part II, CFDA 20.205 funds. The authors would like to acknowledge the FHWA, the Aurora Program partners, and the Iowa Department of Transportation (DOT), which is the lead state for the program, for their financial support and technical assistance.

The researchers used Esri's ArcGIS version 10.4.1 software throughout this study, and its 2015 help directory and general questions aided in this study.

LIST OF ABBREVIATIONS AND ACRONYMS

AADT	annual average daily traffic
AVHRR	advanced very high resolution radiometer
BPSO	binary particle swarm optimization
CDF	cumulative distribution function
DEM	digital elevation model
DOT	department of transportation
FAA	Federal Aviation Administration
FHWA	Federal Highway Administration
GAM	generalized additive model
ITS	intelligent transportation systems
MODIS	moderate-resolution imaging spectroradiometer
MST	mean surface temperature
NAM	North American Mesoscale Forecast System
NDVI	normalized difference vegetation index
NIP	nonlinear integer programming
NOMADS	National Operational Model Archive and Distribution System
NST	normal score transformation
NWS	National Weather Service
OK	ordinary kriging
PSO	particle swarm optimization
RK	regression kriging
RST	road surface temperature
RWIS	road weather information system
SGS	Sequential Gaussian simulation
SK	simple kriging
SNODAS	Snow Data Assimilation System
SSA	spatial simulated annealing
TMMS	traffic monitoring management system
TPI	topographic position index
UK	universal kriging
WSI	winter severity index

EXECUTIVE SUMMARY

The prevention of weather-related road crashes continues to be a vital and challenging issue particularly for countries in cold regions. As an important part of modern transportation engineering, intelligent transportation systems (ITS) play an essential role in everyday life by improving transportation safety and mobility. A road weather information system (RWIS), a critical piece of ITS infrastructure, is a combination of advanced technologies that collect, process, and distribute road weather and condition information.

RWIS information is used by road maintenance agencies to make operative decisions during winter season to ensure traffic safety and mobility of the travelling public. For this reason, many North American transportation agencies have invested millions of dollars to deploy additional RWIS stations onto their road network to improve the winter road monitoring coverage. Because of the significant cost associated with RWIS station installation, it is essential to develop an RWIS network planning and deployment guideline. To address such challenging issues and improve the generalization potential, this project investigated the dependency of optimal RWIS densities on readily available zonal characteristic data to help agencies determine a long-term strategic RWIS deployment plan. The topographic characteristics and weather severity of the associated study area were selected as zonal classification standards and used for developing optimal RWIS density guidelines. The main findings and key contributions of this project are summarized in the following sections.

Topographic Position Index

This study's topography-based zonal classification was determined using the topographic position index (TPI), which defines the relative topographical variation of an area of interest and its neighborhood. The TPI value of each point was calculated by comparing the elevation of every point with the average elevation of a user-defined neighborhood region. A higher TPI value indicates a varied topographic region, while a lower TPI value indicates a flatland area. According to the TPI values, the study area was classified into three different landform groups: flatland, hilly, and mountainous.

Weather Severity Index

This study's weather severity-based zonal classification was determined using an integrated winter weather measure, winter severity index (WSI), which provides a numerical estimate of weather severity using annual average snowfall accumulation and duration, annual duration of blowing snow, and annual duration of freezing rain. A WSI map of the United States generated by Iteris, Inc. (formerly known as Meridian Environmental Technology, Inc.) was adopted for this study for weather severity classification. According to the WSI values, the study area was categorized into four WSI-based classes: less, moderate, high, and extremely high severe weather zones. Generally speaking, weather severity increases from the southern to the northern parts of the study area.

Investigation of Spatiotemporal Characteristics of Road Weather and Topographic Factors

Geostatistical spatiotemporal semivariogram modeling was used in this study to incorporate both spatial and temporal variations of several weather variables monitored by an RWIS. A semivariogram measures the similarity between two measurements as a function of separation distance. Larger autocorrelation ranges indicate greater spatiotemporal continuity of RWIS measurements and vice versa. The findings suggest that flatland areas with less-varied weather are shown to have a greater continuity range than hilly or mountainous regions and more severe weather regions; thus, comparatively fewer RWIS stations are needed to provide a certain level of monitoring coverage.

Development of Region-wide RWIS Deployment Strategies

An innovative optimization framework was developed and enhanced to optimize the spatial design of a regional RWIS network by incorporating the ultimate use of RWIS information for spatiotemporal inference as well as traffic distribution. The problem was formulated on a basic premise that data from each individual RWIS in a region should collectively be used to maximize their overall monitoring quality. The spatial simulated annealing (SSA) algorithm was employed to solve the optimization problem in an efficient manner. The optimization was run for two distinct scenarios: (1) all-new optimal locations for the existing RWIS network and (2) an expansion of the current RWIS network. The all-new plan may also be used by agencies that would like to install an entirely new RWIS network from scratch. The first analysis was to evaluate the location quality of the current RWIS network in relation to the optimal solution obtained from the research team's model using the two location criteria (i.e., weather and traffic). Since relocating the entire set of existing stations may not be a feasible option, the second analysis was undertaken to suggest a few hypothetical expansion plans over the current RWIS network.

Evaluation of the Leveraging Effect of Existing RWIS Stations in Neighboring Regions

The effect of neighboring RWIS stations for RWIS network planning was evaluated by comparing the coverage of the existing RWIS network and an equal number of all-new RWIS stations generated by considering available RWIS stations in neighboring states. This is considered essential, particularly for developing a statewide RWIS implementation plan, where the primary goal is to leverage all available assets and existing infrastructure in a way that minimizes expending unnecessary resources to further reduce the cost of implementation. Furthermore, by making use of “extra” information available at neighboring sites (i.e., different jurisdictions), nowcasting and forecasting capabilities of an RWIS network will likely be enhanced when compared to that of using information available from only in-state RWIS stations. The results indicated that the deployment of RWIS should take the RWIS of bordering states into consideration.

RWIS Density Guidelines and Their Statewide Applications

The spatiotemporal semivariogram analysis results were used as inputs for RWIS density optimization in order to develop RWIS siting guidelines. RWIS density per unit area for different topographic and weather severity regions were determined from the density optimization outputs. Lastly, density optimization results were used to generate an RWIS density chart for TPI-WSI zones. The RWIS density chart included upper bound, lower bound, and average number of RWIS stations needed for a defined unit area. Using the density chart, RWIS density was determined for 14 states. The study area is made up of a total of nine different TPI-WSI zones.

Development of a Web-Based Visualization Tool

The developed solutions were integrated into LoRWIS, a prototype web-based RWIS location visualization platform for demonstrating the proposed models and the resulting solutions.

1. INTRODUCTION

Background

Intelligent transportation systems (ITS) are an important part of modern transportation engineering and have a significant impact on society and everyday life. Their main contribution is to the improvement of transportation mobility and safety, particularly in how they relate to the prevention of weather-related road crashes, a vital and challenging issue, especially for countries with cold regions. In the US, over 1.5 million road crashes, 800,000 injuries, and 7,000 fatalities occur annually due to adverse weather (Jin et al. 2014). In Canada, about 3,000 fatalities result from weather-related accidents, and more than 1 in 135 people experience driving-related injuries annually (Andrey et al. 2001).

A road weather information system (RWIS) consists of a set of weather and road condition sensors installed at a station near a road side. This combination of advanced sensors gathers, processes, and disseminates the road weather and condition information that is then used by road maintenance authorities to make operative decisions before and/or during inclement weather events in order to enhance overall road safety and decrease weather-related crashes. It is also used by travelers via RWIS-connected dynamic message signs to help them make more informed decisions when traveling during inclement weather events. However, the cost of investment in these technologies is significant. Indeed, many North American transportation agencies have invested millions of dollars to deploy RWIS stations to improve the monitoring coverage of winter road surface conditions (White et al. 2006, Kwon and Fu 2017). As transportation authorities are constantly challenged by limited budgets for installing additional stations, it is of paramount importance to address the questions of how many stations are necessary (optimal RWIS density) and where to locate them (optimal RWIS location) to maximize the return on their investment.

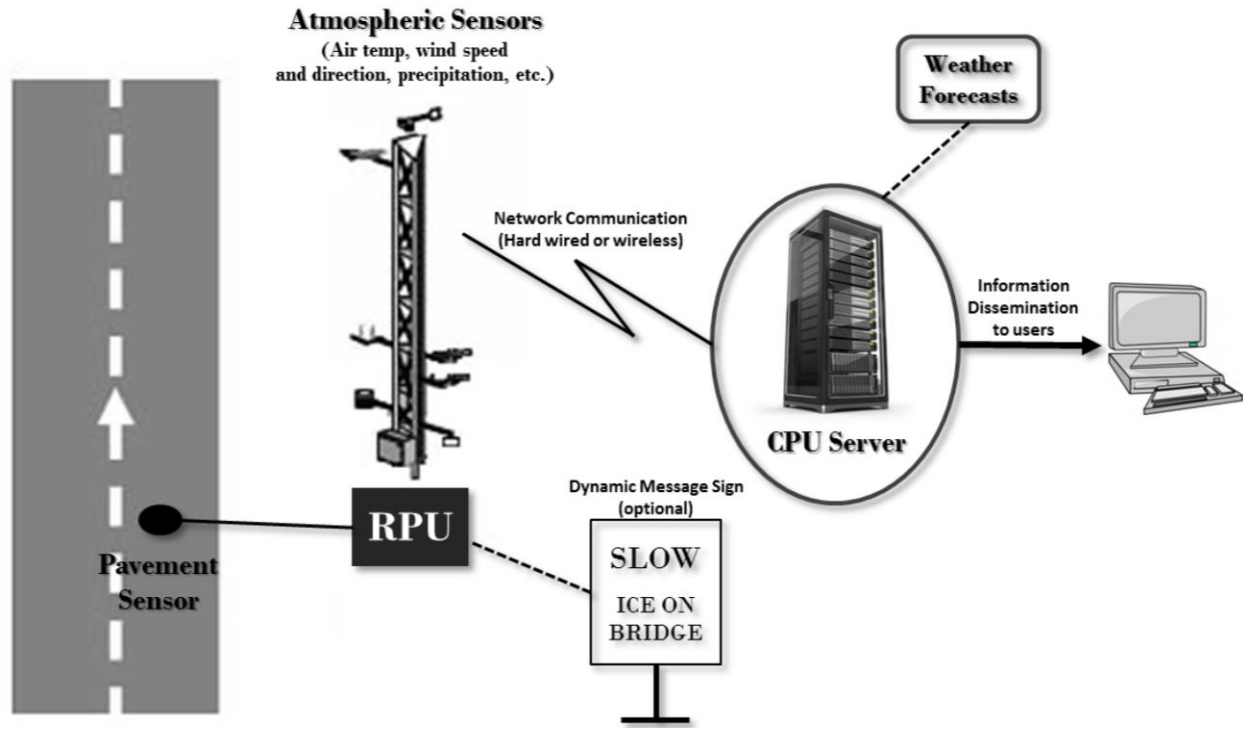
Numerous studies conducted by researchers around the world have sought to quantify the spatial coverage of RWIS data and determine the optimal RWIS density and location based on available RWIS data (Eriksson and Norrman 2001; Manfredi et al. 2008; Kwon and Fu 2013, 2017; Kwon et al. 2017). The Federal Highway Administration (FHWA) initiated extensive efforts to provide RWIS siting guidelines based on the knowledge and experience of field operators (Manfredi et al. 2008). A more recent study by Kwon and Fu (2017) evaluated the dependency of optimal RWIS density on topographic conditions of the regions under investigation by examining three US states (Iowa, Utah, and Minnesota) and one Canadian province (Ontario). Their findings indicated that more RWIS stations would be needed in mountainous areas than in flatland areas. The study also asserted that a region with a longer spatial autocorrelation range would require fewer stations than a region with a shorter range (Kwon and Fu 2017). In this research, the project team has expanded on the former work by investigating the dependency of optimal RWIS density on two different measures, topographic and weather severity, in an effort to improve generalization potentials and design a long-term strategic RWIS deployment plan. Since, road surface conditions vary over space and also over time, there is, therefore, a need to incorporate the temporal domain in the optimization of RWIS location and density.

Spatiotemporal data analysis is a well-known geostatistical analysis technique that is commonly used to analyze the variability of parameters that have a tendency to fluctuate over space and time. It combines spatial and time series analysis concurrently to preserve the interactive effect of time variation on spatial domain and vice versa. Previous research reveals that spatiotemporal analysis is more accurate than spatial analysis as both time and space are included in spatiotemporal analysis (Gräler et al. 2016). The underlying techniques have been previously used to model air pollutants by quantifying the space-time variability of certain particles' concentrations (Gräler et al. 2016, RESSTE Network 2017, Li et al. 2017, Ahmed et al. 2018). Spatiotemporal regression kriging has been used to predict precipitation using Moderate Resolution Imaging Spectroradiometer (MODIS) and normalized difference vegetation index (NDVI) data (Hu et al. 2017). In a study more relevant to the topic of interest, Wang et al. (2019) investigated spatiotemporal variation of road weather and surface conditions using RWIS data from Alberta, Canada. In this study, the authors developed space-time semivariogram models using RWIS measurements from Alberta in order to examine the applicability of the method. The study's findings provided the spatiotemporal feature of the RWIS database (Wang et al. 2019). However, the dependency of the spatiotemporal feature of RWIS measurements on topographic and weather severity has yet to be scrutinized.

There exists a large gap in current literature for determining spatiotemporally optimal density and location of an RWIS network. Equally important, there are no existing guidelines available for winter road maintenance agencies to use and decide its optimality, especially for regions with no RWIS data, which has been deemed a prerequisite for undertaking any RWIS-related analyses including location and density.

Road Weather Information Systems (RWIS)

An RWIS is a significant part of an ITS infrastructure, especially for countries with regions where winter conditions can significantly affect the mobility and safety of their transportation networks. Information regarding the road surface and weather condition is collected, processed, and distributed by RWIS stations that are generally installed alongside roads and highways. An RWIS station consists of atmospheric, pavement, and water-level monitoring sensors. The types of data collected by RWIS stations include air, surface, and sub-surface temperatures; precipitation rate, type and intensity; atmospheric pressure; wind speeds and direction; and road surface condition. Major components of an RWIS stations are presented in Figure 1.



Kwon and Fu 2016, Aurora Program

Figure 1. Major components of an RWIS station

Information disseminated by an RWIS station is collectively used by road operations personnel to make effective and timely winter road maintenance decisions, and to help travelers make more informed decisions related to scheduling their trips. In addition, RWIS information is also used for initializing the road weather and surface conditions forecasts to improve the quality of winter road maintenance services. With forecasted road weather information (e.g., subsurface and surface temperatures), proactive maintenance strategies such as anti-icing operations become possible to further improve the quality of road surface conditions (Sato et al. 2004). The accuracy of forecasts depends on various factors, such as climate characteristics, geographical and topographical settings, etc. (Ahrens 2009). The key benefits of an RWIS are improved traffic safety, mobility, and winter road maintenance (Kwon et al. 2017).

Despite these benefits, there are a few limitations associated with both RWIS and the data collected by the stations. The biggest limitation is installation cost, which could be as high as \$100,000 USD per station depending on the type and number of sensors (Kwon and Fu 2017). In addition, RWIS data provides point-based measures, which are often limited to capturing the spatial heterogeneity of the surrounding road surface conditions. For this reason, it is important to measure the spatial range of continuity of the measured data and associated variance of the data within the continuity range in order to understand the monitoring coverage of the stations for RWIS network planning issues.

Current Practice of RWIS Network Planning

The determination for RWIS station sites entails several critical challenges, requiring full understanding and quantification of spatiotemporal variation of road weather conditions and needs for RWIS data. To address these challenges, several studies were conducted to establish proper guidelines for RWIS station installation (e.g., Kwon et al. 2017, Kwon and Fu 2017). An extensive effort was first initiated by the FHWA to provide a standard for RWIS network planning based on the analysis of published information on siting criteria for weather and pavement sensors and interviews with state departments of transportation (DOT) RWIS managers. The study recommended 30 to 50 km (20 to 30 mi) spacing for RWIS station installation based on the knowledge and experience of field operators (Manfredi et al. 2008). Given that the recommended guidelines are based on expert opinion, several researchers attempted to implement a more objective way to quantify the spatial coverage of RWIS data and identify an optimal set of locations and densities of RWIS stations (Eriksson and Norrman 2001; Manfredi et al. 2008; Kwon and Fu 2013, 2017; Jin et al. 2014; Kwon et al. 2017).

Several studies were conducted to identify the location and number of RWIS stations required for specific regions. A study was conducted in Sweden to determine the hazardous conditions on a roadway by multiple regression analysis of RWIS data. In this research, 10 types of slipperiness were identified to classify road climate, and the RWIS site locations were recommended based on the slipperiness (Eriksson and Norrman 2001). Kwon and Fu (2013) presented a Geographic Information System- (GIS-) based framework to evaluate RWIS locations in Ontario, Canada, by modeling local road weather conditions (i.e., variability of road surface temperature [RST], mean surface temperature [MST], and snow water equivalent) and topographic location attributes (Kwon and Fu 2013). Jin et al. (2014) proposed an RWIS location optimization method that maximized spatial coverage of existing RWIS sensors based on weather-related crash data, which was converted into a safety concern index (Jin et al. 2014). Kwon et al. (2017) also proposed a new methodological framework, which implemented advanced geostatistical analyses for quantifying the underlying spatial structure of RWIS measurements, and then used an efficient combinatorial optimization algorithm, namely, spatial simulated annealing (SSA), for performing an RWIS network location allocation analysis (Kwon et al. 2017). In their study, the optimization problem was formulated as a nonlinear integer programming (NIP) problem to maximize the monitoring capability while minimizing kriging errors (Kwon et al. 2017).

Several other studies were conducted in the past with a specific focus on developing an understanding of factors influencing road weather and surface conditions during inclement weather events. Factors influencing road conditions were listed and categorized in a detailed study by White et al. (2006). According to the literature, meteorological, geographical, road construction, and traffic parameters are the factors contributing to the spatial variation in RST. Amongst all the factors, topography was noted as the major factor influencing RST variation over a region (Gustavsson 1990, Boselly et al. 1993, Manfredi et al. 2005, Chapman and Thornes 2005, White et al. 2006). For this reason, Kwon and Fu (2017) further extended their previous work by examining a hypothesis that the optimal RWIS density or spacing of a region may be dependent on the spatiotemporal variability of road weather conditions as well as their respective topographic settings (Kwon and Fu 2017). To do so, the authors conducted case studies using

three US states (Iowa, Utah, and Minnesota) and one Canadian province (Ontario). Their results indicated that the number of RWIS stations required would depend on the topographical characteristics of the regions under investigation (i.e., more stations are needed in mountainous regions than in flatter areas). Although their findings have been well-received, the study would benefit from incorporating larger case studies and other variables that can be used to establish a concrete RWIS planning guideline for regions with no RWIS stations.

Motivation of the Study

The main motivation of this study was to extend the research team's previous work by including more case studies and by further investigating the dependency of optimal RWIS densities on data that are readily available in regions that need a long-term strategic RWIS deployment plan. The two measures that the research team is particularly interested in are topographic position index (TPI) and winter severity index (WSI). TPI is a commonly used topographic measure that defines the relative topographical variation of an area of interest and its neighborhood, whereas WSI is an aggregate indicator of weather severity using yearly average snowfall accumulation and duration, annual duration of blowing snow, and yearly duration of freezing rain (Weiss 2001, Jenness 2006, Mewes 2012). Since both measures are commonly available and believed to influence the number of RWIS stations required, they could be used to develop new RWIS siting guidelines. Furthermore, previous studies dealt solely with spatial domain, which does not account for the inherent temporal correlation of road weather and surface conditions. As road surface conditions vary over both space and time, it is necessary to include the temporal domain to achieve more accurate results of RWIS density and location optimization.

Objectives

RWISs play an important role by helping transportation maintenance operations to keep roadways clear of ice and snow for improved safety and mobility of the traveling public. To maximize the benefits of such systems, transportation agencies strive to answer two key questions: where should we locate RWIS stations, and how many do we need in a region with varying environments to provide sufficient coverage over space and time? In this study, the researchers attempted to answer both questions by proposing a new method based on a spatiotemporal geostatistical semivariogram analysis of RWIS data in an effort to determine the topographical and weather characteristics of a region, and how they are related to optimal RWIS densities. In particular, the study examined the connection between the spatiotemporal autocorrelation range of RWIS measurements and the topographic and weather characteristics of different zones. The project had the following specific objectives:

- Investigate the topographic and weather characteristics of the study area
- Investigate spatiotemporal autocorrelation of RWIS measurements (i.e., RST) using large scale case studies
- Examine the effect of topography and weather severity of regions on spatial and temporal continuity of RST data
- Develop an RWIS optimal density chart that can facilitate the decision-making process for planning a long-term RWIS deployment strategy

- Evaluate the leveraging effect of existing RWIS stations in neighboring regions

The outcome of this study can be used as a guideline for an RWIS network expansion plan that applies to different topographic and weather severity zones without having to gather any additional data.

2. PROPOSED METHODOLOGY

The topographic and weather characteristics of the study area were analyzed to create several topographically unique regions within the study area with varying levels of winter severity. Spatial semivariogram models were generated for each TPI and WSI class and the change of spatial ranges was evaluated with terrain variability and weather severity classes. Spatiotemporal semivariogram models were then developed to examine spatial and temporal autocorrelation of RWIS data. The effective spatial and temporal range of continuity was determined under different topographic and weather settings, and the dependency of weather data on the topographic variation and weather severity of the region were also evaluated. Then, the optimal density of RWIS stations was determined using the modified particle swarm optimization (PSO) method for different topographic and weather classes to develop a TPI-WSI zone-based optimal RWIS density chart. Lastly, the density optimization results were used for state-wise application and location allocation under different criteria. An overview of the proposed methodology is presented in Figure 2.

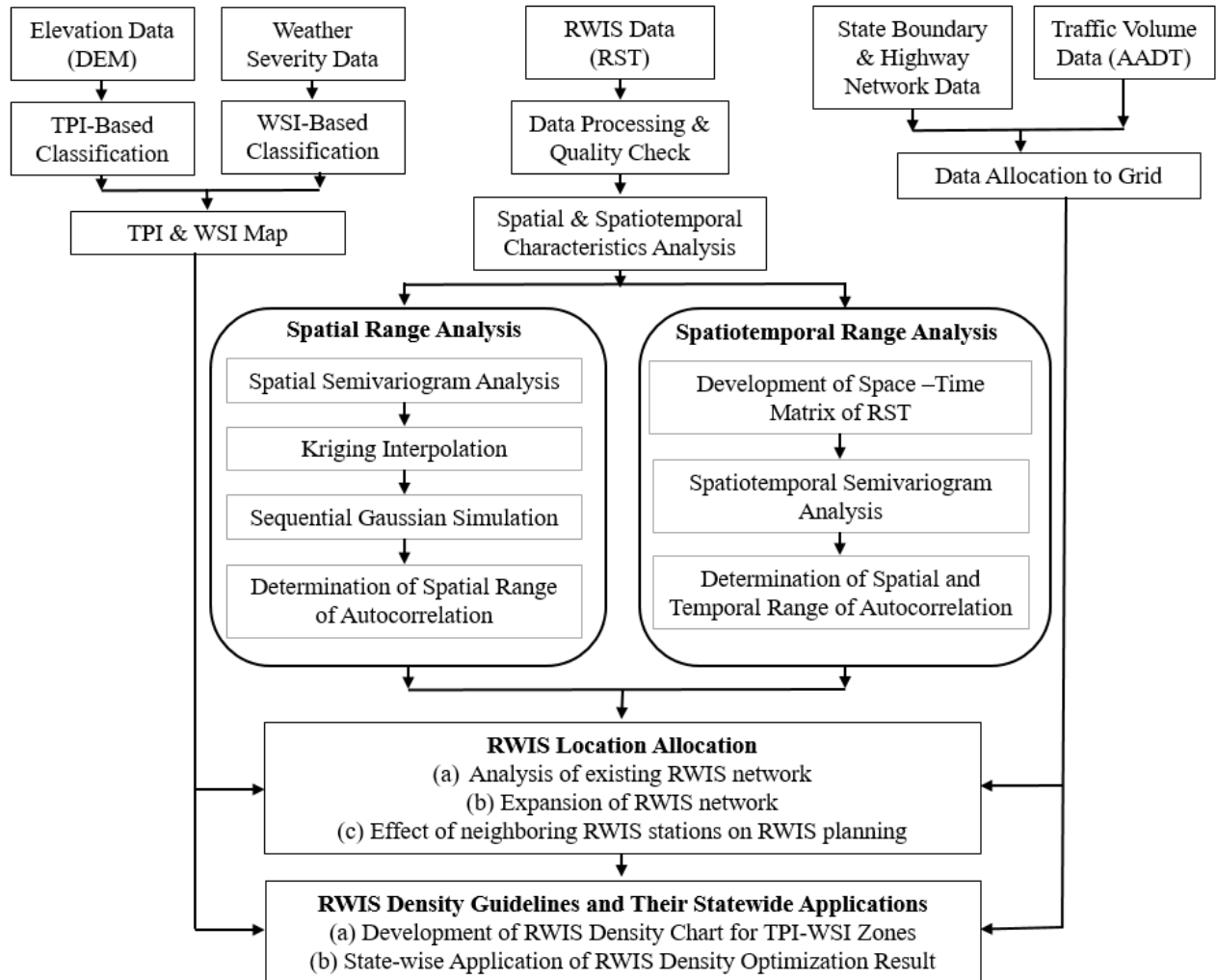


Figure 2. Overview of the proposed methodology

Characterizations of Topography and Weather

To evaluate the relationship among RWIS station density, topographic variability, and weather characteristics for the regions under investigation, the study area was initially classified into topography and weather-based classes. TPI was calculated using the digital elevation model (DEM) data based on Jenness's algorithm (Jenness 2006). According to the TPI values, the study area was classified into three different landform groups (flatland, hilly, and mountainous). The WSI parameter was used for weather-based classifications using the software ArcGIS and the shapefile generated for the United States by Meridian Environmental Technology, Inc. (Mewes 2012). Lower WSI values indicate a less severe weather zone, whereas higher severe weather zones are associated with higher WSI values.

Topography Based Analysis

Topographic analysis was performed using the TPI. TPI values compare the elevation of every point in a DEM to the mean elevation of a specified neighborhood around that cell. Hence, the value of TPI defines the topographic variation of a region. Higher TPI values indicate hilly and mountainous areas whereas lower TPI values represent flatlands (Weiss 2001, Jenness 2006). The TPI calculation algorithm, which was provided by Jenness Enterprises, is the most promising and widely used algorithm for landform classification (Jenness 2006, Seif 2014a, Mokarram et al. 2015). The equation for TPI for a given location, i , is calculated as follows:

$$TPI_i = M_0 - \sum_{n=1} M_n / n \quad (1)$$

where,

M_0 = elevation of the model point, i

M_n = elevation of neighboring points

n = total number of surrounding points employed in the evaluation

A neighborhood is defined as a circle or square around the model point. In this study, TPI values for each point were calculated by considering a circular neighborhood with a diameter of 50 km (31.07 mi) around the point. TPI values are sensitive to the neighborhood size, and this circle diameter was selected based on the application. For example, a smaller diameter is appropriate for analysis of small landforms such as individual ridges or valley lines, whereas a larger neighborhood diameter is appropriate for major topographic landforms (Weiss 2001).

Positive TPI values indicate that a point is higher than the average elevation of the neighborhood while negative TPI values represent locations that are lower than the average elevation. TPI values close to zero indicate regions where the elevation is similar to the average elevation of the surroundings (Seif 2014b). Relatively speaking, lower average TPI values indicate flatland, and higher ranges represent hilly and mountainous regions. An illustrated example of TPI values is presented in Figure 3.

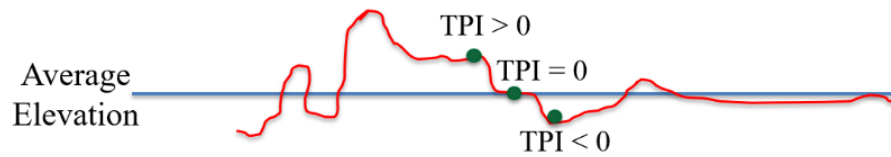


Figure 3. Example of positive and negative TPI values for a typical land surface

An elevation map of the study area was generated in ArcGIS using DEM data. A TPI value was calculated for every 30 m (98.43 ft) grid point (at the resolution of the DEM) using the topography tool that follows Jenness's algorithm. Later, the area was classified into three zones based on the TPI values.

Weather Severity Index

A number of previous studies have introduced methods to calculate WSI, which is generally used as a decision-support tool to benchmark the expected amount of road maintenance resources (e.g., salts) that are required for a given region in a winter season. A common practice of winter severity investigation is to generate a daily-basis WSI number using some weather parameters and to summarize the numerical values for weekly, monthly, and seasonal WSI (Matthews et al. 2017a, 2017b). There are many different methods currently available to measure winter severity; however, most of the methods are for small geographic area-use only and may not be suitable for use for a large area. A large-scale weather severity mapping method was recently developed by Meridian Environmental Technology, Inc. for calculating winter severity over the entire US and was adopted for use in this study. Parameters used for WSI calculation are yearly average accumulation and duration of snowfall and average annual duration of freezing rain and blowing snow. Parameters representing weather severity were selected through an iterative process based on previous experiences of Meridian and the solicitor's interest. Data acquisition details for WSI measurement are as follows:

- Snowfall accumulation data from National Weather Service's (NWS's) United States Climate Normals for the time period of 1971 to 2000 and snow precipitation data from Snow Data Assimilation System (SNODAS) for the winter seasons of 2004 to 2011
- Snowfall duration data from the Meteorological Terminal Aviation Routine Weather Report (METAR) observation of weather stations from the Federal Aviation Administration (FAA) and NWS for the winter seasons of 2000 to 2010 and analysis of precipitation type from the North American Mesoscale Forecast System (NAM) through the National Operational Model Archive and Distribution System (NOMADS) for the winter season of 2004 to 2011
- Average annual duration of freezing rain data from METAR observation from 2000 to 2010 winter seasons and analysis of precipitation type from NAM model from 2004 to 2011 winter seasons
- Hours of blowing or drifting snow was estimated from wind speed data using the NAM model through NOMADS and 1 km advanced very high resolution radiometer (AVHRR) based land cover data from the University of Maryland for the winter seasons of 2004 to 2011

The formula used for WSI calculation provides equal weights for all listed factors. As the unit of snowfall accumulation was in inches and annual duration of snowfall, blowing snow, and freezing rain was calculated in hours, the typical inches to hours weighting ratio of 10:1 was applied. For extra caution and to be proactive, a double weighting factor was provided for the duration of freezing rain. There is no specific explanation for the index values other than it being a relative comparison of winter severity from a winter maintenance viewpoint (Mewes 2012). The resulting WSI formula is shown as follows:

Winter Severity = $0.50 \times (\text{annual average snowfall in inches}) + 0.05 \times (\text{annual snowfall duration in hours}) + 0.05 \times (\text{annual duration of blowing snow in hours}) + 0.10 \times (\text{annual duration of freezing rain in hours})$

Spatial Variogram Modeling

In this study, geostatistical approaches were used for spatial continuity analysis. A semivariogram is a plot of mean semivariance on the y-axis versus separation distance between point pairs on the x-axis (i.e., lag size). Semivariance is a statistic that measures the level of similarity or dissimilarity between two measurements as a function of separation distance (Olea 1999). Semivariance can be calculated by taking the average of the squared differences between measurements in a spatial domain separated by a specific and defined lag distance, as defined in equation 2.

$$\gamma(h) = \frac{1}{2n(h)} \sum_{i=1}^{n(h)} [z - z(x_i)]^2 \quad (2)$$

where, $\gamma(h)$ is the semivariance; $z(x_i + h)$ and $z(x_i)$ are two measurements taken at location x_i and $(x_i + h)$, which are separated by a lag with distance, h . Figure 4 shows a typical semivariogram plot.

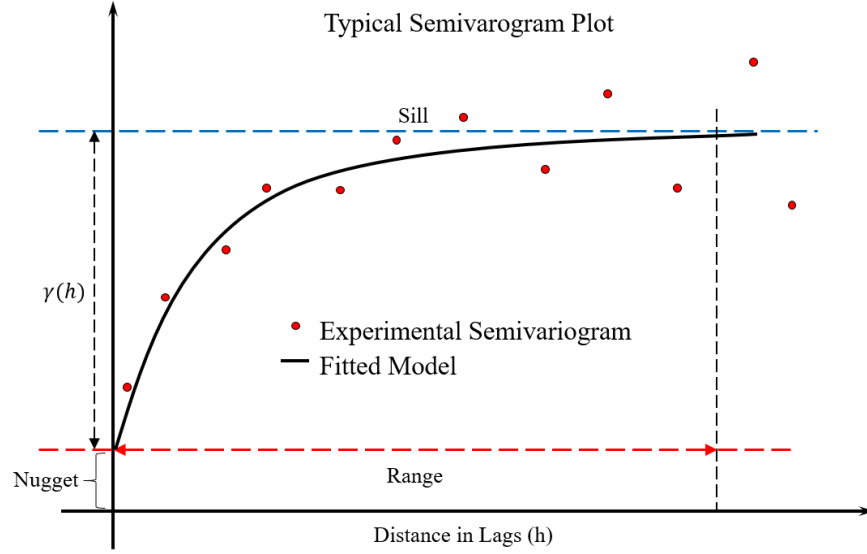


Figure 4. Typical semivariogram with parameters

Three basic parameters are used to define a semivariogram model: range, nugget, and sill. The value at the origin (zero separation distance) should theoretically be zero. However, due to measurement and sampling errors, the value of the semivariogram at the origin could differ significantly from zero, and this error is known as the nugget effect. The semivariance value at which the semivariogram levels off is known as the sill parameter. Generally, a partial sill is the difference between the actual sill value and the nugget effect, which is often the case in a semivariogram analysis. The distance at which the semivariogram reaches the sill value is known as the spatial range of autocorrelation, or autocorrelation range. Autocorrelation is considered as zero beyond this spatial range. Three commonly used semivariogram model forms were considered in this analysis (Bohling 2005, Olea 2006, Solana-Gutiérrez and Merino-de-Miguel 2011). The underlying models are shown in equations 3 to 5.

$$\text{Spherical model: } g(h) = \begin{cases} c \cdot \left(1.5 \left(\frac{h}{a} \right) - 0.5 \left(\frac{h}{a} \right)^3 \right) & \text{if } h \leq a \\ c & \text{otherwise} \end{cases} \quad (3)$$

$$\text{Gaussian model: } g(h) = c \cdot \left(1 - \exp \left(\frac{-3h^2}{a^2} \right) \right) \quad (4)$$

$$\text{Exponential model: } g(h) = c \cdot \left(1 - \exp \left(\frac{-3h}{a} \right) \right) \quad (5)$$

where,

h = lag distance

a = spatial range of continuity

c = sill

The best-fitting semivariogram models were selected based on their cross-validation results (mean standardized error, correlation between the predictors and observed values, and root mean square error). The semivariogram parameters are used for linear interpolation using kriging, which is a commonly used geostatistical interpolation technique that predicts values at unsampled locations using the weighted averages of surrounding measured observations. Weights are assigned based on the semivariogram model. Commonly used kriging methods are simple kriging (SK), ordinary kriging (OK), and regression or universal kriging (RK or UK). The main difference between simple and ordinary kriging estimation methods is that SK assumes a constant and known mean over the sampling domain, whereas OK assumes an unknown and constant mean. RK and UK are equivalent interpolation techniques that model the trend component of the response variable as a function of either a set of independent predictor variables (as in the deterministic trend component in RK) or as a function of spatial coordinates (X and Y). The basic equation of kriging is given in equation 6.

$$Z^*(X_0) = \sum_{i=1}^n \lambda_i Z(X_i) \quad (6)$$

where, $Z^*(X_0)$ is the estimated value at location X_0 , $Z(X_i)$ is the measured observations at sampling sites X_i , λ_i is the kriging weight, and n is the number of sampling locations within the search neighborhood. The kriging weight for each sampling location is estimated based on the parameters of the semivariogram model as well as relative distance of the specific point with other sampling points and the unknown point (Lichtenstern 2013, Kwon et al. 2017). However, uneven smoothing is observed in the kriging interpolated surface where smoothing is inversely proportional to data density. This smoothing issue is addressed by geostatistical simulation methods. Sequential Gaussian simulation (SGS) is one of the most commonly used stochastic simulation methods that generates an infinite number of equiprobable realizations using a kriged surface generated from a normal-score-transformed dataset (Olea 1999). Normal score transformation (NST) transforms the dataset to a standard normal distribution. The formula for NST for a variable of interest, Z , is given in equation 7.

$$Y(X_a) = G^{-1}[F^*(Z(X_a))] \quad (7)$$

where, X_a is sampling location with $a = 1, 2, 3, \dots, n$; F^* is the cumulative distribution function (CDF) of Z , and $G^{-1}(\cdot)$ is the inverse Gaussian CDF of the random function $Y(X_a)$. The normal score transformed data is back-transformed by applying the inverse of the NST equation. The basic procedure for generating a realization is to define a regularly spaced grid surface of the study area and create a random path through the grids in such a way that each grid is visited once in each sequence. A simulated value for each grid is generated from the estimated conditional CDF, which is estimated using the kriged surface generated from the available dataset. The simulated value of each grid cell is added to the conditioning dataset for simulating the values of other grid points until all the points in the study area are simulated. For generating the next realization, the same procedure is repeated using a different random path (Chen et al. 2012). In this study, a 5×5 km gridded fishnet of points was generated for each TPI or WSI class, and the associated value was extracted from the SGS surface for each specific class. Finally, a semivariogram was generated using the extracted RST values, and the semivariogram range was used for RWIS density optimization.

Spatiotemporal Semivariogram Modeling

Spatiotemporal semivariogram modeling was used in this study to evaluate the spatiotemporal variability of RWIS measurements. RWIS data for a winter season were downloaded and processed, and a space-time matrix was formulated as an input of the spatiotemporal analysis. The dataset was classified based on previously developed TPI and WSI classes, and a separate analysis was conducted for each month and zone, which were aggregated to generate a seasonal spatiotemporal autocorrelation range for the TPI and WSI classes. Optimal RWIS densities were then determined by relying on spatiotemporal semivariogram analysis results. Density per unit area was calculated and compared for different topographic and weather-based zones.

Geostatistical spatiotemporal semivariogram modeling was used in this study for spatial and temporal continuity analysis. The traditional spatial analysis is incorporated with temporal analysis to consider both spatial and temporal effect. Spatiotemporal analysis is conducted for variables that vary over space and time. A set of variables in a spatiotemporal field can be defined as $z = \{z(s, t) | s \in S, t \in T\}$, where, S = spatial domain and T = temporal domain. Thus, the general equation of a random field, Z , is $-z_i = Z(s, t), i = 1, 2, 3, \dots, n \times T$, where, n = number of stations and T = number of time points. The random fields $Z(s, t)$ can be modeled as $Z(s, t) = \mu(s, t) + \varepsilon(s, t)$, where, $\mu(s, t)$ = the deterministic part (trend) and $\varepsilon(s, t)$ = the stochastic part (RESSTE Network 2017). The stochastic part is used for spatiotemporal semivariogram modeling. Spatial and temporal variance is estimated as half of the mean squared difference between pairs of data separated by a user-defined spatial (h_s) and temporal lag (h_t) as given in equation 8 (Gething et al. 2007, Shekhar and Xiong 2008).

$$\gamma(h_s, h_t) = \frac{1}{2n(h_s, h_t)} \sum_{k=1}^{n(h_s, h_t)} [z(s_k, t_k) - z(s_k + h_s, t_k + h_t)]^2 \quad (8)$$

where,

$\gamma(h_s, h_t)$ = estimated semivariance value

$n(h_s, h_t)$ = total number of pairs in analysis domain

$z(s_k, t_k)$ = measurement at spatial location s_k and temporal location t_k

A three-dimensional spatiotemporal semivariogram is presented in Figure 5.

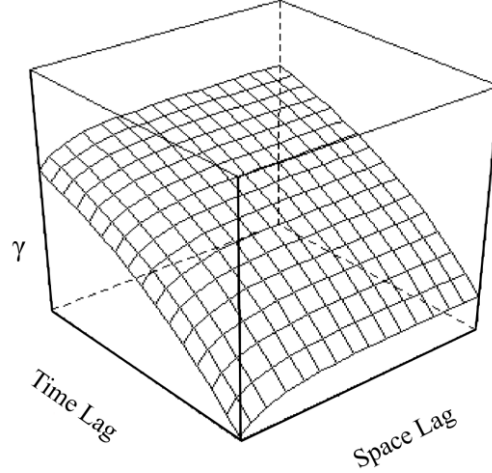


Figure 5. Typical spatiotemporal semivariogram

As the estimated model is irregular, a mathematical model was used for smoothening the empirical variogram. The covariance models generally used for spatiotemporal variogram modeling are discussed in the following section.

Covariance Models

A number of covariance models are used for spatiotemporal semivariogram modeling. The most popular and widely used models are described in the following sections (Pebesma and Gräler 2012, Pebesma et al. 2019; Gräler et al. 2016).

Separable Covariance Model

It is assumed in this model that the spatiotemporal covariance function can be represented as the product of a spatial and temporal term. The covariance function can be written as $C_{sep}(h, u) = C_s(h)C_t(u)$. Thus, the equation of the variogram is $\gamma_{sep}(h, u) = sill. (\gamma_s(h) + \gamma_t(u) - \gamma_s(h)\gamma_t(u))$. Spatial and temporal sill is ignored in this model and kept constant at 1. A joint sill (= 1) is used; which combines both spatial and temporal effects.

Product-Sum Covariance Model

This model assumes a new parameter, k , as a weighting factor of the product ($k > 0$). The equation for the covariance function is $C_{ps}(h, u) = k. C_s(h)C_t(u) + C_s(h) + C_t(u)$. The equation for the variogram can be written as $\gamma_{ps}(h, u) = (k. sill_t + 1)\gamma_s(h) + (k. sill_s + 1)\gamma_t(u) - k\gamma_s(h)\gamma_t(u)$. The expression of joint sill is $sill_{st} = k. sill_s. sill_t + sill_s + sill_t$, where, the spatial and temporal nugget is ignored and kept constant at 0; joint nugget is used to account for both spatial and temporal effects.

Metric Covariance Model

Identical spatial and temporal covariance functions are assumed in this model, except for spatiotemporal anisotropy. Spatial, temporal, and spatiotemporal distances are treated equally in a joint covariance model by matching space and time by spatiotemporal anisotropy parameter, $k(stAni)$. The equation for the covariance function is $C_m(h, u) = C_{joint}(\sqrt{h^2 + (k \cdot u)^2})$. The equation for the metric variogram can be written as $\gamma_m(h, u) = \gamma_{joint}(\sqrt{h^2 + (k \cdot u)^2})$. Temporal distances are internally re-scaled to an equivalent spatial distance to determine the equivalent factor in terms of dependence of 1 m separation in a second or a minute. The expression of spatiotemporal anisotropy is $k(StAni) = \frac{\text{Spatial unit}}{\text{Temporal unit}} = \frac{\text{m}}{\text{Sec/min}}$.

Sum-Metric Covariance Model

This model is a combination of spatial, temporal, and metric models. The equation for a covariance function is $C_{sm}(h, u) = C_s(h) + C_t(u) + C_{joint}(\sqrt{h^2 + (k \cdot u)^2})$. The equation for a sum-metric variogram can be written as $\gamma_{sm}(h, u) = \gamma_s(h) + \gamma_t(u) + \gamma_{joint}(\sqrt{h^2 + (k \cdot u)^2})$. Spatial, temporal, and joint nugget are estimated separately in this model.

Simple Sum-Metric Covariance Model

This model is the simplified version of the sum-metric model to restrict the spatial, temporal, and joint variograms to nugget free models. A single spatiotemporal nugget is introduced in this model. The equation for a variogram is $\gamma_{ssm}(h, u) = nug \cdot 1_{h>0, u>0} + \gamma_s(h) + \gamma_t(u) + \gamma_{joint}(\sqrt{h^2 + (k \cdot u)^2})$, where spatial, temporal, and joint nuggets are set to 0; only joint nugget is fitted.

As several previous studies attested to the superior performance of sum-metric model in fitting the spatiotemporal variogram using environmental parameters (i.e., smallest mean squared errors), this model was selected and used in this analysis (Hu et al. 2017, Ahmed 2018).

Location Optimization via SSA

Few research studies have used geostatistical approaches to determine an optimal RWIS density and set of locations. In a study by Kwon et al. (2017), location optimization of RWIS stations was formulated as an integer programming problem, where the objective function was designed to minimize the spatially averaged kriging variance across the road network (Kwon et al. 2017). The problem was formulated on a basic premise that data from individual RWIS in a region should collectively be used to maximize their overall monitoring quality. The method developed, for the first time, provided decision-makers with the freedom to simulate and optimize their RWIS network by balancing the needs of the road users, winter road maintenance requirements, and other respective priorities in locating RWIS stations. As such, the underlying idea presented therein has been adopted and implemented in this study.

To improve the generalization potential, spatiotemporal semivariogram parameters generated from different weather and topographic classes were used in the location optimization process as representative of the spatial characteristics of the zones. The highway road network of each state was used as the boundary wherein the solution was limited for location optimization of that specific state. A 5×5 km prediction grid was generated along the road network in ArcGIS to create the candidate sites for RWIS station placement. The objective function was formulated to minimize the mean kriging estimation variance.

The equations of the objective function and its related computation process are shown in equations 9 through 12.

$$G = \begin{bmatrix} \gamma(x_1, x_1) & \gamma(x_2, x_1) & \dots & \gamma(x_k, x_1) & 1 \\ \gamma(x_1, x_2) & \gamma(x_2, x_2) & \dots & \gamma(x_k, x_2) & 1 \\ & & \dots & & \\ \gamma(x_1, x_k) & \gamma(x_2, x_k) & \dots & \gamma(x_k, x_k) & 1 \\ 1 & 1 & \dots & 1 & 0 \end{bmatrix} \quad (9)$$

where, x_i ($i=1, 2, \dots, k$) is the sampling site of a sample subset of size k , and in this case, k is equal to the number of RWIS stations, and $\gamma(x_i, x_j)$ is the semivariance between sampling site i and j .

$$g = [\gamma(x_0, x_1) \ \gamma(x_0, x_2) \ \dots \ \gamma(x_0, x_k) \ 1]' \quad (10)$$

where, x_0 is the estimation location and x_i ($i=1, 2, \dots, k$) is the sampling site of a sample subset of size k . Then, the minimum mean squared error for ordinary kriging for the estimation location x_0 is:

$$\sigma_{OKI}^2(x_0) = g'G^{-1}g \quad (11)$$

Based on above three equations, the objective function of this work can be formulated as follows:

$$f(w) = \frac{\sum_{i=1}^{n-k} \sigma_{OKI}^2(x_0)}{n} \quad (12)$$

where,

n = total number of candidate RWIS station locations in the study area

Spatial optimization requires mathematical and computational methods to find optimal solutions for an objective function, which is usually performed under some constraints. For the large-size optimization problem, a heuristic algorithm is a suitable and effective method for finding the solutions (Revelle et al. 2008). The optimization method implemented in this study was SSA (Kwon et al. 2017), which is a spatial counterpart to simulated annealing (SA) (Kirkpatrick et al.

1983). SSA is a popular heuristic algorithm used to solve spatial optimization problems (van Groenigen and Stein 1998, van Groenigen et al. 1999, Heuvelink et al. 2006, Brus and Heuvelink 2007, Kwon et al. 2017). SSA works by slightly perturbing previous sampling designs using random search techniques (van Groenigen et al. 1999). As optimization continues, it is necessary to avoid local minima, and thus SSA not only accepts improving solutions but also worsening solutions based on a certain probability (van Groenigen and Stein 1998). The probability of accepting worsening solutions is typically set initially at 0.2, and this probability decreases exponentially to zero as a function of the number of iterations (Kirkpatrick et al. 1983, Heuvelink et al. 2006, Brus and Heuvelink 2007). The workflow of SSA for a certain number of RWIS stations is displayed in Figure 6.

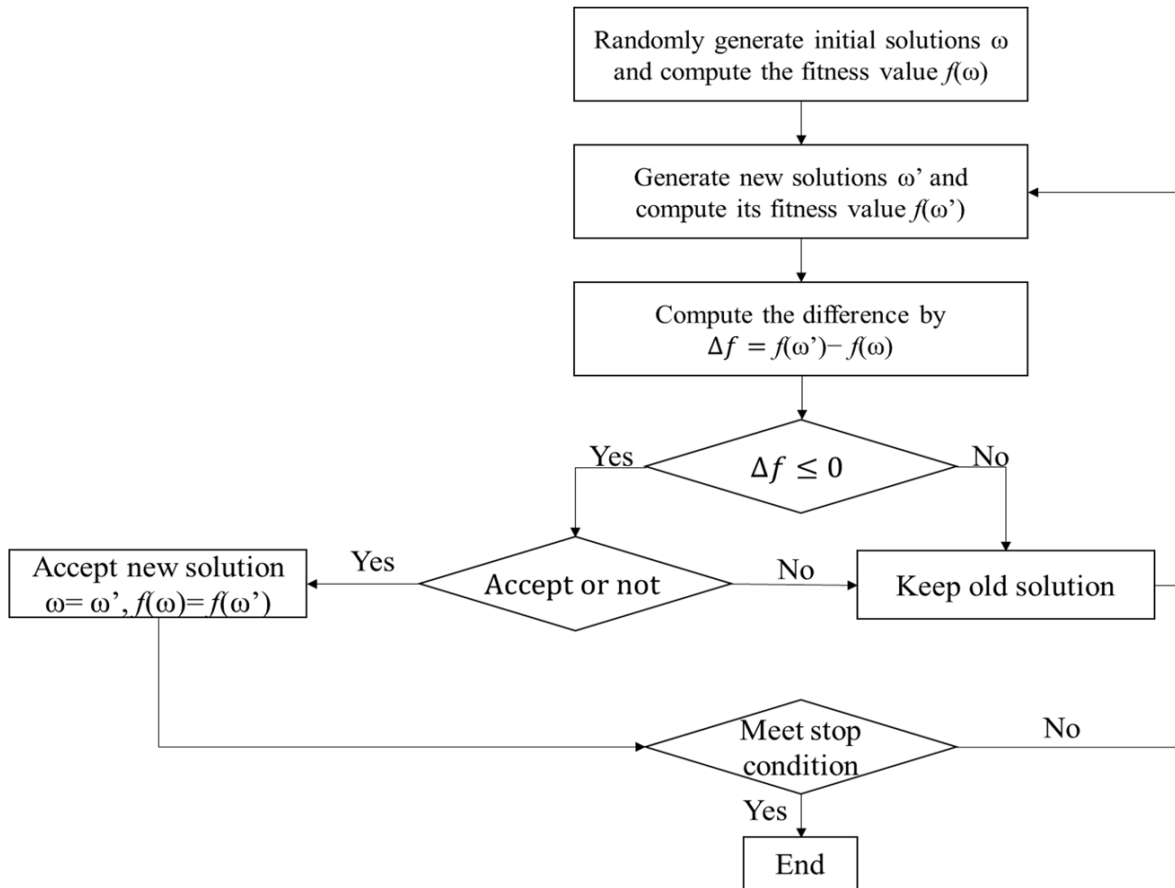


Figure 6. Workflow of spatial simulated annealing

The objective function of this algorithm was the mean OK prediction error variance based on a predefined number of RWIS stations. Optimization follows an iterative process where stations are added one by one into the study area, and locations are selected based on heuristic attempts to minimize the objective function. Location and density distribution optimization was performed in the study area made up of 14 states. This was done over two installation strategies effectively known as all-new and expansion plans. The all-new plan explores a case where all existing RWIS stations are relocated to their optimal locations for comparison. It is called all-new as it also may be used to optimize the installation of a new RWIS network from scratch. The

expansion plan assumes a staged expansion program where 10 RWIS stations are installed per stage to an existing network. Two expansion stages were implemented for this study.

Three different scenarios were used for location optimization: (1) considering weather only, (2) considering traffic only, and (3) considering both (both weather and traffic). The number of iterations was set to 10,000, after which the search process for new RWIS station locations was set to stop. An additional stopping criterion was also used such that if there was no improvement in the objective function after 200 iterations, the algorithm is set to automatically stop. The results of the location optimization are shown in Chapter 4.

Density Optimization via PSO

Density optimization in this study was conducted in order to compare the number of RWIS stations needed per unit area in different TPI- and WSI-based classes. Semivariogram parameters generated from different classes were used in the optimization process as representative of the spatial characteristics of the zones. A randomly selected square region (area of 10,000 km²) within the study area was used as the experimental boundary wherein the solution was limited for density optimization of all classes. Following the same procedure for generating the optimal location solutions, RWIS density curves for different TPI and WSI zones were generated based on a predefined number of RWIS stations. The marginal increment of benefit associated with each additional RWIS station was calculated to determine the optimal RWIS density.

Density optimization in this project was conducted using PSO. PSO is an evolutionary computation technique and population-based global optimization method developed by Kennedy and Eberhart in 1995 (Eberhart and Shi 2001). PSO is widely used and popular in scientific computations, because it is easily implemented and computationally inexpensive. In this optimization process, a number of n-dimensional candidate points (particle) are placed in the search space of a function and each of the particles evaluates the objective function at its current location. Each particle can be assumed as a potential solution presented by velocity and position (Wang et al. 2013, Gu et al. 2019). Movement of each particle is determined based on its best fit location with one or more swarms, and the algorithm searches for optima by updating the generations (Kennedy and Eberhart 1995, Poli et al. 2007). The *i*th particle in the search space can be represented as $x_i = (x_{i1}, x_{i2}, \dots, x_{in})$. Each particle in the swarm flies to the previous best position and global best position; those are named as *pbest* and *gbest*, respectively. The best previous position of the *i*th particle can be presented as $p_i = (p_{i1}, p_{i2}, \dots, p_{in})$. The index of the best particle in the swarm is represented by the subscript *g*. The velocity of particle movement is represented by $v_i = (v_{i1}, v_{i2}, \dots, v_{in})$. The particle is attracted by *pbest* and *gbest* during the search process according to equations 13 and 14.

$$v_{id} = \omega v_{id} + c_1 \zeta (p_{id} - x_{id}) + c_2 \eta (p_{gd} - x_{id}), \quad (13)$$

$$x_{id} = x_{id} + v_{id}, \quad (14)$$

where, d = dimension, representing the total number of candidate RWIS sites, where $1 \leq d \leq n$; c_1 and c_2 are positive constant; ζ and η are random adjustment factors with a range of 0 to 1; and ω is the inertia weight. The performance of each particle is measured using a predefined fitness function. A binary particle swarm optimization (BPSO) was proposed by Kennedy and Eberhart (1997) for solving integer-programming problems, as the original PSO was not suitable in this case. The basic difference between these two methods is in updating of the particles' position. The sigmoid function is utilized in BPSO where every dimension in the position becomes a number between 0 and 1. A modified BPSO was proposed by Gu et al. (2019) to solve the RWIS location optimization problem. A similar method was adapted for use in this current study for region-wise RWIS density optimization. Position of particle was updated using equation 15.

$$x_{id} = \frac{1}{1+e^{-v_{id}}}, \quad (15)$$

In the modified BPSO, a threshold probability, r , is set to control whether the x_{id} becomes 1 or not, where 1 represents the selection of the element. During optimization, the total number of RWIS stations (m) is set as a constant, and the algorithm is set to select best-fit ' m ' number of locations in the search space. The original BPSO shows premature convergence because of a quick loss of diversity. To treat this problem, more randomness is added into the internal mechanism of the modified BPSO in order to expand the search space and allow the particle to escape from any possible local minima. Another addition is that if more than one location has the same probability for an RWIS station, a mechanism is set in the modified BPSO to randomly select one of them as the solution. Lastly, in addition to the maximum velocity set to control the speed of convergence, the inertia weight (ω) and self-learning factor (c_1) are set to decrease from 0.9 to 0.4 and 2 to 0, respectively, in the search process. On the other hand, the society-learning factor (c_2) is set to increase from 0 to 2. The parameters were chosen to ensure that the particles can fly slowly while eliminating their ability for self-learning and enhancing social-learning. The steps associated with the modified BPSO algorithm are as follows (Poli et al. 2007, Wang et al. 2013, Gu et al. 2019):

- **Step 1.** ' m ' particles are initialized with dimensions of velocity.
- **Step 2.** Velocities are converted to positions (probabilities) using the sigmoid function (equation 8).
- **Step 3.** Two top probabilities are selected in each particle's position, and they are set to the selected candidate points for locating RWIS stations; then, ordinary kriging variance is calculated for all the unknown points as the fitness value.
- **Step 4.** Memorize the current individual best positions and the global best positions.
- **Step 5.** Update ω , c_1 , and c_2 using equations 16, 17, and 18.

$$\omega_{new} = \omega_{old} - \frac{\omega_{max} - \omega_{min}}{\text{number of iterations}}, \quad (16)$$

$$c_{1new} = c_{1old} - \frac{c_{1max} - c_{1min}}{\text{number of iterations}}, \quad (17)$$

$$c_{2new} = c_{2old} - \frac{c_{2max} - c_{2min}}{\text{number of iterations}}, \quad (18)$$

- **Step 6.** Update each particle's velocity using equation 19.

$$v_{id} = \omega v_{id} + c_1 * \zeta_{id} * \Delta x_{pid} + c_2 * \eta_{id} * \Delta x_{gid}, \quad (19)$$

If the $v_{id} > v_{max}$, then $v_{id} = v_{max}$.

- **Step 7.** Update particles' positions using equation 8.
- **Step 8.** Update the individual best position and global best position by comparing fitness values. If updated fitness value is smaller than before, accept the new solution and check if the new solution meets the stopping criterion (i.e., a predefined number of RWIS). If not, repeat the process from Step 2.

3. STUDY AREAS AND DATA DETAILS

Study Areas and RWIS Network

The study area is comprised of 14 states, which also happens to be a part of the Aurora RWIS project. These 14 states were chosen based on the availability of the necessary datasets to run both the location optimization and the density distribution of the RWIS stations. A calibration and exploration of the methodology was done on eight states that had the required data availability and level of completeness in order to do so. This subgroup is called the calibration states. However, three of the eight states, namely Wyoming, Nebraska, and Kentucky, did not have sufficient transportation-related data available at the time to run the optimization analysis and thus were not included as part of the study area for optimization. Once the calibration was done, it was then applied to the 14-state study area. This section details the study area and the data used.

The study area for spatiotemporal analysis and RWIS density optimization was selected based on RWIS data availability and distribution of RWIS stations to cover a variety topography and weather conditions that may pose challenging driving conditions. Only eight states had sufficient data, RWIS station coverage, and the minimum number of stations for the team's analysis; those states include Colorado, Iowa, Kansas, Kentucky, Minnesota, Nebraska, Ohio, and Wyoming. These eight states provided a broad enough region, as well as a range of topographic and weather conditions, in which to explore the research team's approach. The total available RWIS station count for the states are 147, 86, 56, 38, 98, 70, 182, and 81, respectively. The study period selected for this project included a winter season (October 2016 to March 2017) to best capture challenging winter driving conditions. The distribution of RWIS stations for the study area is presented in Figure 7.

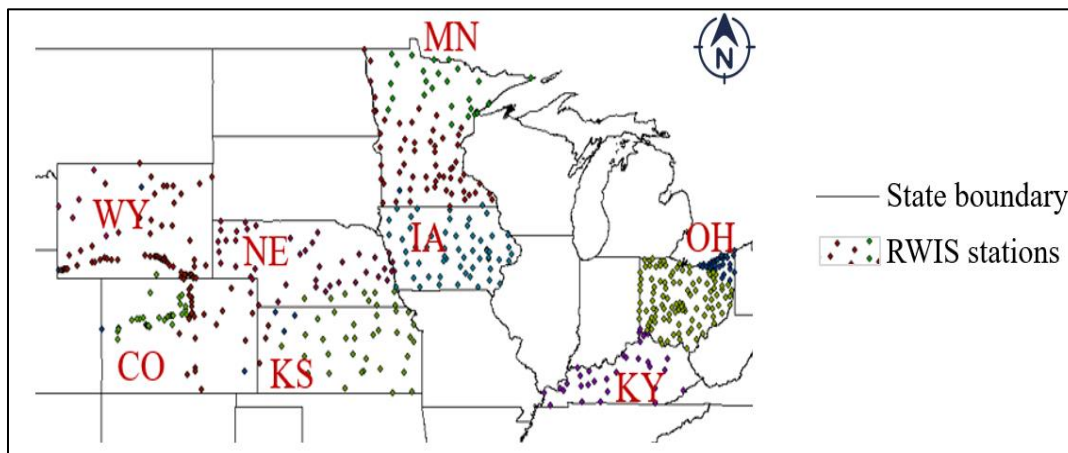


Figure 7. Distribution of RWIS stations for eight US states

The spatiotemporal semivariogram analysis results were then applied to RWIS location optimization for 14 states presented in Figure 8. These 14 states already have RWIS stations installed and served as a basis for comparing the optimized locations to the current locations.

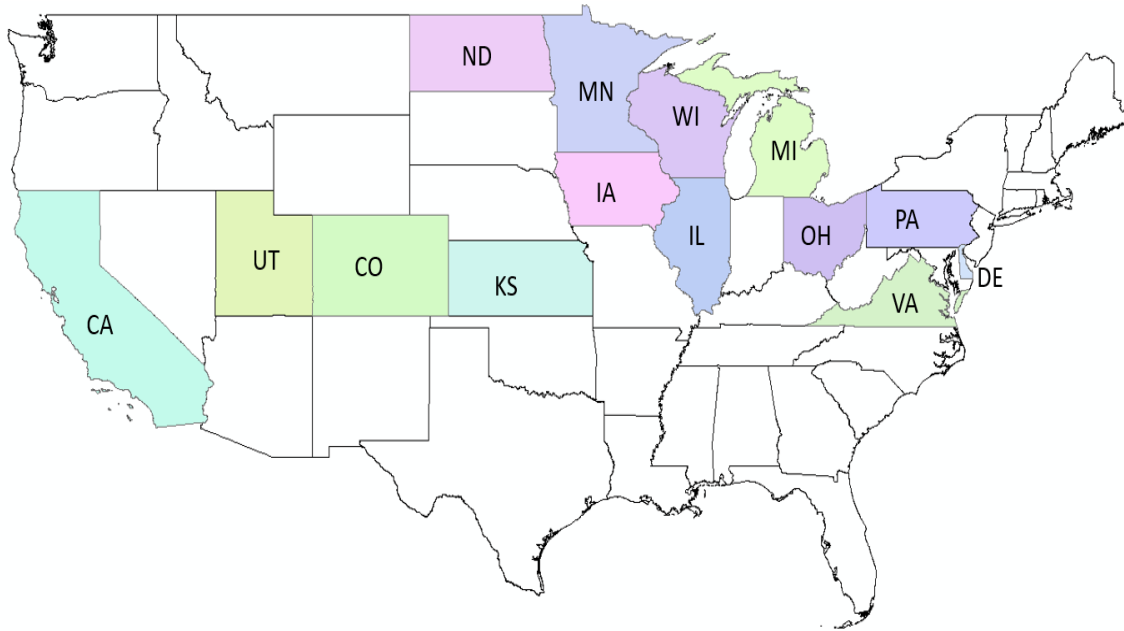


Figure 8. Study area for location optimization

The total available RWIS station count for the additional states are: 23 for California, 19 for Delaware, 59 for Illinois, 97 for Michigan, 29 for North Dakota, 19 for Pennsylvania, 98 for Utah, 52 for Virginia, and 59 for Wisconsin.

Data Description

The description of various data sources that are used in this study are described in this section.

Topography Data

A DEM with resolution of 30 m data (28 GB) was downloaded from the U.S. Geological Survey website (<https://earthexplorer.usgs.gov/>) for topographic characteristic analysis in ArcGIS 10.4.1, which happens to encompass 20 state DOTs. The resulting TPI map file has a size of 49 GB. However, only the 14 aforementioned states in the study area were used in this report.

Weather Severity Data

The ArcGIS shapefile generated by Meridian Environmental Technology, Inc. was used for weather severity analysis.

RWIS Data

RWIS data for the states of Colorado, Iowa, Kansas, Kentucky, Minnesota, Nebraska, North Dakota, Ohio, Virginia, Wisconsin, and Wyoming were downloaded from the Iowa State

University mesonet project site (<http://mesonet.agron.iastate.edu/RWIS/>). The RWIS data for California, Delaware, Michigan, Pennsylvania, and Utah were obtained from their respective DOT open data database network. The statewide RWIS data were downloaded as an Excel file. Measurements from a typical RWIS station include, but are not limited to, air and surface temperature, visibility, wind speed, and road surface conditions, collected at 15 to 20 minute intervals. In total 1,026 stations were included in the analysis, and 4,368 hours of data were used.

Traffic Volume Data

Annual average daily traffic (AADT) data for the year 2017 were downloaded from the Traffic Monitoring Management System (TMMS) section of the Ohio DOT website (<http://www.dot.state.oh.us/Divisions/Planning/TechServ/Pages/default.aspx>). AADT data include location description, details of route, AADT, and some other information. The size of the AADT data covering 8,760 hours of observations was 2.22 GB.

Data Processing

The RWIS data were processed to remove the missing and erroneous data using five steps:

1. Conducting data completeness test to identify missing data
2. Conducting reasonable range test to find erroneous data
3. Cross-checking RST data with air-temperature data
4. Analyzing RST data pattern
5. Detrending RST data with respect to time using the generalized additive model (GAM)

Data completeness was checked by identifying the total missing data for each sensor. If the total missing data was more than 15%, the associated sensor ID was marked, and the data from that sensor were not used for analysis. Reasonable range was tested based on historical data ranges for the associated region and month. Filtered RST data were then cross-checked with air-temperature data ranges for any possible outliers. An RST data pattern analysis was performed by plotting the day of the month versus the average daily temperature for all selected sensors, for each state, and each month. All selected sensors were expected to show a similar pattern throughout the month. If any unusual pattern was noticed, the RST data for the associated sensors were further investigated for the time period of the unusual pattern. In total, 48 sets of data (six months for the eight calibration states) were analyzed using the above-described process. Finally, RST data was detrended with respect to time using a GAM, where GAM worked as a generalized linear model with linear predictors. The GAM function was formulated as $m = \beta_0 + f_1(x_1) + f_2(x_2) + \dots + f_i(x_i)$, where, m = variable of interest, β_0 = intercept, $f_i(x_i)$ = smooth function of predictor x_i . The smooth function can be expressed as $f_i(x_i) = \sum_{n=1}^m s(x_n)$ (Hastie and Tibshirani 1990, Wang et al. 2019).

Descriptive statistics (means and standard deviations) revealed relatively less variation in average monthly temperatures in the mid-winter months than in the shoulder months. Overall minimum and maximum temperatures for the study area were: -30.3°C to 51.5°C (-22.5°F to

124.7°F). Table 1 presents the maximum, minimum, average, and standard deviations of RST for the study area. Because of erroneous data in November 2016 in Kentucky, it was excluded from the analysis.

Table 1. Descriptive statistics of RST for the calibration states

Month-Yr	RST	States							
		CO	IA	KS	MN	OH	KY	NE	WY
Oct-16	Min	-6.7	-1.1	0.8	-2.6	-1.5	-7.2	-6.2	-9.4
	Average	15.5	16.9	20.8	12.6	18.3	20.0	16.7	11.9
	Max	37.8	41.5	46.2	41.0	47.0	39.5	44.7	45.1
	StDev	9.0	6.9	8.2	7.0	6.9	6.9	7.7	8.1
Nov-16	Min	-29.8	-8.6	-7.6	-9.9	-24.0	-	-12.5	-15.9
	Average	7.6	9.5	12.5	6.0	10.1	-	8.7	5.0
	Max	46.9	38.3	39.5	30.2	35.5	-	34.4	30.6
	StDev	9.2	7.1	7.8	6.2	6.3	-	8.0	8.0
Dec-16	Min	-22.6	-29.5	-24.9	-29.9	-19.6	-10.4	-28.1	-29.5
	Average	-1.5	-2.7	0.8	-6.6	1.7	4.5	-3.3	-5.4
	Max	26.6	18.8	22.9	11.7	51.5	21.1	17.8	17.6
	StDev	7.4	6.4	7.3	6.8	5.7	4.8	6.2	6.3
Jan-17	Min	-26.9	-24.0	-20.9	-30.3	-19.1	-17.2	-26.9	-29.1
	Average	-0.6	-2.1	2.7	-6.8	2.9	6.4	-2.5	-5.5
	Max	37.8	19.6	28.5	14.2	25.5	21.8	19.9	21.0
	StDev	7.7	6.0	7.4	7.9	6.3	5.1	6.3	6.9
Feb-17	Min	-17.7	-15.9	-10.8	-26.0	-22.7	-9.6	-19.4	-23.4
	Average	6.0	5.6	9.8	-1.5	7.1	9.3	4.4	0.9
	Max	37.7	32.4	38.6	27.2	34.5	30.4	36.1	30.7
	StDev	8.9	8.2	9.0	8.1	7.3	5.9	8.0	7.7
Mar-17	Min	-17.2	-16.4	-7.3	-22.0	-10.8	-8.4	-11.5	-17.5
	Average	11.0	7.0	13.9	2.5	9.0	12.1	9.4	7.2
	Max	38.3	36.1	48.7	36.3	36.0	31.7	43.7	39.5
	StDev	10.2	7.6	9.5	8.7	7.1	6.5	8.3	9.3

Figure 9 shows the seasonal maximum, minimum, average, and standard deviation of RST for the calibration states.

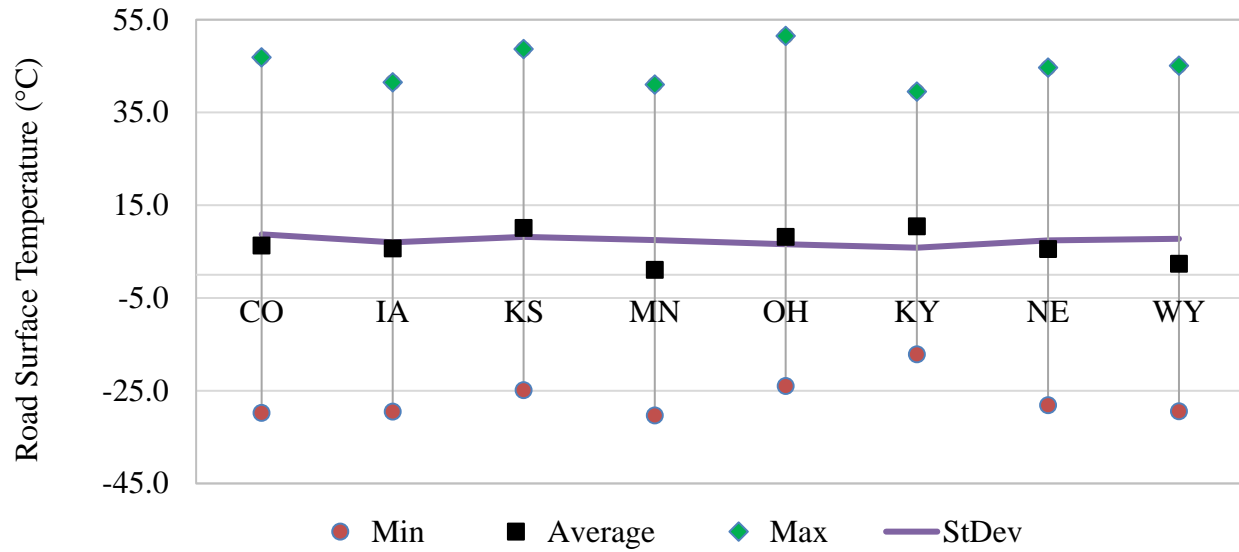


Figure 9. Seasonal road surface temperature details for eight states

Semivariogram modeling and RWIS location optimization were performed using the R statistical package, Version 3.2.5 (Pebesma 2004, Gräler et al. 2016, R Core Team 2018). RWIS density optimization was coded in Python. To improve the computational efficiency, all optimizations undertaken in this study were run on the supercomputer “beluga” from the University of Alberta, managed by Calcul Québec and Compute Canada (<https://www.computecanada.ca/>), with 32 central processing units (CPUs), each of which runs on 2.4 GHz CPU and 1 GB memory.

4. RESULTS AND DISCUSSION

TPI and WSI Classes

Topographic features of 14 US states in the study area were studied, quantitatively described, and classified using the TPI. The TPI map of the study area is shown in Figure 10, and the range of values was between 565 and 5,293.

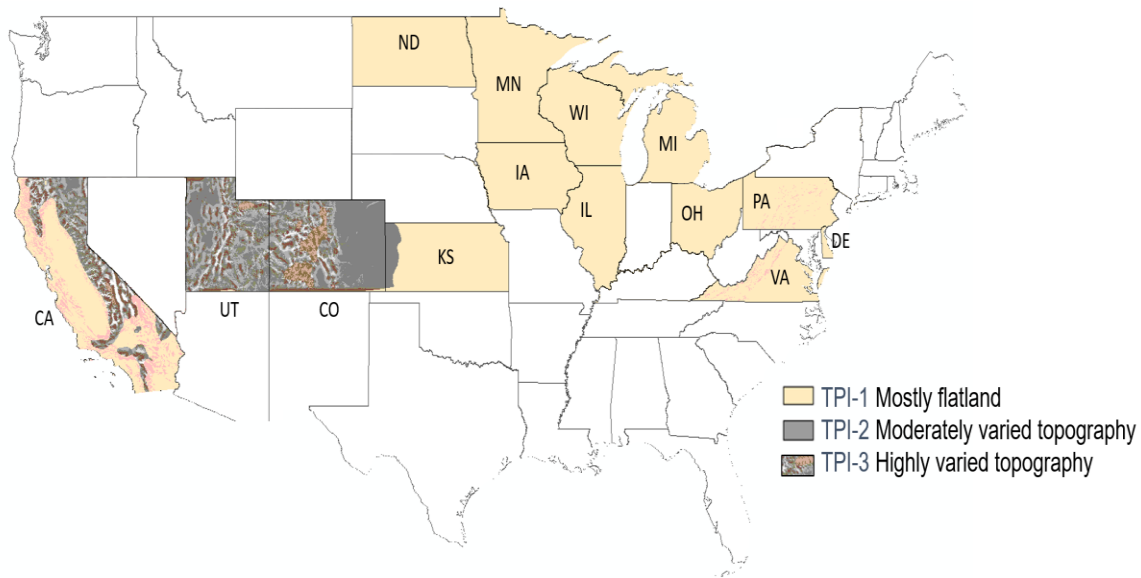


Figure 10. TPI map of the 14 US states of the study area

As the team's main interest in using TPI-based analysis was landform classification over a large geographic area, the absolute value of TPI was used. However, much of the study area had a TPI value below 75. More specifically, Delaware, Illinois, Indiana, Iowa, Kentucky, Michigan, Minnesota, New York, North Dakota, Ohio, Pennsylvania, Virginia, and Wisconsin, and large portions of California, Kansas, and Nebraska had TPI values that were less than 75. This area was designated as TPI-1 (i.e., the beige colored zone in Figure 10), that represents the flatland area. A few points with a TPI value between 75 and 1,500 can be seen at the edges of California, New York, Pennsylvania, and Virginia. Another large part of the study area had a TPI range between 1,900 and 2,100 with a minor area of 1,500 to 1,900. This more hilly zone was designated TPI-2 (i.e., the gray colored zone in Figure 10), which covers a small part of Kansas and sizable portions of Colorado, Nebraska, and Wyoming, and very small parts of California and Utah. Large variations in TPI can be seen in the remaining study area including large parts of California, Colorado, Nevada, Utah, and Wyoming, where the range in TPI varied from 1,900 to 5,293, with a minor area under 1,900. This zone was classified as TPI-3, which is a mountainous region.

The study area was also classified into four WSI classes (Figure 11).

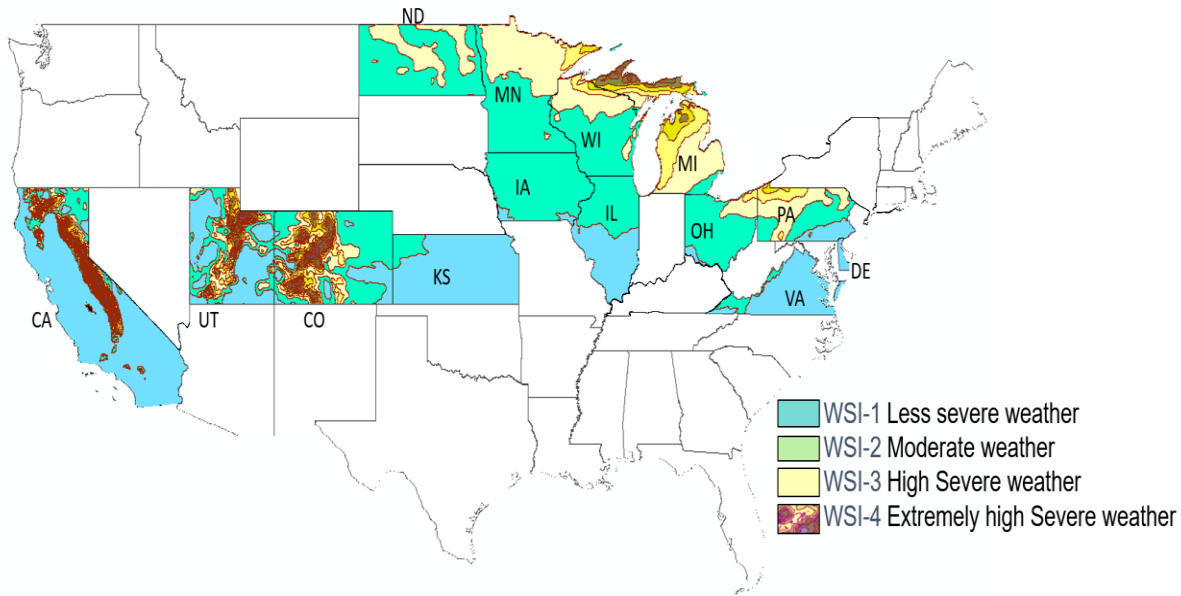


Figure 11. WSI map of the 14 US states of the study area

The range of WSI was 7.6 to 301.7. The class WSI-1 (blue colored zones) includes the areas with WSI values less than 25. This classification covers nearly all of Delaware, Kansas, Kentucky, and Virginia; the lower parts of Illinois and Indiana; small parts of California, Colorado, Nevada, Pennsylvania, and Utah. The class WSI-2 (green colored zones) represents a region with a WSI range of 25 to 50. Nearly all of Iowa, Nebraska, and Ohio; the southern halves of Minnesota, North Dakota, and Wisconsin; the northern parts of Illinois and Indiana; and small portions of Colorado, Pennsylvania, Nevada, New York, and Wyoming are captured by this class. Of the remaining portion of the study area, a relatively large region is between 50 and 75 WSI and between 75 and 100 WSI. This region (50 to 100) was designated WSI-3, and this class includes the northern parts of Minnesota, New York, North Dakota, Pennsylvania, and Wisconsin; small portions of Colorado and Ohio; and part of Wyoming. The remaining area had large variation in WSI values from 100 to 301.7. This area is mountainous and was classified as WSI-4, which is quite similar to TPI-3.

Spatial Semivariogram Modeling Results

The range of spatial autocorrelation for the study area was examined using semivariogram analysis. The RST was selected as the variable of interest for this study as it is one of the most widely used weather variables that represents the road surface conditions properly, and it is a necessity for improved winter road maintenance operations (Kwon and Fu 2017). Raw RST data were processed and semivariogram models were developed using monthly average RST data.

The range of spatial autocorrelation for the three TPI-based classes and the four WSI-based classes are presented in Figure 12.

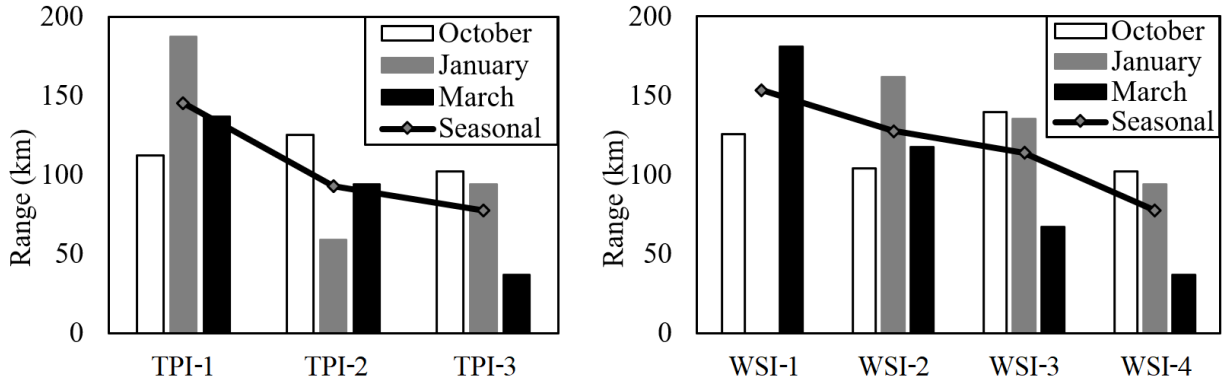


Figure 12. Comparison of spatial range for TPI classes (left) and WSI classes (right)

As shown, for TPI-1, the flatland area, the average spatial range is highest, followed by TPI-2, and TPI-3, suggesting that on average the range of spatial structure (i.e., similarity in conditions) decreases as topography becomes more variable. Similarly, decreasing spatial range is observed from WSI-1 to WSI-4. Given the limited time periods examined here, a lack of data, and clustering of RWIS stations when multiple states were considered together, monthly estimates for spatial ranges (the vertical bars in Figure 12) do not always follow the average trend. In addition, the spatial range for WSI-1 for the month January is missing because the semivariogram developed for this particular month failed to converge, possibly due to a lack of samples to capture the underlying spatial autocorrelation structure of the variable of interest. This result reveals that the predictive coverage of an RWIS station is dependent on the topographic and weather features of a region. Flatter areas had higher spatial ranges and thus require a smaller number of RWIS stations to achieve a similar level of monitoring coverage than hilly or mountainous regions. Correspondingly, areas with more severe weather conditions require more stations to achieve the same level of spatial coverage than areas with less severe weather. This phenomenon is examined using density optimization in the following section.

Spatiotemporal Semivariogram Modeling Results

RWIS data for the study area were also processed considering both space and time domains on a monthly basis, from October 2016 to March 2017. RST data were aggregated using 20 minute interval for time domain analysis. A space-time matrix was then formulated for each TPI and WSI zone. Spatiotemporal autocorrelation of RST for each study zone was then analyzed using spatiotemporal variogram modeling methods using the gstat package in R (Pebesma 2004, R Core Team 2018). A sample of spatiotemporal semivariograms of different TPI and WSI classes is presented in Figure 13.

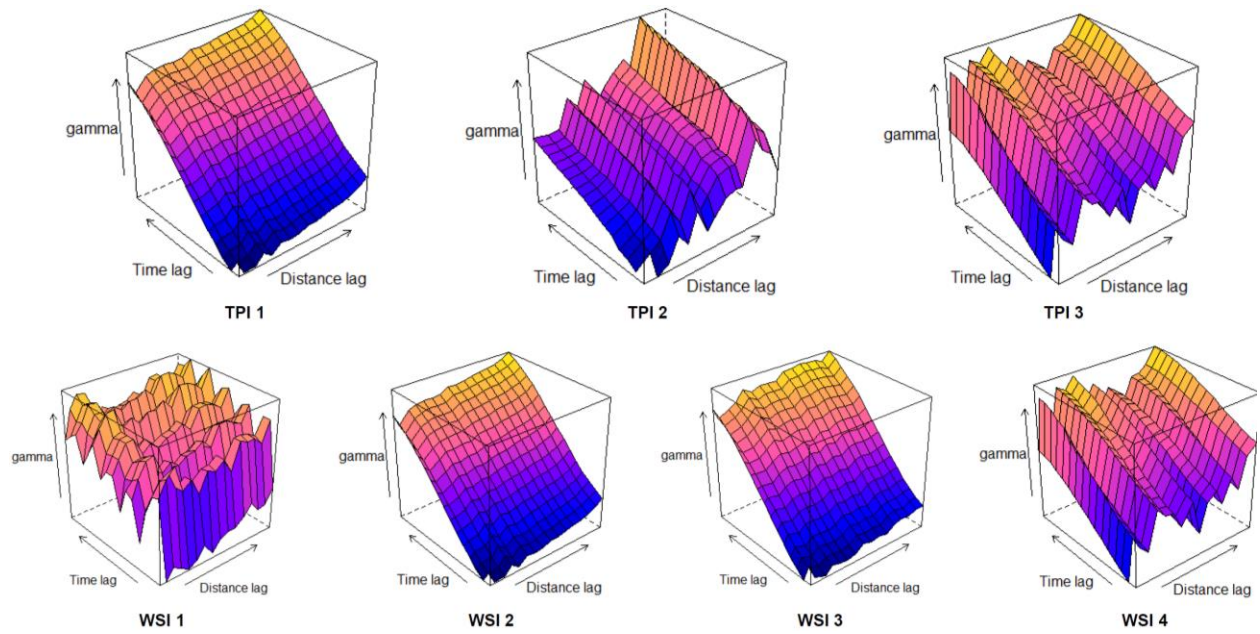


Figure 13. Sample spatiotemporal semivariogram of TPI and WSI classes for November 2016 RWIS data

Seasonal spatiotemporal analysis results for TPI and WSI zones are presented in Figure 14.

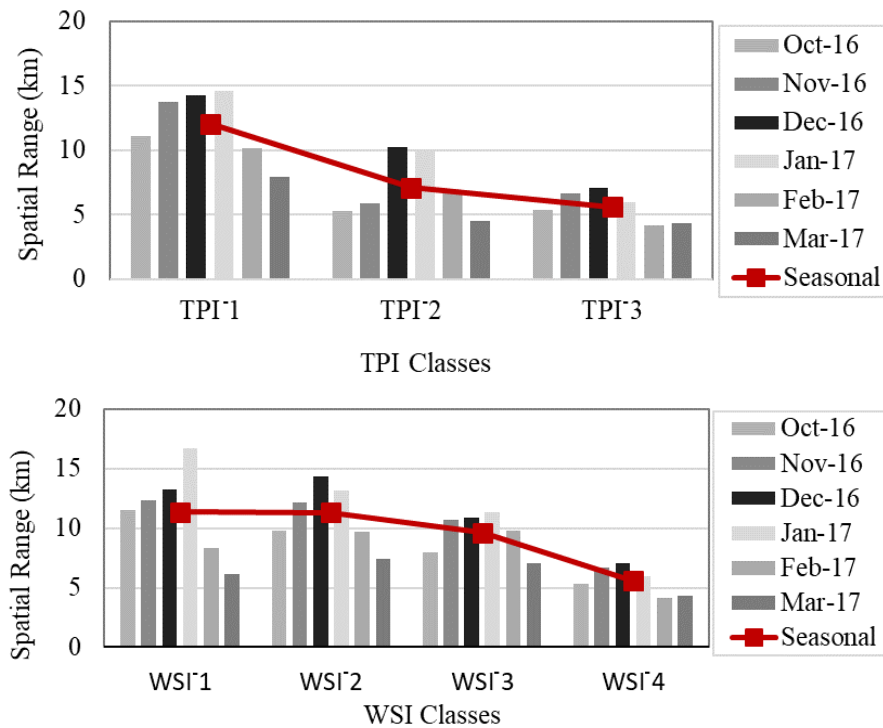


Figure 14. Spatial semivariogram ranges for TPI classes (top) and WSI classes (bottom)

According to Figure 14, relatively higher spatial and temporal ranges are obtained for TPI-1 (flatland area), followed by TPI classes 2 and 3, representing hilly and mountainous areas, respectively. Similar results were obtained for weather-based classes, where regions with less topographic variation and less severe weather have a higher spatial and temporal range as depicted in Figure 15.

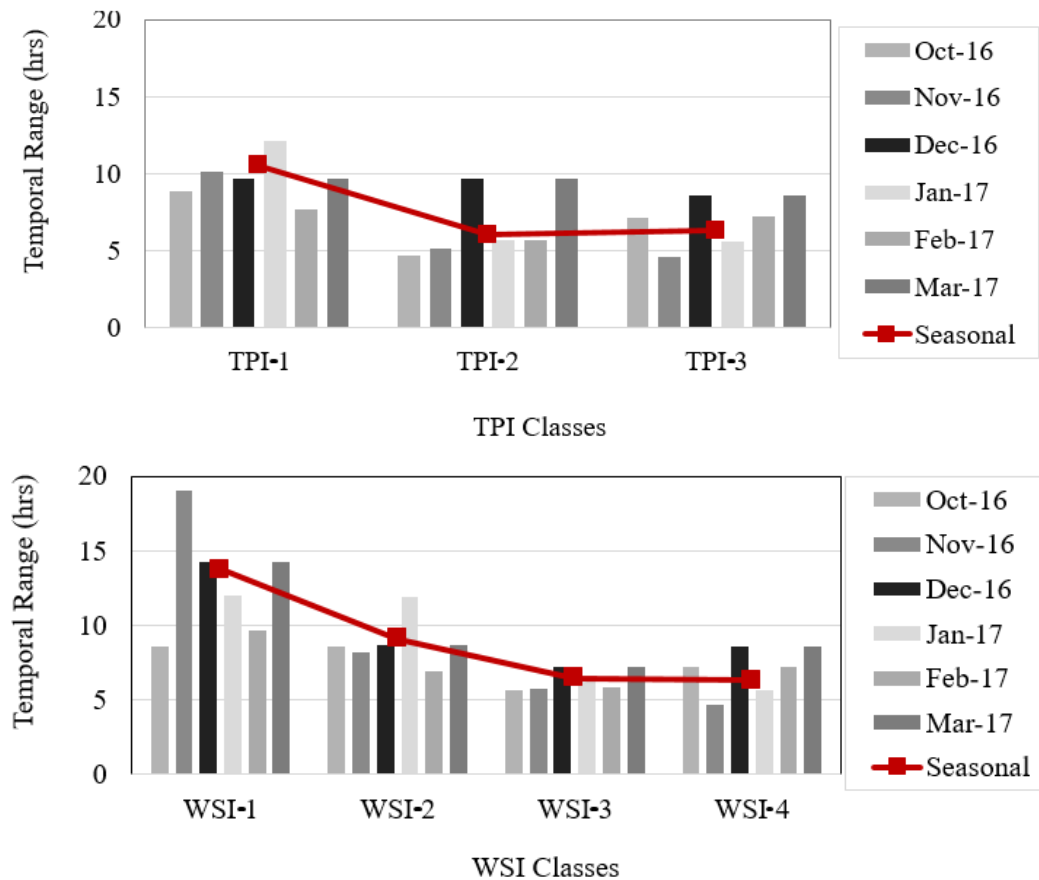


Figure 15. Temporal semivariogram ranges for TPI classes (top) and WSI classes (bottom)

The range of autocorrelation decreases with an increase in topographic variation and weather severity. In general, there is a trend of higher autocorrelation range during mid-winter months compared to shoulder months, which is as expected.

The effect of weather severity in the TPI-1 zone, which is the flatland area, is presented in Figure 16.

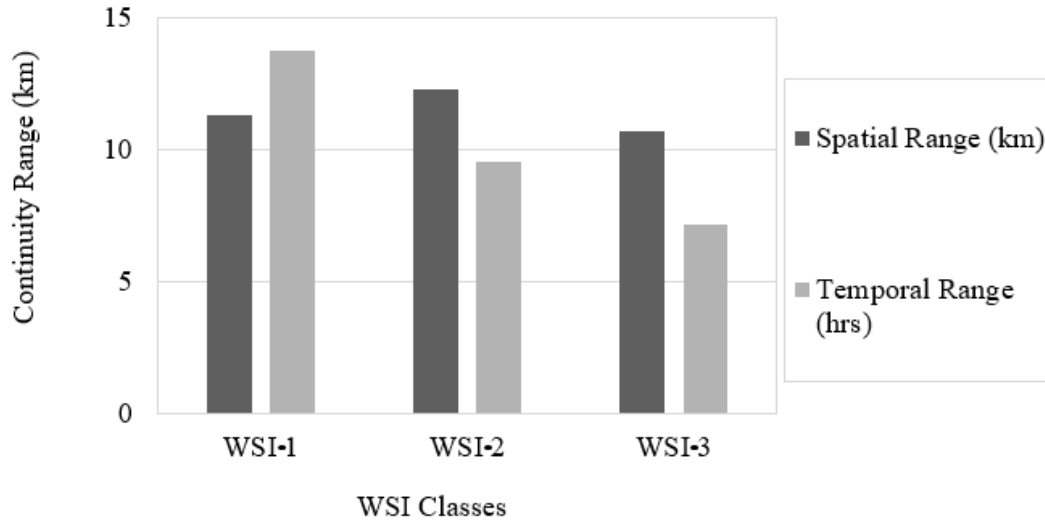


Figure 16. Spatial and temporal range for flatland area (TPI-1) with different weather severity

In the study area, the flatland region consists of three weather severity regions, and there is a trend toward a higher autocorrelation range in areas with less weather severity than in areas with more severe weather severity regions, especially for the temporal range. The effect of weather for the spatial range is negligible as the total difference is only 1.6 km. From this, it can be concluded that topography can serve as a more intuitive measure for RWIS network planning than that of weather severity. Similar comparisons for other TPI zones have not been made because TPI-2 includes WSI-2 and WSI-3 zones; and TPI-3 is identical to WSI-4 (see Figure 10 and Figure 11).

Statewide RWIS Implementation Strategies

Spatiotemporal semivariogram models for different topographic and weather severity regions were used for state-wise RWIS network implementation. This section includes the state-wise relocation of the current RWIS network for different criteria, statewide expansion of the RWIS network, and the effect of spatial demarcation in RWIS network planning.

A Statewide Relocation of the Current RWIS Network

This section includes an analysis of the hypothetical problem of optimizing the RWIS network for the 14 states such that the current network can be effectively evaluated. The main goal of this state-wise relocation was to compare the overall monitoring capabilities of the optimized network with the current location settings. The existing station number and location were collected from the aforementioned Iowa State University website, and an equal number of new RWIS station locations were generated for candidate states using a dual scenario, which considered both weather and traffic data with equal weightage. The resulting new locations for

the same number of RWIS stations per state are presented in Appendix A, and the specific location information is provided in Appendix B.

A Statewide Expansion of the Current RWIS Network

The RWIS network expansion plan described herein is a staged expansion where a set of 10 new RWIS stations are added at each expansion stage. This study implements two expansion stages to the existing RWIS network for the 14-state study area to increase coverage and enhance winter maintenance operations. The optimization problem has, therefore, been modified to include the existing stations as input and locate the additional stations accordingly. Network expansion solutions were generated considering two different criteria: (1) considering weather only and (2) considering dual criteria (both weather and traffic). Location plots for adding new stations to the existing RWIS network for the study area are presented in Appendix C, and the specific location information is provided in Appendix D.

Effects of Spatial Demarcation

This section aims to evaluate how existing RWIS configurations in neighboring states influences the RWIS optimization process. Iowa, with 86 existing RWIS and six border states, was selected as the study area. The methodology was applied to derive two different optimal RWIS location sets under two conditions: (1) by considering the RWIS stations of bordering states and (2) without considering the RWIS stations of bordering states. The comparison between the results for Iowa can be a good reference point with respect to the effects of the bordering states' RWIS stations. Figure 17 presents the RWIS optimization process with and without considering bordering states' effects.

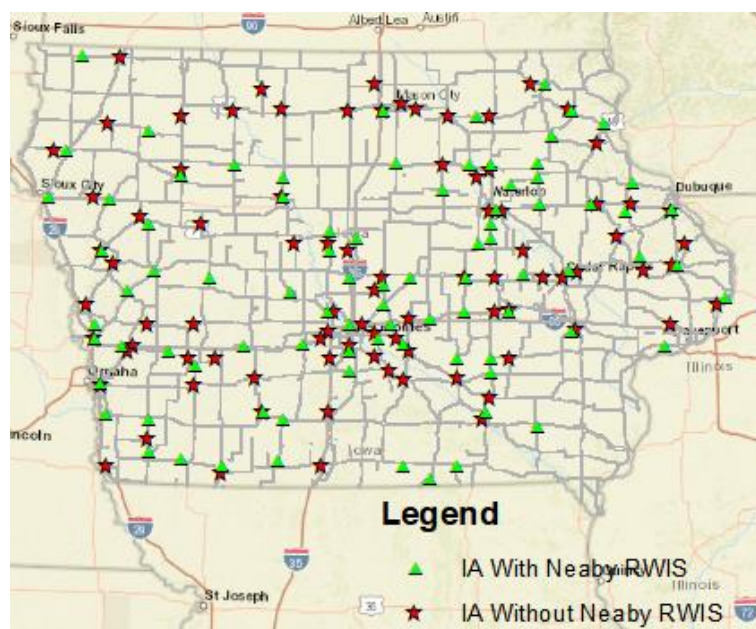


Figure 17. RWIS optimization for Iowa

As is shown, by combining the neighboring states' RWIS, the derived RWIS solutions focus on urban areas. To statistically explain the differences, the research team conducted two different statistical analyses to compare the similarity between the two RWIS patterns. First was the two-sample t-statistic for the mean, which suggested the directionality of the surrounding RWIS effect. If the centroid distance between the two groups is significantly different, then the surrounding RWIS stations can be seen as having an uneven effect on the location optimization process of RWIS. The other part is a two-sample F-statistic for variance test. This test showed the effect of nearby RWIS locations by resulting in a relatively higher RWIS density in the center of the study area.

The two tests evaluated the directionality and effectiveness of the surrounding RWIS location. According to the directionality test, the t-value was found to be 0.21, meaning the effect of bordering states does not pose a directional effect. The F-test result is presented in Figure 18.

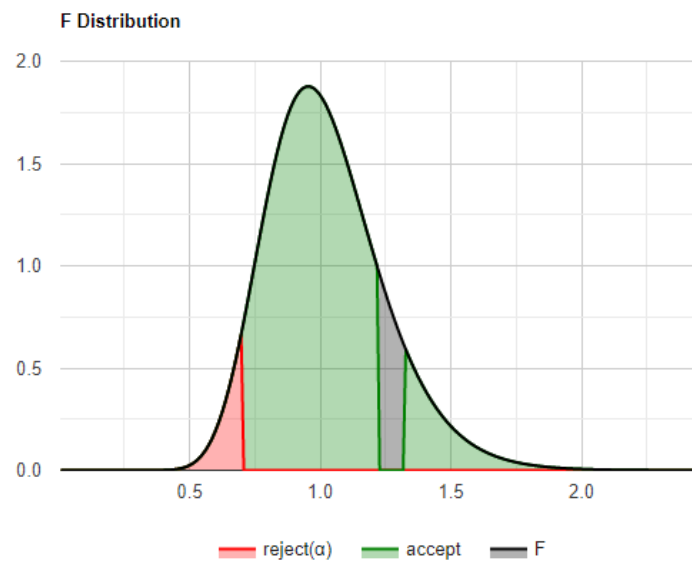


Figure 18. F-statistic distribution

The null hypothesis assumed in the F-test was that, Scenario A has the same variance as B. The resulting p-value was 0.866, which suggested that there was an 86.6% probability to reject the correct null hypothesis. The F-test value was 1.273117, which lies in the 95% critical value accepted range: $[0.699, \infty]$. This result indicated that, Scenario A has a lower variance than B. Hence, the deployment of RWIS should take the RWIS of bordering states into consideration.

RWIS Density Guidelines and Their Statewide Applications

Development of Optimal RWIS Density Guidelines

Spatial parameters of a spatiotemporal semivariogram were used as input for density optimization for topographic and weather severity zones (three TPI classes and four WSI classes). A hypothetical network of 100 km × 100 km was used for density optimization. A 5 km

$\times 5$ km prediction grid was generated in ArcGIS to create the candidate sites for RWIS station placement. The objective function was formulated to minimize the mean ordinary kriging estimation variance and solved via PSO as described earlier.

The algorithm optimizes the location and density of RWIS stations in an iterative process where stations are added one by one into the study area and locations are selected based on heuristic attempts to minimize the objective function. The total number of RWIS stations allowed was arbitrarily limited to 100 in this study to ensure the variation trend of the estimation error as density changes were fully displayed. The number of iterations was set to 5,000, after which the search process for new RWIS station locations was set to stop. Prediction errors were normalized to make a valid and fair comparison among zonal classes.

According to the density optimization results, as shown in Figure 19, topographic and weather severity classes with larger spatial ranges required a lower number of RWIS stations, except WSI-3, which shows a similar trend to WSI-1.

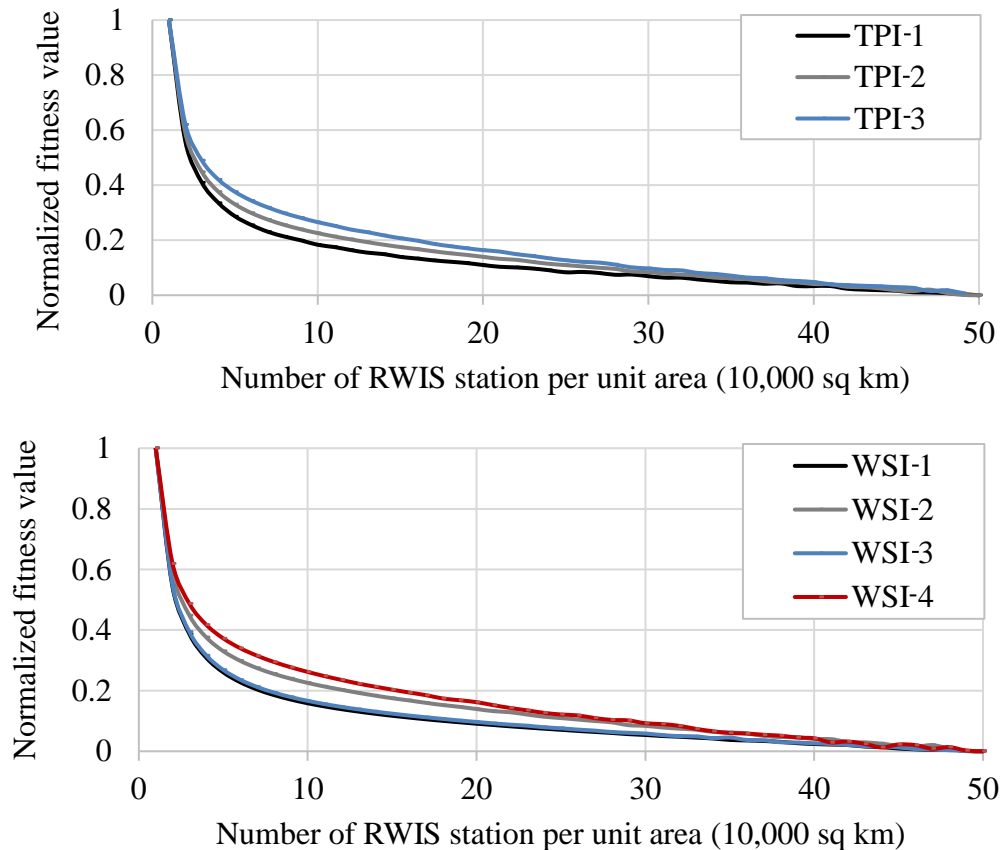


Figure 19. Normalized prediction error as a function of RWIS density for TPI classes (top) and WSI classes (bottom)

From the results shown above, TPI classes follow the same behavioral trend: WSI-3 consists mainly of northern parts of Minnesota, classified as flatland area (TPI-1) and found to have a

lower density of RWIS based on topographic analyses. In addition, the team's density optimization was conducted using all three semivariogram parameters (range, nugget, and sill), though the dependency of the semivariogram range upon topographic-weather characteristics of the region was the team's main concern in this analysis. From this, it can be stated that topographic measures (TPI) provided a more intuitive and direct relationship with the impact than the spatiotemporal range had on optimal density.

The number of RWIS stations needed for 0.1 unit increment of benefit was calculated from Figure 19 and is presented in Figure 20.

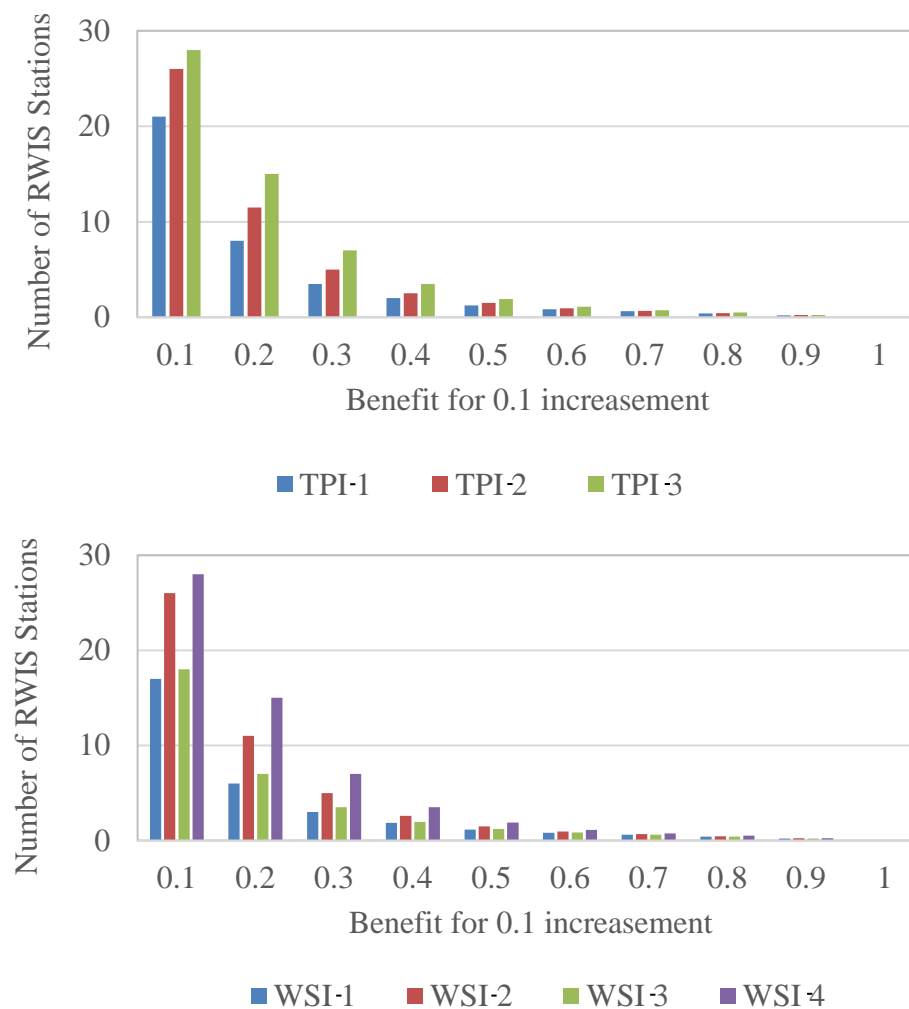


Figure 20. Number of RWIS stations for benefit increment of 0.1 unit for TPI classes (top) and WSI classes (bottom)

According to Figure 20, the initial 0.1 unit of incremental benefit requires the highest number of RWIS stations with each subsequent incremental benefit requiring fewer and fewer additional stations. This is as expected because the amount of marginal benefit from additional RWIS

stations should decrease as station numbers increase. A similar trend is observed for both TPI and WSI classes.

For determining the optimal RWIS density, marginal benefits were calculated from Figure 19 and are presented in Figure 21.

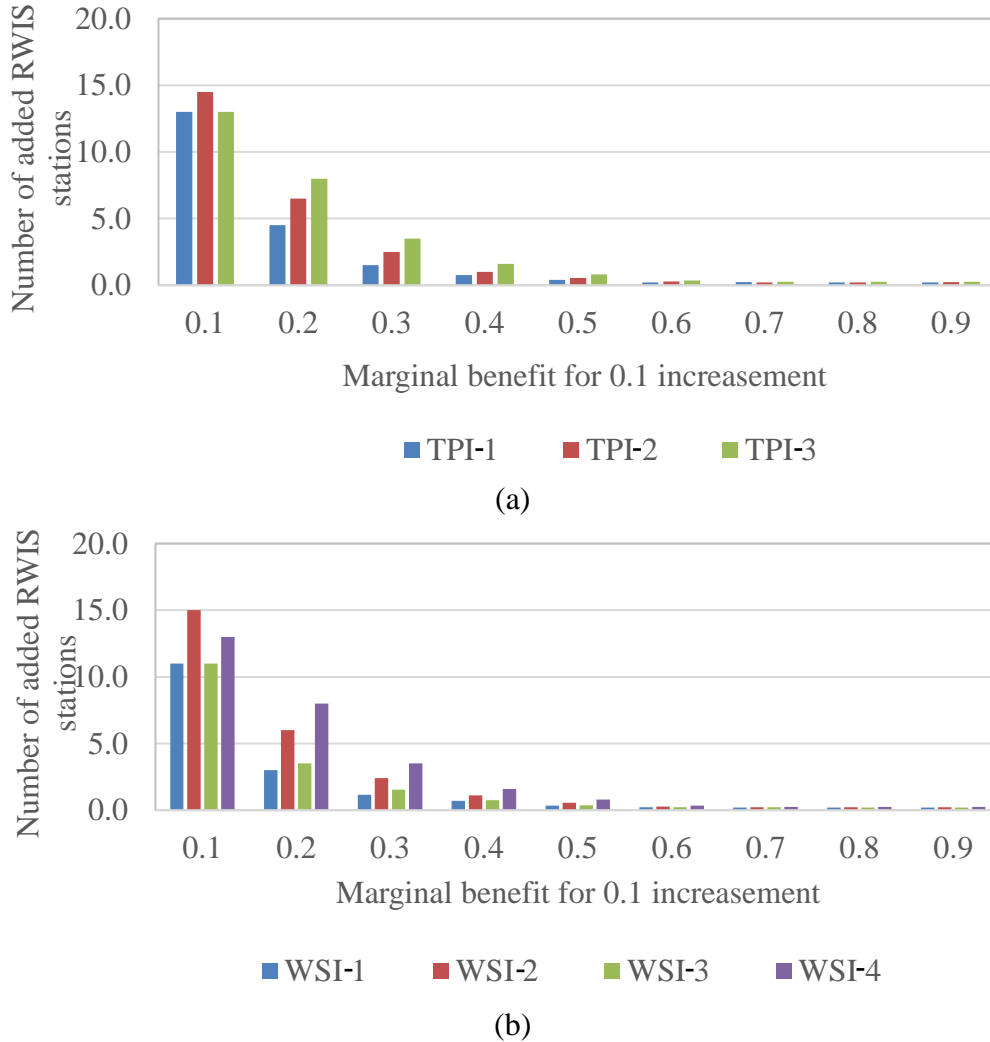


Figure 21. Added number of RWIS stations for marginal benefit increment of 0.1 unit for (a) TPI classes and (b) WSI classes

According to Figure 21, the number of added RWIS stations for an initial marginal incremental benefit of 0.1 unit is the highest and then the number of additional stations decreases for further increments of marginal benefits for both TPI and WSI classes.

As shown in Figure 20 and Figure 21, the marginal benefit decreases significantly after the 0.3 unit increment of benefit mark. This was determined as the median of the range and number of associated RWIS stations for 0.3 unit increment of benefit increase was defined as the optimal

RWIS density. The number of RWIS stations needed for an incremental benefit of 0.2 unit and 0.4 unit were selected as the upper and lower bound, respectively. The number of RWIS stations needed for 0.2, 0.3, and 0.4 unit benefit increment was recorded from Figure 20 and is plotted in Figure 22.

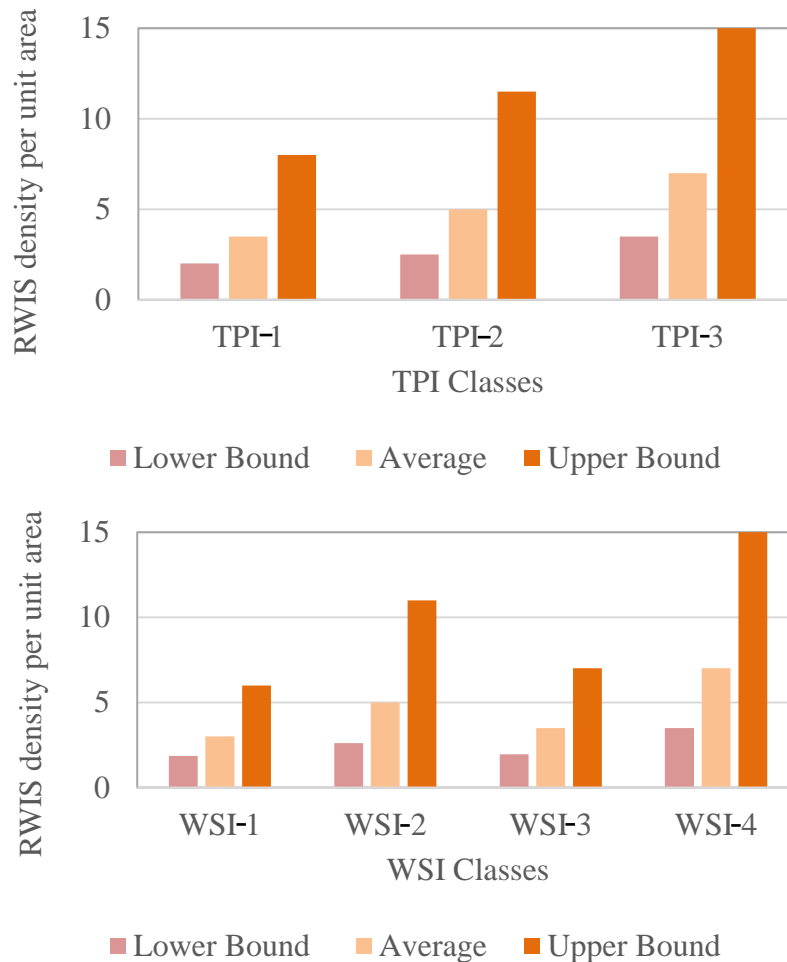


Figure 22. RWIS density comparison for TPI classes (top) and WSI classes (bottom)

As shown, RWIS density is the lowest for TPI-1 and increases with an increase in topographic variation. Similarly, RWIS station numbers for less weather severe regions are the lowest and increase with an increase in weather severity, except WSI-3 for the above noted reasons.

The density optimization results were used to generate an RWIS density chart for TPI-WSI zones and is presented in Table 2.

Table 2. RWIS density for TPI-WSI zones for unit area (1/10000 km²)

RWIS density for unit area		TPI classes								
		TPI-1			TPI-2			TPI-3		
		LB	Avg	UB	LB	Avg	UB	LB	Avg	UB
WSI classes	WSI-1	1.93	3.25	7.00	2.18	4.00	8.75	2.68	5.00	10.50
	WSI-2	2.30	4.25	9.50	2.55	5.00	11.25	3.05	6.00	13.00
	WSI-3	1.98	3.50	7.50	2.23	4.25	9.25	2.73	5.25	11.00
	WSI-4	2.75	5.25	11.50	3.00	6.00	13.25	3.50	7.00	15.00

On average, three to seven RWIS stations are required for a unit area of 10,000 km² depending on the topographic feature of the landform and weather severity of the region. Such findings can readily be used by winter road maintenance agencies for planning a region-wide RWIS network, especially for regions with limited or no available RWIS stations.

Statewide RWIS Density Determination

The optimal RWIS density was determined for each of the 14 states using Table 2. The optimal RWIS density map is presented in Figure 23.

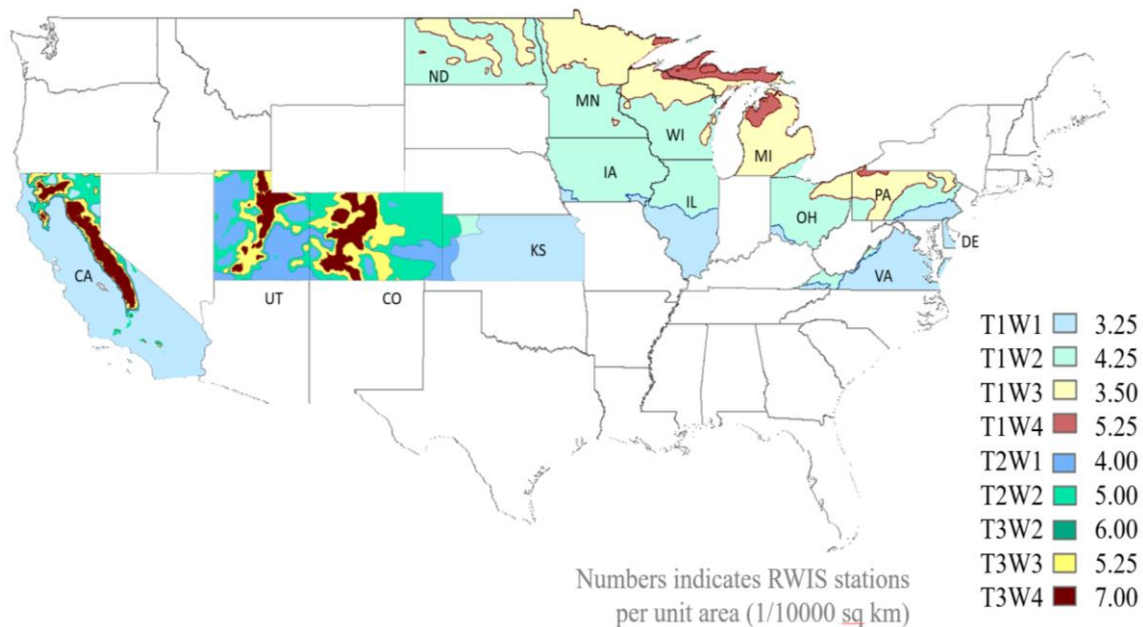


Figure 23. Optimal RWIS density map

Nine different TPI-WSI combined zones were identified in the study area. The flatland area (TPI-1 zone) includes four different weather severity zones named as T1W1, T1W2, T1W3, and T1W4 (lighter colored blue area in Figure 23). Weather severity increases from the southern to the northern parts of the study area. The optimal RWIS density in these regions varies from 3.25 to 5.25 stations per unit area (1/10000 km²). The TPI-2 zone, which are hilly areas, combines

two different types of weather severity zones in the study area and were named as T2W1 and T2W2. These areas include a smaller parts of Colorado, Kansas, and Utah. Four to five RWIS stations are needed per unit area in these zones. Mountainous areas (TPI-3 zone) include three different types of weather severity zones named as T3W2, T3W3, and T3W4. Very small areas of California, Colorado, and Utah are under the T3W2 and T3W3 zones. Most of the mountainous areas are under extremely high severe weather regions.

The area under each TPI-WSI zone was calculated to determine the optimal RWIS density for each state. Table 3 presents the suggested RWIS densities for the 14 states in the study area.

Table 3. Suggested RWIS density for the 14 states

States	CA	CO	DE	IA	IL	KS	MI	MN	ND	OH	PA	UT	VA	WI
RWIS density	198	156	2	61	54	73	61	86	75	45	46	127	37	58

The findings from the density analyses showed that the number of RWIS stations needed for adequate monitoring coverage of mountainous regions with highly varied climates (i.e., California, Colorado, and Utah) are relatively higher than regions that are relatively flat and experience less varied weather. This makes intuitive sense since highly varied regions in terms of weather and topography would typically require more frequent monitoring of road weather and surface conditions during inclement weather events to provide timely and cost-efficient winter road maintenance operations. A suggested RWIS density for Delaware was found to be the lowest for having the smallest area with relatively less-varying weather and topographic conditions.

The values provided are for reference only and further investigation may be warranted to determine optimal densities based on different weighting schemes (i.e., traffic versus weather) and budgetary constraints since the more RWIS stations there are, the better coverage they will provide.

5. CONCLUSION AND RECOMMENDATIONS

Winter road maintenance is one of the most critical activities for transportation agencies, especially for cold-region countries. The significant and critical information needed for making winter road maintenance decisions is related to road condition and weather data, which are often collected, processed, and transmitted by RWIS. Effective and efficient planning of RWIS networks is a must and needed for maximizing the monitoring coverage and benefit of RWIS. The effectiveness of an RWIS network depends on its density and spatial distribution.

In this study, the research team investigated the representativeness of RWIS measurements in two analysis domains: space and time. Spatial and temporal continuity of the variable of interest, RST, was investigated using geostatistical spatiotemporal semivariogram analysis and compared to different topographic and weather regions. Lastly, optimal RWIS density for three TPI and four WSI zones were estimated from the density optimization output. The key findings of this study are as follows:

- A spatiotemporal analysis concluded strong dependency of spatial and temporal autocorrelation ranges of RWIS measurements with TPI and WSI values from their associated regions. The zone with the highest topographic variation (TPI-3, mountainous region) had a shorter range of spatiotemporal structure, whereas zones with lower TPI values (TPI-1, flatland region) had a higher range. Similarly, areas with less severe weather tended to have a higher spatial range (e.g., WSI-1), whereas areas with more severe weather had a lower range in spatial autocorrelation.
- The RWIS location allocation framework was extended to account for both spatial and temporal attributes of road weather conditions and provided more complete and conclusive location solutions. In addition, the framework reestablished in this work provides an important basis for strategically locating regional RWIS stations, which are optimal in collecting measurements over space and time.
- A series of RWIS density curves were generated and an optimal RWIS chart was created for the first time in literature, providing a decision-support tool to transportation authorities that need to plan an RWIS network without having road weather and surface condition data.
- The desired RWIS density shows a strong dependency on topography and weather characteristics of the region under investigation. Higher RWIS density is required for regions with high topographic variation and high incidence of severe weather, while lower RWIS density is needed for less varied topographic regions with less incidence of severe weather to achieve similar levels of monitoring coverage.
- The solutions developed in this project were integrated into LoRWIS (www.lorwis.com), a prototype web-based RWIS location visualization platform for demonstrating the proposed models and the resulting solutions.

Recommendations for further research on this subject are as follows:

- The geographic study area included in this project consisted largely flatlands, with few hilly and mountainous regions due to data availability issues. Hence, more case studies consisting of wider geographic regions should be conducted for a better understanding of the relationship between spatial range of autocorrelation in RST and the topographic and weather features to develop a more robust quantitative relation between these parameters.
- The study period of this project was limited to one winter season including six months from October 2016 to March 2017. Thus, larger temporal ranges could be considered to improve the level of confidence in the outcomes.
- Universal kriging or kriging with external drift could be applied considering meteorological parameters (wind speed and direction, precipitation, humidity, cloud cover, vegetation cover, etc.) to better capture the dependency of RST data (or other key parameters, including road surface condition index) on local meteorological parameters.
- Lastly, a sensitivity analysis could be conducted to investigate how the resulting optimal densities would change with respect to some of the factors considered in the analysis, especially those coefficients used to generate WSI (or even a winter severity index model) and TPI classification schemes.

REFERENCES

- Ahmed, S. O., R. Mazloun, and H. Abou-Ali. 2018. Spatiotemporal Interpolation of Air Pollutants in the Greater Cairo and the Delta, Egypt. *Environmental Research*, Vol. 160, pp. 27–34.
- Ahrens, C. D. 2009. *Meteorology Today: An Introduction to Weather, Climate, and the Environment*. Brooks/Cole, Cengage Learning, Inc., Belmont, CA.
- Andrey, J. C., B. Mills, and J. Vandermolen. 2001. *Weather Information and Road Safety*. Institute for Catastrophic Loss Reduction (ICLR), Toronto, Ontario, Canada.
- Bohling, G. 2005. *Introduction to Geostatistics and Variogram Analysis*. Kansas Geological Survey, University of Kansas, Lawrence, KS.
- Boselly, S. E., G. S. Doore, J. E. Thornes, C. Ulbery, and D. D. Ernst. 1993. *SHRP-H-350: Road Weather Information Systems Volume 1: Research Report*. Strategic Highway Research Program, Washington, DC.
- Brus, D. J. and G. B. M. Heuvelink. 2007. Optimization of Sample Patterns for Universal Kriging of Environmental Variables. *Geoderma*, Vol. 138, No. 1–2, pp. 86–95.
- Chapman, L. and J. E. Thornes. 2005. The Influence of Traffic on Road Surface Temperatures: Implications for Thermal Mapping Studies. *Meteorological Applications*, Vol. 12, pp. 371–380.
- Chen, F., S. Chen, and G. Peng. 2012. Using Sequential Gaussian Simulation to Assess Geochemical Anomaly Areas of Lead Element. *International Conference on Computer and Computing Technologies in Agriculture*, Vol. 393, pp. 69–76.
- Eberhart, R. C. and Y. Shi. 2001. Particle Swarm Optimization: Developments, Applications, and Resources. *Proceedings of the 2001 Congress on Evolutionary Computation*, May 27–30, Seoul, South Korea, Vol. 1, pp. 81–86.
- Eriksson, M. and J. Norrman. 2001. Analysis of Station Locations in a Road Weather Information System. *Meteorological Applications*, Vol. 8, No. 4, pp. 437–448.
- Flatman, G. T., E. J. Englund, and A. A. Yfantis. 1988. Geostatistical Approaches to the Design of Sampling Regimes. In *Principles of Environmental Sampling: ACS Professional Reference Book*. American Chemical Society, Washington, DC. pp. 73–84.
- Gething, P. W., P. M. Atkinson, A. M. Noor, P. W. Gikandi, S. I. Hay, and M. S. Nixon. 2007. A Local Space–Time Kriging Approach Applied to a National Outpatient Malaria Data Set. *Computers & Geosciences*, Vol. 33, No. 10, pp. 1337–1350.
- Gräler, B., E. Pebesma, and G. Heuvelink. 2016. Spatio-Temporal Interpolation Using Gstat. *R Journal*, Vol. 8, No. 1, pp. 204–218.
- Gu, L., M. Wu, and T. J. Kwon. 2019. An Enhanced Spatial Statistical Method for Continuous Monitoring of Winter Road Surface Conditions. *Canadian Journal of Civil Engineering*, Vol. 0, No. ja.
- Gustavsson, T. 1990. Variation in Road Surface Temperature Due to Topography and Wind. *Theoretical and Applied Climatology*, Vol. 41, No. 4, pp. 227–236.
- Hastie, T. J. and R. J. Tibshirani. 1990. 43 Generalized Additive Models. In *Monographs on Statistics and Applied Probability*. Chapman & Hall/CRC, Boca Raton, FL.
- Heuvelink, G. B., D. J. Brus, and J. J. de Gruijter. 2006. Chapter 11 Optimization of Sample Configurations for Digital Mapping of Soil Properties with Universal Kriging. *Developments in Soil Science*, Vol. 31, pp. 137–151.

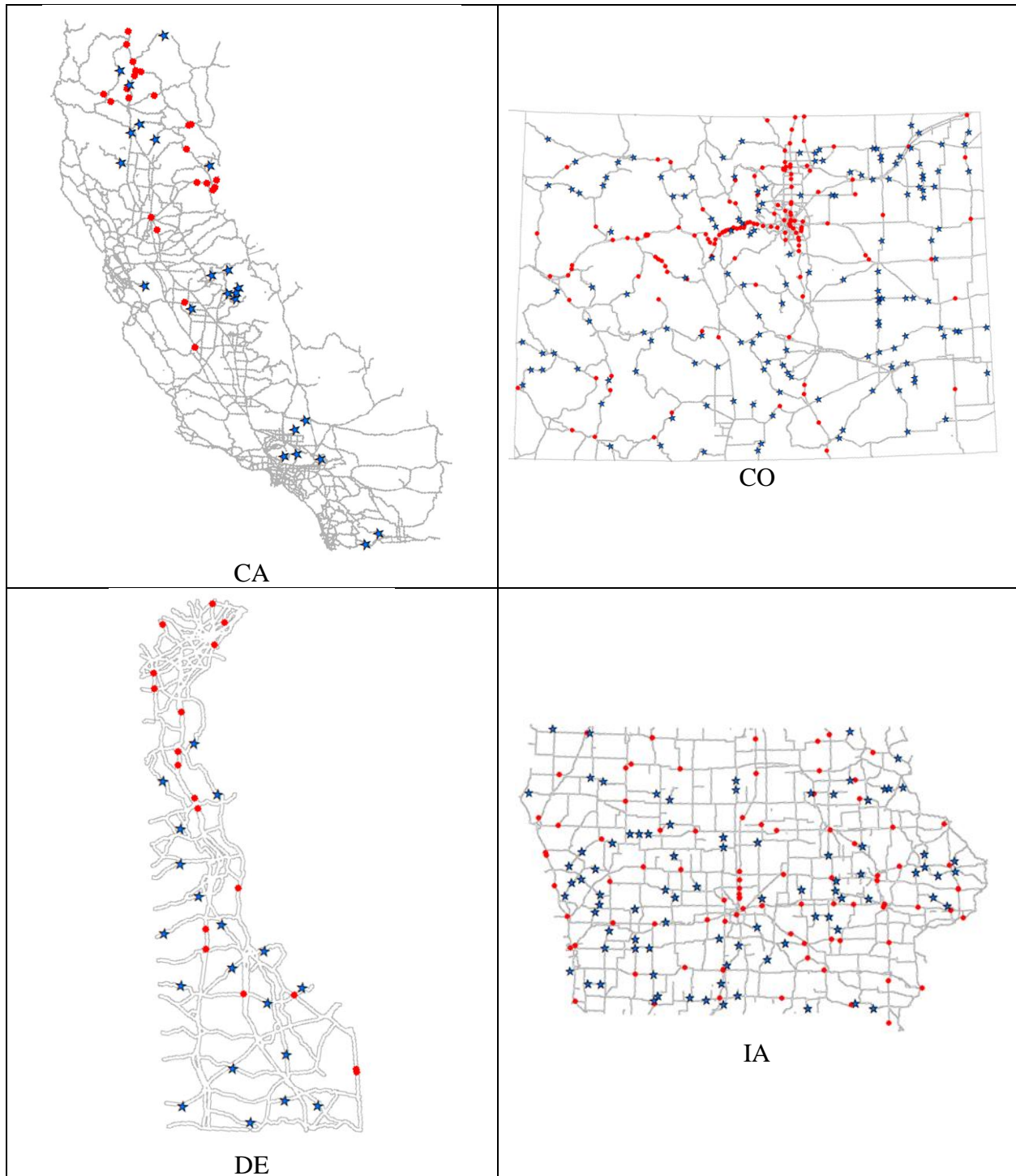
- Hu, D., H. Shu, H. Hu, and J. Xu. 2017. Spatiotemporal Regression Kriging to Predict Precipitation Using Time-Series MODIS Data. *Cluster Computing*, Vol. 20, No. 1, pp. 347–357.
- Jenness, J. 2006. *Topographic Position Index (TPI) v. 1.2*. Jenness Enterprises, Flagstaff, AZ.
- Jin, P. J., A. Walker, M. Cebelak, and C. M. Walton. 2014. Determining Strategic Locations for Environmental Sensor Stations with Weather-Related Crash Data. *Transportation Research Record: Journal of the Transportation Research Board*, No. 2440, pp. 34–42.
- Kennedy, J. and R. Eberhart. 1995. Particle Swarm Optimization. *Proceedings of International Conference on Neural Networks*, pp. 1942–1948.
- Kennedy, J. and R. C. Eberhart. 1997. A Discrete Binary Version of the Particles Swarm Algorithm. *Proceedings of Conference on Systems, Man, and Cybernetics*, pp. 4104–4108.
- Kwon, T. J. and L. Fu. 2013. Evaluation of Alternative Criteria for Determining the Optimal Location of RWIS Stations. *Journal of Modern Transportation*, Vol. 21, No. 1, pp. 17–27.
- Kwon, T. J. and L. Fu. 2016. *RWIS Network Planning: Optimal Density and Location*. Aurora Program, Institute for Transportation, Iowa State University, Ames, IA.
https://intrans.iastate.edu/app/uploads/2018/10/RWIS_network_planning_for_optimal_density_and_location_w_cvr.pdf.
- Kwon, T. J. and L. Fu. 2017. Spatiotemporal Variability of Road Weather Conditions and Optimal RWIS Density—An Empirical Investigation. *Canadian Journal of Civil Engineering*, Vol. 44, No. 9, pp. 691–699.
- Kwon, T. J., L. Fu, and S. J. Melles. 2017. Location Optimization of Road Weather Information System (RWIS) Network Considering the Needs of Winter Road Maintenance and the Traveling Public. *Computer-Aided Civil and Infrastructure Engineering*, Vol. 32, No. 1, pp. 57–71.
- Kirkpatrick, S., C. D. Gelatt Jr., and M. P. Vecchi. 1983. Optimization by Simulated Annealing. *Science*, Vol. 220, No. 4598, pp. 671–680.
- Li, L., J. Zhang, W. Qiu, J. Wang, and Y. Fang. 2017. An Ensemble Spatiotemporal Model for Predicting PM_{2.5} Concentrations. *International Journal of Environmental Research and Public Health*, Vol. 14, No. 5, 549.
- Lichtenstern, A. 2013. Kriging Methods in Spatial Statistics. Bachelor's thesis, Technical University of Munich, München, Germany.
- Manfredi, J., T. Walters, G. Wilke, L. Osborne, R. Hart, T. Incrocci, and T. Schmitt. 2005. *Road Weather Information System Environmental Sensor Station Siting Guide*. FHWA-HOP-05-026. Federal Highway Administration, Washington, DC.
- Manfredi, J., T. Walters, G. Wilke, L. Osborne, R. Hart, T. Incrocci, T. Schmitt, V. K. Garrett, B. Boyce, and D. Krechmer. 2008. *Road Weather Information System Environmental Sensor Station Siting Guidelines, Version 2.0*. FHWA-JPO-09-012. Federal Highway Administration, Washington, DC.
- Matthews, L., J. Andrey, I. Minokhin, and M. Perchanok. 2017a. Operational Winter Severity Indices in Canada – From Concept to Practice. 96th Annual Meeting of the Transportation Research Board, January 8–12, Washington, DC.
- Matthews, L., J. Andrey, D. Hambly, and I. Minokhin. 2017b. Development of a Flexible Winter Severity Index for Snow and Ice Control. *Journal of Cold Regions Engineering*, Vol. 31, No. 3, pp. 04017005-1–14.

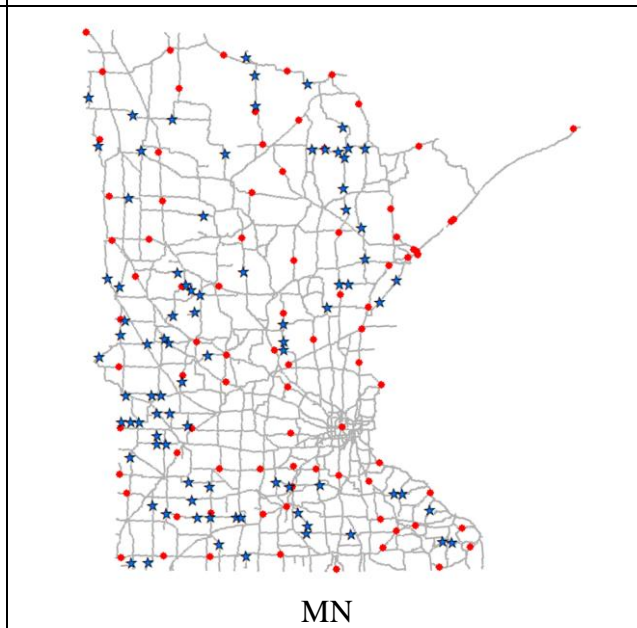
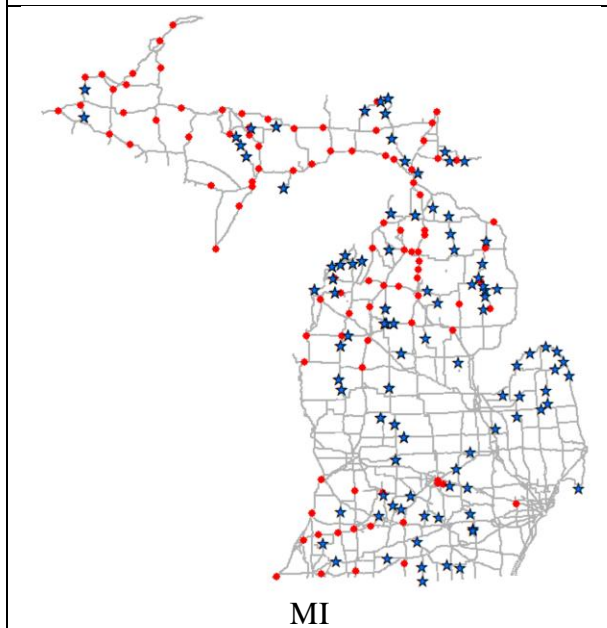
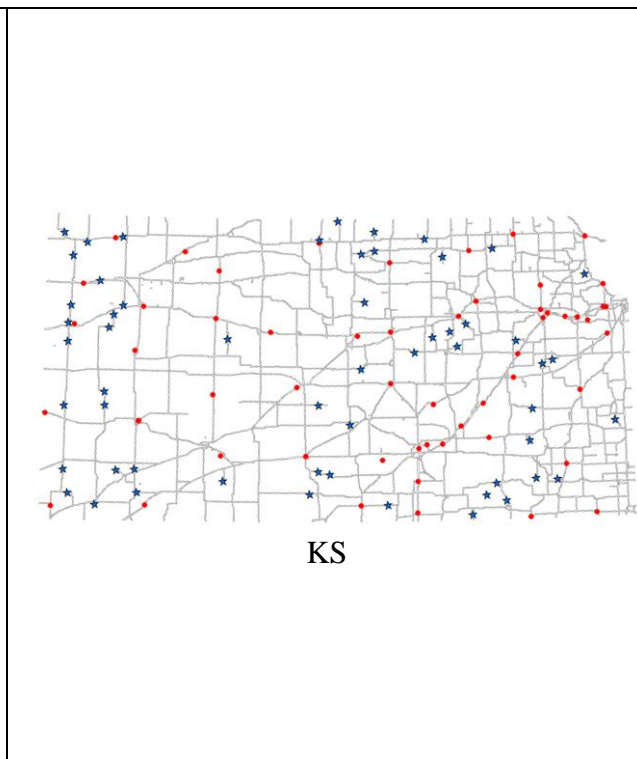
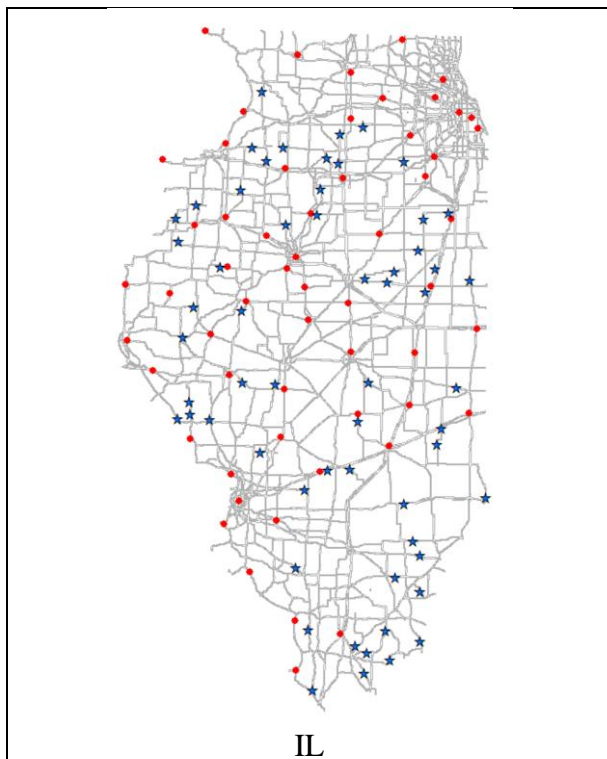
- Mewes, J. J. 2012. *Mapping Weather Severity Zones*. Clear Roads Pooled Fund Study, St. Paul, MN.
- Mokarram, M., G. Roshan, and S. Negahban. 2015. Landform Classification using Topography Position Index (Case Study: Salt Dome of Korsa-Darab Plain, Iran). *Modeling Earth Systems and Environment*, Vol. 1, No. 40.
- Olea, R. A. 1999. *Geostatistics for Engineers and Earth Scientists*. Springer-Science+Business Media, LLC, New York, NY.
- Olea, R. A. 2006. A Six-Step Practical Approach to Semivariogram Modeling. *Stochastic Environmental Research and Risk Assessment*, Vol. 20, No. 5, pp. 307–318.
- Pebesma, E. J. 2004. Multivariable Geostatistics in S: the Gstat Package. *Computers & Geosciences*, Vol. 30, pp. 683–691.
- Pebesma, E. and B. Gräler. 2012. *Spatial and Spatio-Temporal Geostatistical Modelling, Prediction, and Simulation*.
- Pebesma, E., B. Gräler, and M. E. Pebesma. 2019. *Package ‘Gstat’*
- Poli, R., J. Kennedy, and T. Blackwell. 2007. Particle Swarm Optimization. *Swarm Intelligence*, Vol. 1, No. 1, pp. 33–57.
- R Core Team. 2018. *R: A Language and Environment for Statistical Computing*. R Foundation for Statistical Computing, Vienna, Austria. <https://www.R-project.org/>.
- RESSTE Network. 2017. Analyzing Spatio-Temporal Data with R: Everything You Always Wanted to Know – But Were Afraid to Ask. Submitted to *Journal de la Société Française de Statistique*, Vol. 158, No. 3, pp. 124–158.
- Revelle, C. S., H. A. Eiselt, and M. S. Daskin. 2008. A Bibliography for Some Fundamental Problem Categories in Discrete Location Science. *European Journal of Operational Research*, Vol. 184, No. 3, pp. 817–848.
- Sato, N., J. E. Thornes, T. Maruyama, A. Sugimura, and T. Yamada. 2004. Road Surface Temperature Forecasting: Case Study in a Mountainous Region of Japan. Sixth International Symposium on Snow Removal and Ice Control Technology, June 7–9, Spokane, WA.
- Seif, A. 2014a. Using Topography Position Index for Landform Classification (Case Study: Grain Mountain). *Bulletin of Environment, Pharmacology, and Life Sciences*, Vol. 3, No. 11, pp. 33–39.
- Seif, A. 2014b. Landform Classification by Slope Position Classes. *Bulletin of Environment, Pharmacology, and Life Sciences*, Vol. 3, No. 11, pp. 62–69.
- Shekhar, S. and H. Xiong, editors. 2008. *Encyclopedia of GIS*. Springer, Boston, MA.
- Solana-Gutiérrez, J. and S. Merino-de-Miguel. 2011. A Variogram Model Comparison for Predicting Forest Changes. *Procedia Environmental Sciences*, Vol. 7, pp. 383–388.
- van Groenigen, J. W. and A. Stein. 1998. Constrained Optimization of Spatial Sampling using Continuous Simulated Annealing. *Journal of Environmental Quality*, Vol. 27, pp. 1078–1086.
- van Groenigen, J. W., W. Siderius, and A. Stein. 1999. Constrained Optimization of Soil Sampling for Minimisation of the Kriging Variance. *Geoderma*, Vol. 87, No. 3–4, pp. 239–259.
- Wang, H., H. Sun, C. Li, S. Rahnamayan, and J-S. Pan. 2013. Diversity Enhanced Particle Swarm Optimization with Neighborhood Search. *Information Sciences*, Vol. 223, pp. 119–135.

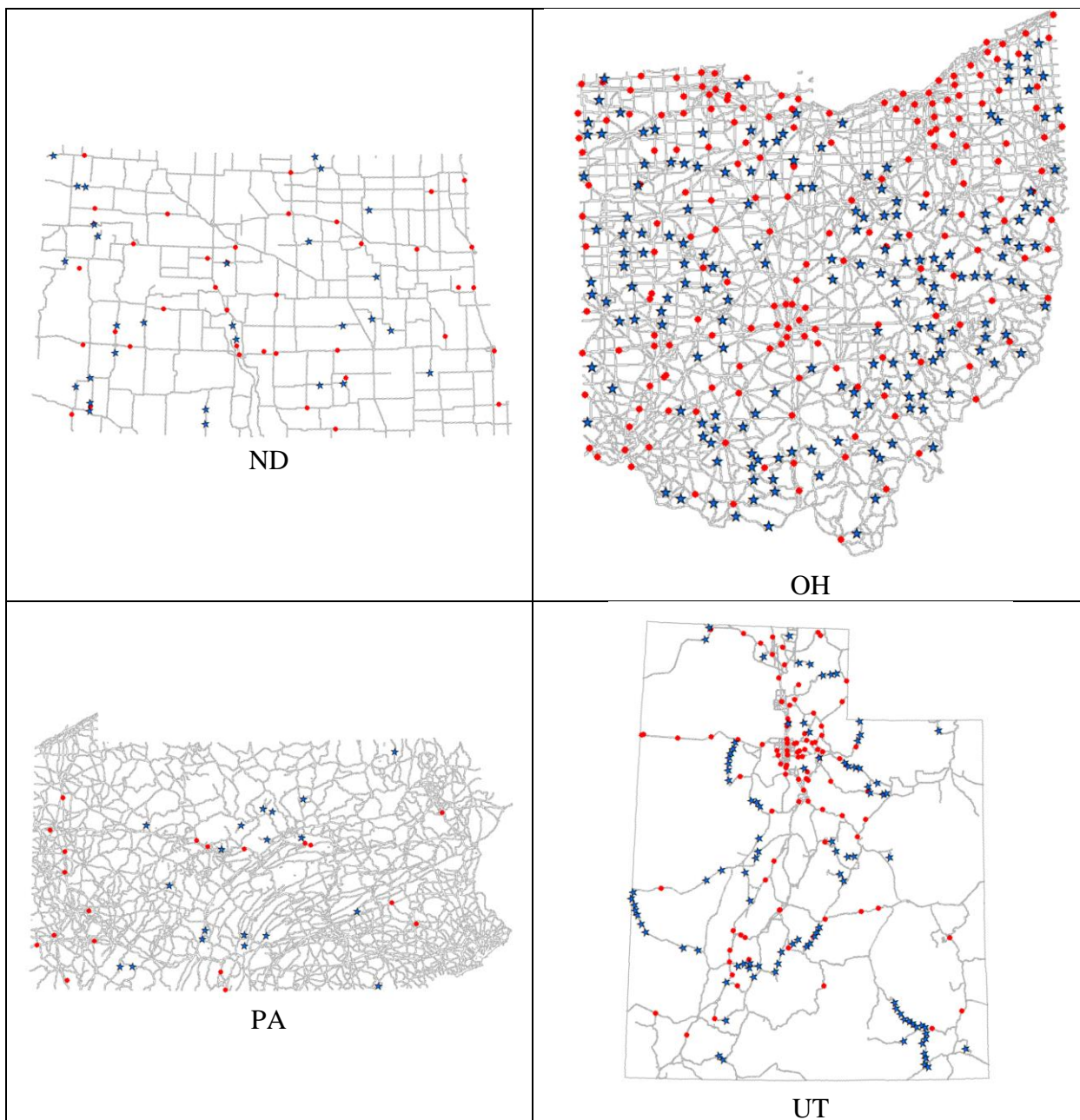
- Wang, X., L. Gu, T. J. Kwon, and T. Z. Qiu. 2019. Determining the Spatiotemporal Coverage of Road Weather Information Systems – A Case Study in Alberta, Canada. 98th Annual Meeting of the Transportation Research Board, January 13–17, Washington, DC.
- Weiss, A. D. 2001. Topographic Positions and Landforms Analysis. Conference poster. Esri International User Conference, July 9–13, San Diego, CA.
- White, S. P., J. E. Thornes, and L. Chapman. 2006. *A Guide to Road Weather Information Systems: Version 2*. Standing International Road Weather Commission (SIRWEC).

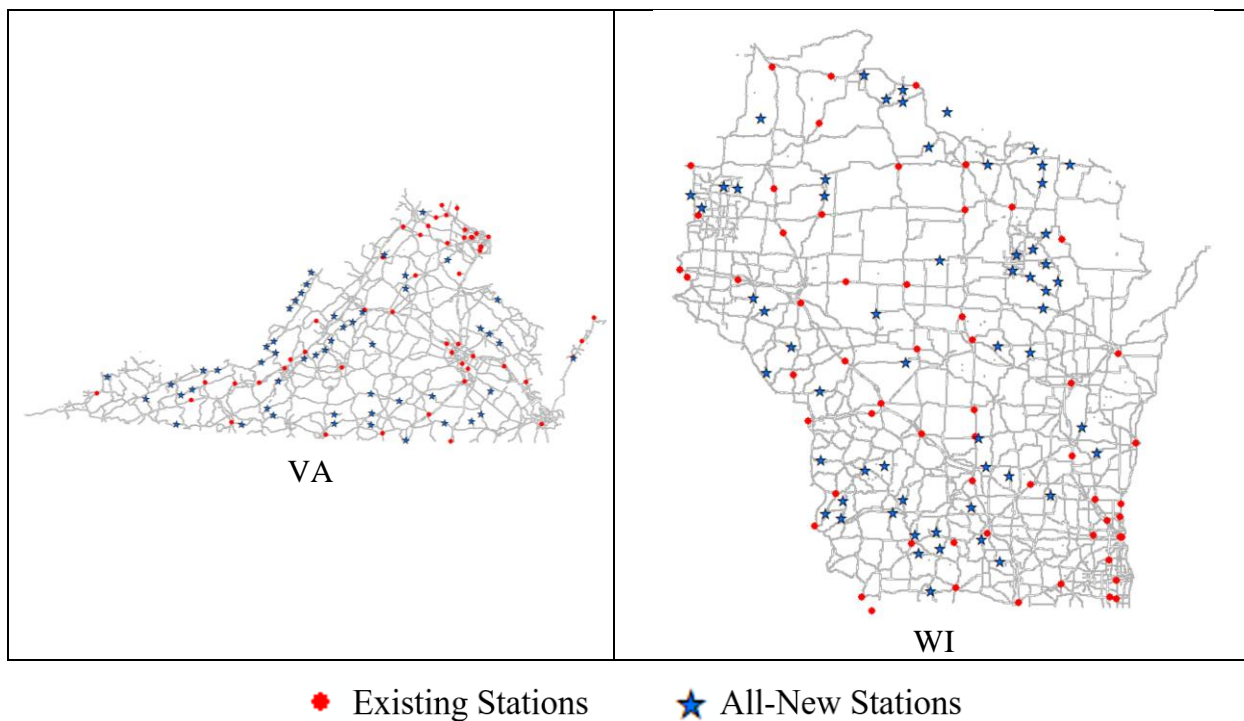
APPENDIX A. PLOTS OF EXISTING AND OPTIMIZED RWIS LOCATIONS FOR THE ALL-NEW STRATEGY

In the figure, the current location of the existing stations are shown in red, and the optimal new locations are shown in blue.









APPENDIX B. LOCATIONS OF THE ALL-NEW OPTIMIZED RWIS NETWORK

Note that in the following tables the new locations for the existing RWIS network were generated using dual criteria (considering both weather and traffic data), and the locations are given by longitude and latitude.

Table B.1. Optimized new locations for RWIS stations in California

Station #	Long.	Lat.	Station #	Long.	Lat.	Station #	Long.	Lat.
1	-117.28	34.26	9	-120.22	39.67	17	-122.22	40.12
2	-121.51	37.34	10	-119.57	37.31	18	-121.61	40.05
3	-122.67	41.25	11	-122.41	41.01	19	-117.87	34.81
4	-122.02	40.31	12	-118.11	34.31	20	-120.39	36.97
5	-122.36	39.55	13	-117.64	35	21	-115.96	32.87
6	-116.25	32.66	14	-119.38	37.21	22	-117.83	34.34
7	-119.31	37.43	15	-121.71	42.01	23	-119.6	37.75
8	-119.98	37.63	16	-119.37	37.33			

Table B.2. Optimized new locations for RWIS stations in Colorado

Station #	Long.	Lat.	Station #	Long.	Lat.	Station #	Long.	Lat.
1	-106.44	38.13	50	-103.31	40.52	99	-105.55	39.67
2	-107.8	37.66	51	-102.96	40.29	100	-105.71	39.04
3	-105.19	37.79	52	-105.74	40.71	101	-105.08	38.28
4	-103.12	40.88	53	-106.13	39.72	102	-106.58	39.13
5	-107.67	37.17	54	-104.31	40.08	103	-105.78	39.81
6	-102.5	38.44	55	-103.6	40.53	104	-107.84	40.18
7	-102.66	40.64	56	-103.14	40.61	105	-103.71	38.23
8	-108.26	40.44	57	-103.48	38.27	106	-104.55	40.62
9	-104.08	40.35	58	-105.61	39.63	107	-104.37	40.08
10	-108.31	40.13	59	-104.34	37.24	108	-103.01	40.42
11	-104.28	37.33	60	-105.89	39.68	109	-103.7	38.59
12	-102.95	38.8	61	-104.49	40.48	110	-106.03	40.53
13	-102.97	40.11	62	-106.77	37.5	111	-105.42	38.05
14	-106.49	40.3	63	-102.96	40.24	112	-105.08	39.04
15	-103.31	38.09	64	-107.08	38.39	113	-103.66	40.61
16	-107.62	40.46	65	-102.23	40.77	114	-106.19	39.81
17	-103.49	40.25	66	-108.69	40.7	115	-108.49	38.95
18	-106.27	37.64	67	-104.73	39.18	116	-105.02	37.96
19	-105.14	38.1	68	-102.97	40.02	117	-103.87	38.18
20	-105.87	37.69	69	-103.18	38.85	118	-105.49	40.13
21	-102.79	40.15	70	-106.1	38.09	119	-102.75	39.65

Station #	Long.	Lat.	Station #	Long.	Lat.	Station #	Long.	Lat.
22	-102.56	38.44	71	-104.61	40.58	120	-108.19	40.08
23	-103.2	37.86	72	-106.34	38.45	121	-107.79	40.27
24	-104.84	40.08	73	-108.66	38.04	122	-103.62	39.53
25	-105.14	38.82	74	-105.58	38.37	123	-106.6	40.07
26	-106.85	38.54	75	-104.61	40.48	124	-103.2	37.91
27	-103.7	38.54	76	-103.9	40.3	125	-105.48	37.19
28	-103.7	38.86	77	-106.18	39.36	126	-102.1	38.47
29	-105.01	39.4	78	-103.37	40.43	127	-107.69	37.93
30	-108.67	38.22	79	-103.83	37.78	128	-108.5	38.23
31	-102.3	40.63	80	-105.43	39.99	129	-102.79	38.48
32	-103.43	37.77	81	-102.73	38.39	130	-103.01	40.79
33	-103.69	39.18	82	-107.38	40.51	131	-105.59	37.65
34	-108.84	38.03	83	-102.76	37.41	132	-105.49	38.68
35	-105.53	37.11	84	-103.53	38.05	133	-108	38.6
36	-107.7	39.65	85	-103.7	38.95	134	-108.97	38.35
37	-106.96	40.29	86	-102.72	40.33	135	-105.85	40.3
38	-107.3	38.04	87	-103.29	38.85	136	-103.64	38.86
39	-105.94	39.17	88	-103.72	40.61	137	-107.19	38.48
40	-108.16	38.06	89	-108.66	40.16	138	-102.12	37.93
41	-103.6	40.48	90	-104.21	39.09	139	-103.03	40.15
42	-105.07	38.01	91	-102.25	40.32	140	-103.33	37.28
43	-105.49	39.9	92	-106.31	37.1	141	-102.82	39.3
44	-102.87	39.52	93	-105.72	39.76	142	-103.73	40.26
45	-105.36	38.15	94	-103.21	40.07	143	-105.48	38.46
46	-103.3	38.4	95	-105.76	38.37	144	-107.45	38.93
47	-106.94	37.18	96	-104.63	37.69	145	-107.97	39
48	-105.3	37.52	97	-106.78	40.07	146	-105.38	40.17
49	-104.84	40.58	98	-108.94	37.85	147	-103.7	38.81

Table B.3. Optimized new locations for RWIS stations in Delaware

Station #	Long.	Lat.	Station #	Long.	Lat.	Station #	Long.	Lat.
1	-75.65	39.15	8	-75.24	38.82	15	-75.64	38.51
2	-75.59	39.06	9	-75.3	38.53	16	-75.36	38.78
3	-75.42	38.47	10	-75.19	38.52	17	-75.61	39.46
4	-75.71	39.37	11	-75.48	38.88	18	-75.71	38.97
5	-75.65	38.83	12	-75.3	38.65	19	-75.37	38.92
6	-75.47	38.61	13	-75.65	39.24			
7	-75.53	39.33	14	-75.51	38.99			

Table B.4. Optimized new locations for RWIS stations in Iowa

Station #	Long.	Lat.	Station #	Long.	Lat.	Station #	Long.	Lat.
1	-91.02	42.19	30	-94.96	42.42	59	-93.74	41.08
2	-93.58	41.29	31	-93.82	40.89	60	-95.49	41.69
3	-90.84	41.96	32	-93.27	41.76	61	-95.32	42.32
4	-94.58	41.52	33	-93.62	42.88	62	-95.65	42.99
5	-92.72	41.85	34	-91.35	43.19	63	-93.32	42.34
6	-95.54	41.61	35	-93.79	42.3	64	-93.62	42.97
7	-94.16	41.89	36	-93.33	41.47	65	-95.96	41.77
8	-92.17	41.76	37	-95.08	42.42	66	-95.61	40.87
9	-92.35	41.57	38	-91.54	42.88	67	-95.86	41
10	-94.47	42.2	39	-96.19	43.47	68	-95.48	41.78
11	-90.6	42.01	40	-92.25	41.84	69	-95.87	41.9
12	-93.8	42.39	41	-90.61	42.11	70	-92.01	43.47
13	-94.45	41.78	42	-95.91	42.08	71	-94.53	42.52
14	-92.53	41.58	43	-91.87	42.29	72	-91.02	42.06
15	-92.95	41.31	44	-95.74	42.23	73	-91.78	42.76
16	-95	41.65	45	-95.34	41.42	74	-93.19	41.14
17	-94.67	40.76	46	-94.72	40.71	75	-92.03	42.97
18	-92.65	40.63	47	-95.44	40.87	76	-90.72	41.65
19	-93.85	41.35	48	-92.24	41.94	77	-94.24	40.75
20	-94.72	42.83	49	-94.54	42.77	78	-94.58	41.85
21	-91.8	41.75	50	-95.74	41.95	79	-92.01	40.67
22	-95.46	42.94	51	-95.4	41.24	80	-94.98	41.25
23	-92.23	41.44	52	-95.55	42.05	81	-91.14	42.01
24	-94.98	41.34	53	-94.73	40.98	82	-93.79	40.68
25	-91.77	40.62	54	-94.83	42.42	83	-95.68	43.44
26	-92.26	42.83	55	-91.48	42.87	84	-94.02	40.72
27	-91.9	42.01	56	-94.79	41.25	85	-92.34	42.2
28	-96.5	42.81	57	-92.58	42.84	86	-91.29	42.88
29	-90.91	41.74	58	-93.6	40.77			

Table B.5. Optimized new locations for RWIS stations in Illinois

Station #	Long.	Lat.	Station #	Long.	Lat.	Station #	Long.	Lat.
1	-89.91	41.45	21	-90.65	41.07	41	-88.19	38.26
2	-90.87	40.95	22	-88.54	37.64	42	-88.18	37.56
3	-90.73	39.99	23	-89.32	41.23	43	-90.09	39.64
4	-88.37	38.67	24	-88.87	41.75	44	-88.27	38.37
5	-88.87	39.34	25	-88.84	37.51	45	-88.18	40.41
6	-89.88	39.07	26	-88.51	40.57	46	-89.4	38.77
7	-89.98	42.02	27	-88.03	39.16	47	-90.18	41.2
8	-89.74	39.63	28	-89.26	41.49	48	-89.27	37.14
9	-89.73	41.56	29	-89.34	41.02	49	-88.2	41
10	-88.45	38.08	30	-90.63	40.23	50	-87.52	38.73
11	-87.93	41.06	31	-88.58	40.48	51	-88.18	37.96
12	-88.49	37.4	32	-90.42	39.32	52	-88.73	37.46
13	-87.83	39.63	33	-89.13	41.68	53	-88.42	41.47
14	-90.12	40.22	34	-88.26	40.75	54	-90.76	39.32
15	-89.48	38.14	35	-89.17	38.94	55	-88.82	40.51
16	-88.75	37.29	36	-90.07	41.55	56	-90.63	39.36
17	-88.75	39.67	37	-87.99	39.3	57	-90.82	40.77
18	-89.13	41.44	38	-90.37	40.57	58	-89.68	40.93
19	-89.32	37.63	39	-90.64	39.46	59	-88.94	38.95
20	-87.7	40.51	40	-88.07	40.6			

Table B.6. Optimized new locations for RWIS stations in Kansas

Station #	Long.	Lat.	Station #	Long.	Lat.	Station #r	Long.	Lat.
1	-100.87	37.51	20	-101.27	38.13	39	-101.18	39.03
2	-98.03	38.52	21	-98.02	39.67	40	-101.09	39.8
3	-101.06	39.13	22	-98.33	39.99	41	-95.87	38.09
4	-97.71	37.16	23	-95.72	38.54	42	-96.8	38.74
5	-97.85	39.69	24	-96.9	38.89	43	-96.47	37.25
6	-98.18	37.96	25	-101.36	37.15	44	-95.59	38.58
7	-95.91	37.78	26	-95.57	37.39	45	-101.37	39.36
8	-96.35	37.36	27	-101.27	38.27	46	-96.05	38.78
9	-99.77	37.4	28	-101.55	39.74	47	-98.58	37.5
10	-101.72	39.61	29	-98.69	37.27	48	-98.56	39.8
11	-101.75	38.75	30	-101.69	37.26	49	-96.22	37.19
12	-98.57	38.16	31	-96.69	38.96	50	-97.86	39.89
13	-101.76	37.49	32	-101.85	39.83	51	-95.14	39.43
14	-97.21	39.81	33	-101.75	38.94	52	-95.85	37.4
15	-101.72	39.11	34	-96.98	39.63	53	-94.82	37.96
16	-99.72	38.81	35	-101.1	37.49	54	-97.35	38.68
17	-101.24	38.9	36	-97.12	38.83	55	-96.65	37.05
18	-96.33	39.7	37	-100.84	37.28	56	-97.98	39.19
19	-101.77	38.12	38	-98.43	37.47			

Table B.7. Optimized new locations for RWIS stations in Michigan

Station #	Long.	Lat.	Station #	Long.	Lat.	Station #	Long.	Lat.
1	-86.18	44.7	34	-89.56	46.43	67	-87.17	46.06
2	-83.14	43.99	35	-84.17	43.92	68	-85.23	41.94
3	-84.57	44.66	36	-85.42	46.52	69	-85.74	45.04
4	-85.93	41.92	37	-85.63	44.95	70	-84.62	44.18
5	-84.51	42.34	38	-84.19	45.98	71	-84.21	45.23
6	-85.71	44.22	39	-84.65	45.86	72	-84.23	41.82
7	-84.95	43.18	40	-82.77	43.99	73	-85.14	42.49
8	-84.23	42.84	41	-83.77	44.46	74	-84.81	42.1
9	-84.03	43	42	-82.93	43.46	75	-85.18	46.61
10	-85.9	44.66	43	-83.56	44.66	76	-82.8	43.81
11	-82.91	44.04	44	-85.19	44.34	77	-87.1	46.35
12	-83.34	43.87	45	-85.08	42.94	78	-83.93	44.72
13	-85.17	44.34	46	-83.37	43.34	79	-84.75	41.7
14	-87.31	46.26	47	-83.83	44.78	80	-83.97	45.97
15	-83.68	43.23	48	-85.15	43.68	81	-85.02	46.23
16	-85.02	42.44	49	-84.83	45.99	82	-85.06	45.46
17	-85.49	44.98	50	-82.94	43.6	83	-83.77	44.92
18	-82.68	43.89	51	-86.72	46.36	84	-83.76	44.69
19	-85.08	43.31	52	-83.32	43.56	85	-84.17	45.07
20	-85.18	44.49	53	-86.1	42.1	86	-85.26	42.59
21	-85.92	44.81	54	-82.56	42.58	87	-84.7	42.37
22	-83.74	44.65	55	-84.71	45.44	88	-85.82	43.67
23	-84.46	45.51	56	-84.96	44.03	89	-83.55	43.57
24	-84.42	44.54	57	-84.75	41.85	90	-85.32	42.38
25	-85.27	43.38	58	-85.06	44.34	91	-85.93	44.93
26	-84.88	42.57	59	-85.8	44.95	92	-84.09	42.64
27	-89.56	46.72	60	-83.7	45.15	93	-85.06	46.64
28	-84.41	41.86	61	-85.82	44.12	94	-84.34	42.66
29	-82.62	43.74	62	-86.62	45.73	95	-84.04	42.22
30	-83.03	43.41	63	-85.86	42.42	96	-84.03	42.2
31	-85.1	45.09	64	-83.75	44.59	97	-84.07	42.37
32	-85.85	43.78	65	-85.1	46.49	98	-87.24	46.18
33	-84.24	46.08	66	-84.23	45.41			

Table B.8. Optimized new locations for RWIS stations in Minnesota

Station #	Long.	Lat.	Station #	Long.	Lat.	Station #	Long.	Lat.
1	-95.83	48.12	30	-95.47	46.37	59	-94.09	45.86
2	-92.93	47.03	31	-96.53	46.39	60	-96.17	45.00
3	-92.50	44.29	32	-95.38	44.22	61	-92.88	46.71
4	-94.00	44.37	33	-92.86	47.84	62	-96.38	45.27
5	-95.86	45.28	34	-93.48	47.84	63	-95.47	44.98
6	-95.31	44.04	35	-93.17	47.22	64	-94.99	43.77
7	-95.92	45.10	36	-96.22	43.57	65	-95.77	45.83
8	-95.40	46.15	37	-94.70	46.57	66	-95.84	45.87
9	-93.88	44.10	38	-96.00	45.28	67	-95.56	45.43
10	-92.68	46.27	39	-94.19	44.41	68	-93.19	47.75
11	-96.43	46.04	40	-95.91	44.88	69	-96.93	47.82
12	-92.38	44.28	41	-93.12	43.87	70	-94.76	44.05
13	-95.98	43.57	42	-97.11	48.31	71	-95.67	46.55
14	-95.91	44.79	43	-95.33	46.33	72	-95.77	44.79
15	-95.75	44.07	44	-93.12	47.85	73	-95.13	44.36
16	-93.74	43.97	45	-96.28	44.64	74	-94.56	48.60
17	-93.27	47.81	46	-96.27	47.79	75	-96.43	45.01
18	-91.69	43.78	47	-94.10	46.04	76	-95.20	45.71
19	-95.12	44.04	48	-96.49	45.90	77	-95.31	47.14
20	-96.42	48.15	49	-95.44	44.40	78	-93.45	46.22
21	-93.27	46.45	50	-93.20	47.43	79	-96.71	46.47
22	-93.76	43.89	51	-94.62	43.65	80	-95.72	46.11
23	-95.00	47.78	52	-93.75	48.51	81	-94.55	48.28
24	-95.72	45.11	53	-92.41	46.49	82	-93.13	46.45
25	-96.44	47.30	54	-96.30	45.01	83	-95.94	44.16
26	-96.09	45.82	55	-93.20	48.06	84	-95.53	46.43
27	-94.70	48.77	56	-92.00	44.11	85	-96.78	45.66
28	-91.83	43.79	57	-93.67	47.84	86	-94.68	44.05
29	-94.09	45.77	58	-93.57	44.38			

Table B.9. Optimized new locations for RWIS stations in North Dakota

Station #	Long.	Lat.	Station #	Long.	Lat.	Station #	Long.	Lat.
1	-99.56	46.51	11	-100.88	47	21	-103.14	46.17
2	-99.56	48.86	12	-98.43	47.1	22	-103.53	48.58
3	-98.76	48.41	13	-103.39	48.58	23	-103.37	46.42
4	-100.94	47.15	14	-99.66	48.99	24	-103.95	48.89
5	-103.15	48.05	15	-102.35	47.15	25	-103.65	47.76
6	-99.2	47.15	16	-102.78	47.1	26	-101.06	47.82
7	-103.14	46.26	17	-99.18	46.53	27	-97.82	46.63
8	-99.74	48.07	18	-102.79	46.81	28	-98.73	47.23
9	-101.33	46.23	19	-101.33	46.07	29	-98.65	47.68
10	-103.22	48.18	20	-103.16	46.52			

Table B.10. Optimized new locations for RWIS stations in Ohio

Station #	Long.	Lat.	Station #	Long.	Lat.	Station #	Long.	Lat.
1	-84.06	40.19	62	-84.26	40.49	123	-82.61	40.4
2	-84.43	41.44	63	-83.87	41.09	124	-84.35	40.05
3	-81.37	40.24	64	-81.12	40.35	125	-82.07	40.23
4	-83.9	40.29	65	-81.36	39.74	126	-84.22	41.31
5	-80.82	40.41	66	-81.13	41.31	127	-80.78	41.68
6	-83.99	41.1	67	-84.37	40.27	128	-83.72	40.25
7	-82.26	40.95	68	-83.2	38.95	129	-84.72	41.3
8	-81.84	40.23	69	-83.98	39.43	130	-84.78	39.37
9	-84.6	41.3	70	-82.75	40.89	131	-81.48	40.24
10	-84.48	40.04	71	-83.26	38.63	132	-83.09	40.98
11	-82.86	41.39	72	-83.33	39.39	133	-83.25	40.52
12	-81.89	39.37	73	-82.06	40.09	134	-81.66	40.05
13	-82.85	40.9	74	-83.19	38.86	135	-84	38.84
14	-83.27	41.29	75	-82.9	41.08	136	-81.25	39.65
15	-81.3	39.92	76	-82.19	40.29	137	-83.38	39.13
16	-83.8	39.34	77	-80.71	40.69	138	-82.08	40.99
17	-83.58	40.02	78	-81.61	40.68	139	-82.8	38.96
18	-81.82	39.11	79	-80.78	40.64	140	-82.13	40.68
19	-82.29	39.69	80	-84.66	40.66	141	-82.38	40.59
20	-83.32	39.08	81	-80.54	41.31	142	-82	39.46
21	-82.01	40.77	82	-82.63	39.18	143	-81.25	40.23
22	-83.54	38.71	83	-81.31	39.82	144	-83.72	38.8
23	-82.83	39.68	84	-81.05	40.19	145	-80.67	41.76
24	-82.87	39.13	85	-83.7	41.29	146	-84.23	41.09
25	-83.44	39.31	86	-83.19	40.39	147	-81.71	39.73
26	-82.47	39.36	87	-83.8	39.25	148	-81.65	39.47

Station #	Long.	Lat.	Station #	Long.	Lat.	Station #	Long.	Lat.
27	-84.43	40.41	88	-83.16	41.2	149	-83.15	39.09
28	-81.13	39.83	89	-83.38	38.82	150	-82.58	39.55
29	-83.53	40.16	90	-82.18	39.54	151	-82.98	41.26
30	-81.97	40.36	91	-83.85	40.78	152	-82.17	39.15
31	-83.68	39.3	92	-81.01	39.7	153	-83.16	39.53
32	-81.58	40.39	93	-82.47	39.5	154	-82.61	40.27
33	-83.04	41.21	94	-82.34	39.1	155	-81.72	40.37
34	-84.11	40.01	95	-83.51	41.02	156	-82.51	38.56
35	-80.95	40.15	96	-83.55	40.34	157	-82.14	40.86
36	-83.35	41.6	97	-83.82	39.79	158	-81.08	41.26
37	-82.02	40.68	98	-83.68	39.08	159	-80.78	41.46
38	-84.13	38.89	99	-81.78	39.91	160	-81.73	40.18
39	-83.66	40.38	100	-81.59	39.87	161	-84.39	40.74
40	-83.03	39.13	101	-82.38	40.72	162	-80.96	40.41
41	-83.59	39.84	102	-84.71	41.38	163	-82.14	40.45
42	-81.84	40.37	103	-82	39.38	164	-80.66	41.27
43	-81.71	39.82	104	-83.73	40.47	165	-80.95	40.59
44	-84.56	39.59	105	-81.94	39.74	166	-84.43	40.63
45	-83.9	40.55	106	-80.95	41.63	167	-81.25	40.54
46	-82.31	40.67	107	-83.68	39.39	168	-80.88	40.68
47	-80.64	41.54	108	-84.26	40.63	169	-83.73	39.21
48	-82	39.59	109	-84.03	40.6	170	-82.12	39.69
49	-84.73	39.74	110	-81.07	40.46	171	-83.9	40.42
50	-82.45	41.31	111	-84.12	40.1	172	-83.32	40.8
51	-84.29	40.95	112	-80.83	40.77	173	-80.78	41.58
52	-84.43	40.5	113	-84.72	40.22	174	-83.75	41.06
53	-82.02	40.54	114	-83.38	39.04	175	-82.28	39.05
54	-84.72	40.31	115	-81.77	40.09	176	-84.6	40.18
55	-83.38	38.95	116	-81.24	40.65	177	-81.78	40.73
56	-81.89	39.91	117	-81.66	40.31	178	-84.61	41.53
57	-82.25	39.91	118	-84.56	41.67	179	-80.96	41.53
58	-82.35	39.41	119	-81.78	39.69	180	-83.28	41.02
59	-84.76	41.02	120	-84.12	41.32	181	-82.66	41.16
60	-81.88	39.46	121	-80.78	40	182	-80.6	40.91
61	-82.34	38.79	122	-82.37	40.36			

Table B.11. Optimized new locations for RWIS stations in Pennsylvania

Station #	Long.	Lat.	Station #	Long.	Lat.	Station #	Long.	Lat.
1	-70.6	40.43	8	-72.85	40.68	15	-71.67	41.11
2	-72.46	40.2	9	-71.95	40.13	16	-73.14	41.24
3	-71.22	41.48	10	-71.6	41.36	17	-71.95	40.24
4	-71.69	40.22	11	-73.44	39.94	18	-71.71	41.39
5	-72.42	40.28	12	-73.3	39.94	19	-70.09	41.89
6	-72.22	41.02	13	-71.25	41.12			
7	-70.36	39.75	14	-71.99	41.24			

Table B.12. Optimized new locations for RWIS stations in Utah

Station #	Long.	Lat.	Station #	Long.	Lat.	Station #	Long.	Lat.
1	-112.46	38.28	34	-111.92	38.42	67	-113.3	38.44
2	-110.88	40.77	35	-112.74	40.3	68	-111.29	41.5
3	-112.75	40.47	36	-110.09	37.62	69	-111.7	38.56
4	-111.77	41.62	37	-111.65	40.45	70	-111.53	38.52
5	-110.85	40.84	38	-112.32	39.45	71	-111.41	41.49
6	-111.97	38.29	39	-110.45	40.19	72	-112.28	40.02
7	-111.21	41.51	40	-110.31	37.8	73	-110.59	40.3
8	-109.93	37.18	41	-109.7	40.89	74	-109.91	37.59
9	-110.72	40.26	42	-109.97	37.61	75	-110.91	39.49
10	-109.95	37.41	43	-112.75	40.4	76	-112.46	39.29
11	-110.5	40.18	44	-112.37	38.29	77	-112.28	39.52
12	-112.72	37.23	45	-114.05	38.95	78	-112.66	40.71
13	-110.21	37.67	46	-109.92	37.24	79	-112.69	37.66
14	-112.29	41.67	47	-114.03	39.03	80	-110.14	37.66
15	-112.53	38.25	48	-111.93	41.91	81	-111.02	40.48
16	-112.72	40.59	49	-112.69	40.64	82	-110.26	37.73
17	-110.85	40.98	50	-109.91	37.45	83	-114.01	38.89
18	-112.38	38.24	51	-112.24	38.26	84	-113	39.19
19	-113.09	38.42	52	-113.96	38.78	85	-110.4	39.48
20	-110.21	37.43	53	-112.31	38.14	86	-110.69	40.19
21	-112.32	40.06	54	-113.99	38.83	87	-111.07	39.21
22	-111.06	40.52	55	-111.6	41.6	88	-111.44	40.57
23	-111.1	39.29	56	-112.69	38.08	89	-109.88	37.15
24	-111.43	38.64	57	-109.93	37.3	90	-111.24	39.65
25	-112.39	40.08	58	-112.74	40.54	91	-113.16	41.83
26	-110.92	40.47	59	-109.9	37.52	92	-112.28	39.67
27	-111	39.48	60	-112.01	38.2	93	-110.04	37.59
28	-111.77	38.51	61	-110.85	40.46	94	-111.67	40.96
29	-112.77	37.27	62	-110.34	37.86	95	-111.46	38.6

Station #	Long.	Lat.	Station #	Long.	Lat.	Station #	Long.	Lat.
30	-113.12	41.97	63	-111.4	38.7	96	-109.35	37.34
31	-112.8	39.3	64	-113.83	38.6	97	-111.59	40.85
32	-111.17	39.54	65	-112.38	38.98	98	-111.9	40.94
33	-111.57	38.48	66	-113.9	38.69			

Table B.13. Optimized new locations for RWIS stations in Virginia

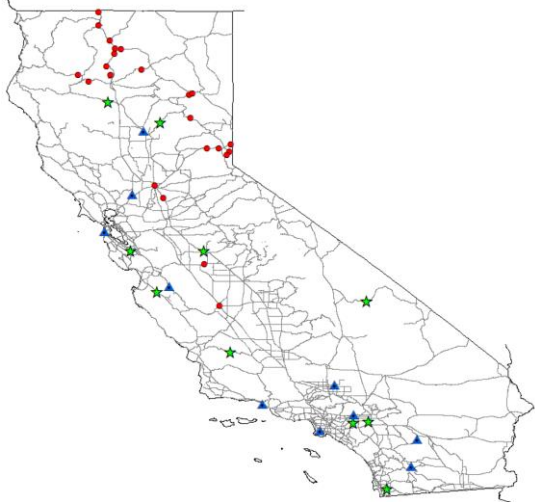
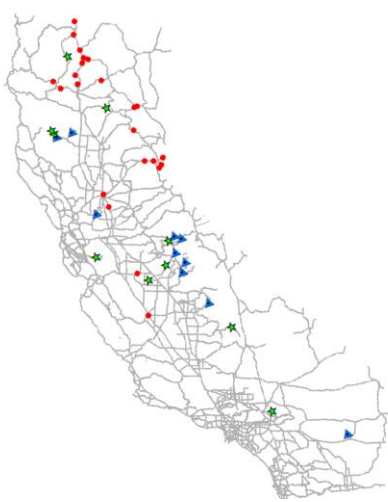
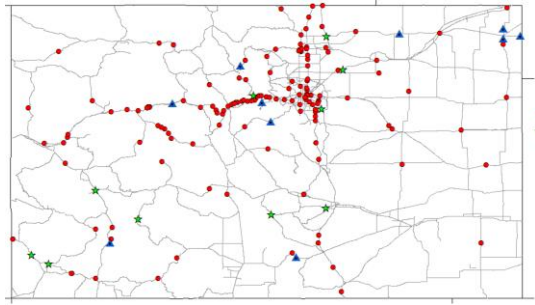
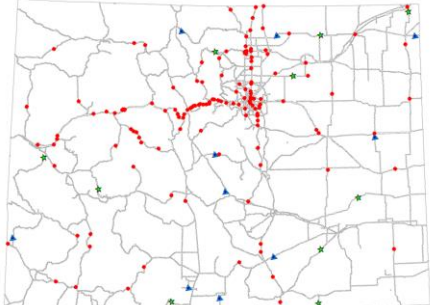
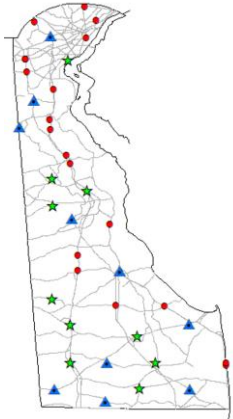
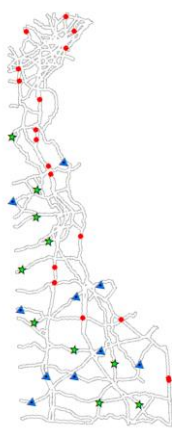
Station #	Long.	Lat.	Station #	Long.	Lat.	Station #	Long.	Lat.
1	-77.85	37.06	19	-79.3	37.96	37	-80.26	37.57
2	-78.73	37.64	20	-79.16	37.83	38	-79.87	38.12
3	-79.71	38.31	21	-78.7	36.85	39	-81.16	37.26
4	-76.92	38.19	22	-80.12	37.51	40	-78.6	38.68
5	-78.04	39.18	23	-77.66	38.63	41	-78.27	38.3
6	-77.66	36.76	24	-77.28	36.78	42	-80.12	36.79
7	-75.83	37.52	25	-79.54	37.5	43	-80.32	37.39
8	-81.6	37.08	26	-76.89	37.69	44	-81.96	36.89
9	-77.17	37.85	27	-79.33	37.67	45	-81.3	37.04
10	-79.95	38.02	28	-80.56	36.66	46	-78.71	36.72
11	-82.54	37.11	29	-77.14	36.87	47	-78.73	37.07
12	-80.21	36.86	30	-77.04	37.79	48	-79.24	36.72
13	-79.79	38.21	31	-79.24	36.82	49	-78.27	38.45
14	-81.45	36.96	32	-79.03	37.89	50	-80.95	37.27
15	-79.41	37.56	33	-78.21	36.55	51	-80.07	37.18
16	-77.01	37.13	34	-80.16	37.64	52	-79.65	38.45
17	-78.32	37	35	-79.71	37.45			
18	-78.88	38.01	36	-81.5	36.62			

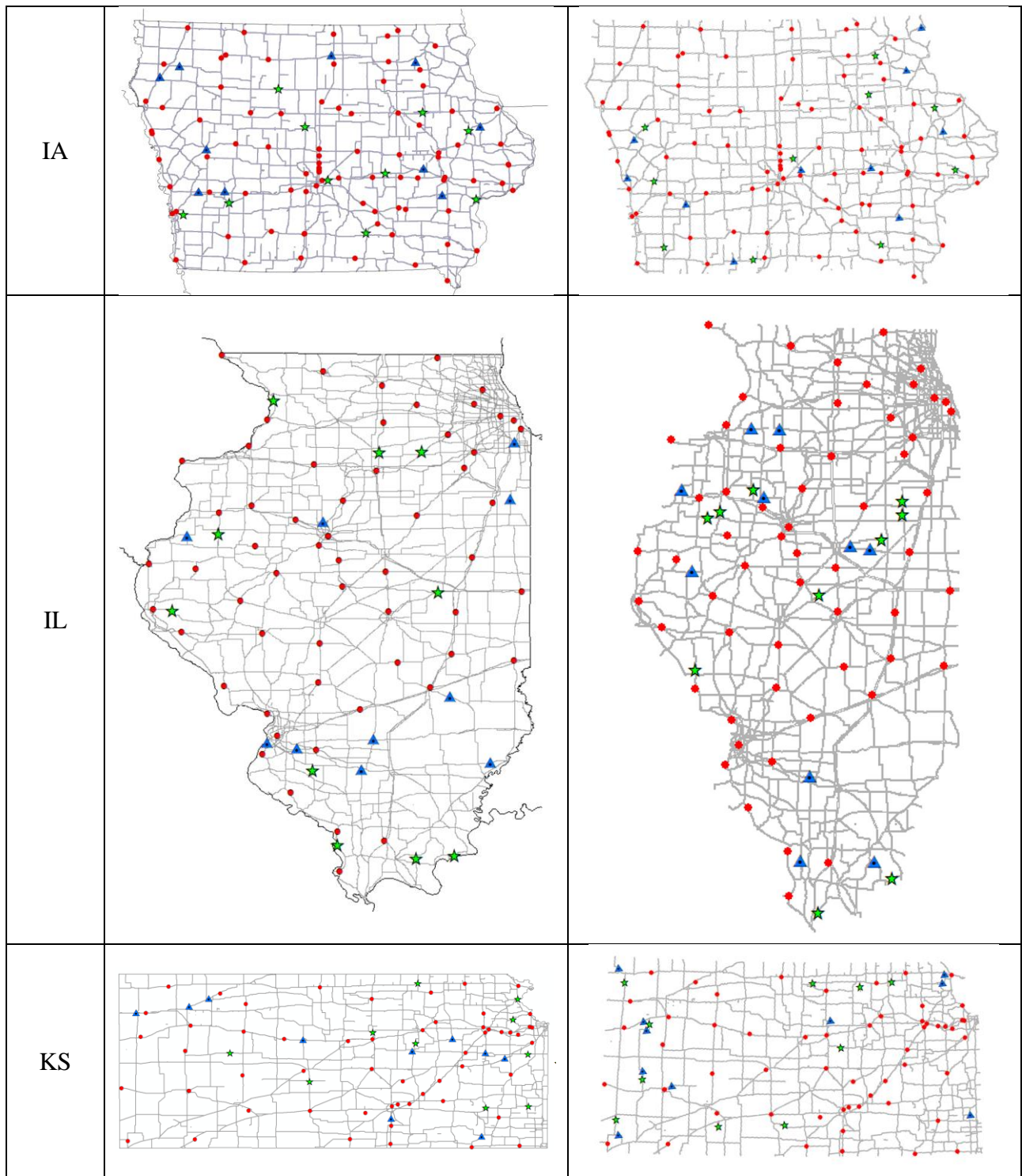
Table B.14. Optimized new locations for RWIS stations in Wisconsin

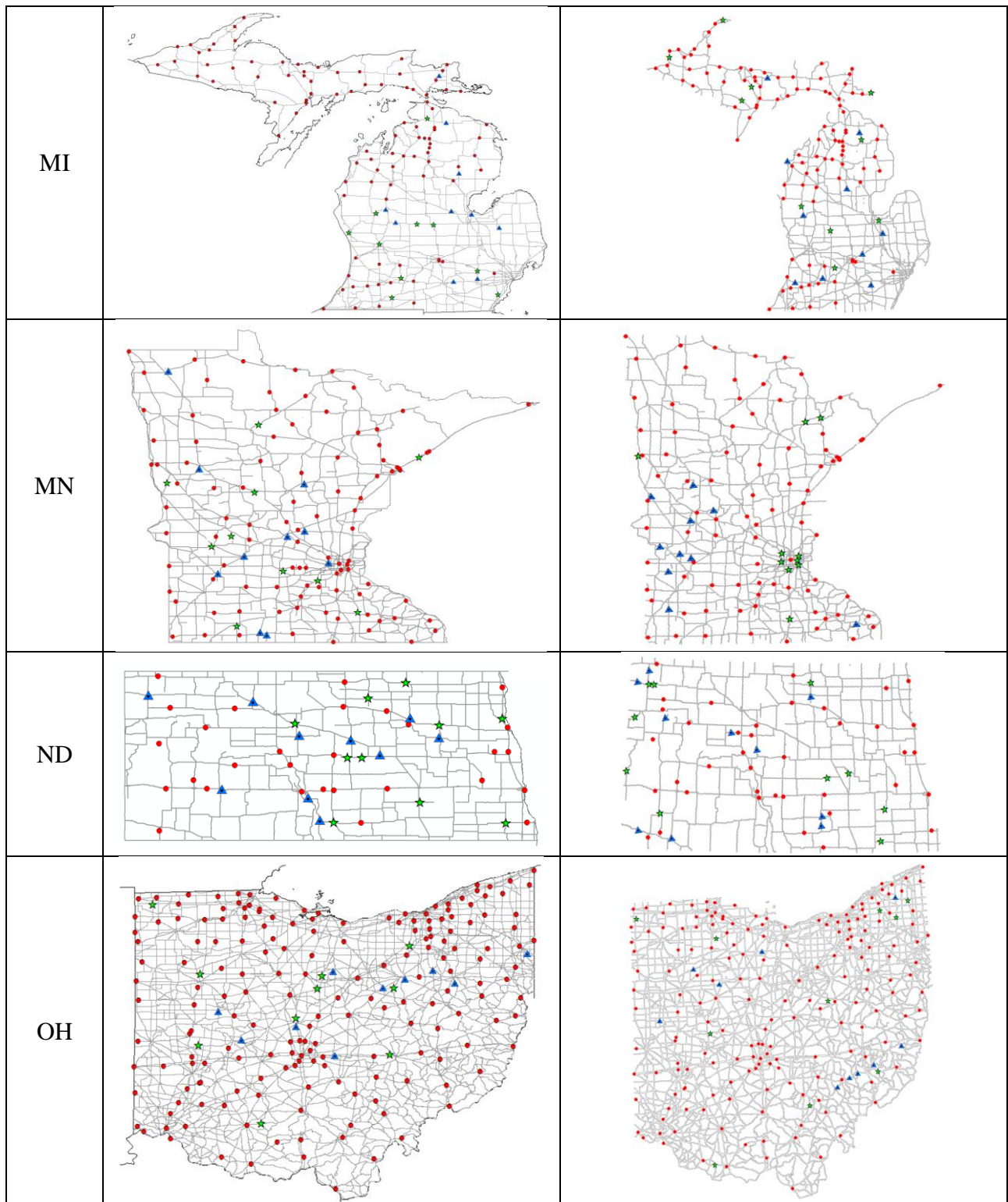
Station #	Long.	Lat.	Station #	Long.	Lat.	Station #	Long.	Lat.
1	-90.22	43.28	21	-88.78	44.8	41	-90.43	43.54
2	-88.93	46.03	22	-90.4	46.36	42	-91.16	44.1
3	-88.34	43.89	23	-89.09	45.21	43	-92.34	45.64
4	-90.09	46.03	24	-88.75	44.94	44	-92.18	45.63
5	-89.38	43	25	-89.35	43.57	45	-90.87	43.12
6	-88.66	43.36	26	-91.98	46.18	46	-89.9	42.59
7	-91.93	44.79	27	-90.64	43.51	47	-88.83	45.91
8	-88.77	45.38	28	-91.11	43.56	48	-90.33	43.18
9	-89.93	45.15	29	-90.25	44.35	49	-88.18	43.69
10	-88.52	45.92	30	-90.08	43.02	50	-89.19	42.83
11	-89.9	46.3	31	-92.69	45.55	51	-88.76	45.15
12	-89.12	45.09	32	-91.49	44.43	52	-88.63	45.02
13	-88.82	45.78	33	-89.44	43.79	53	-88.93	45.05
14	-91.22	45.74	34	-89.82	42.92	54	-90.41	46.46
15	-91.75	44.22	35	-90.04	42.87	55	-91.22	45.61
16	-91.8	44.7	36	-90.86	43.26	56	-89.5	43.25
17	-90.59	44.72	37	-89.43	45.9	57	-89.26	44.5
18	-92.56	45.46	38	-91.04	43.15	58	-90.85	46.56
19	-89.11	43.5	39	-90.59	46.38	59	-89.87	43.04
20	-88.92	44.46	40	-88.91	45.26			

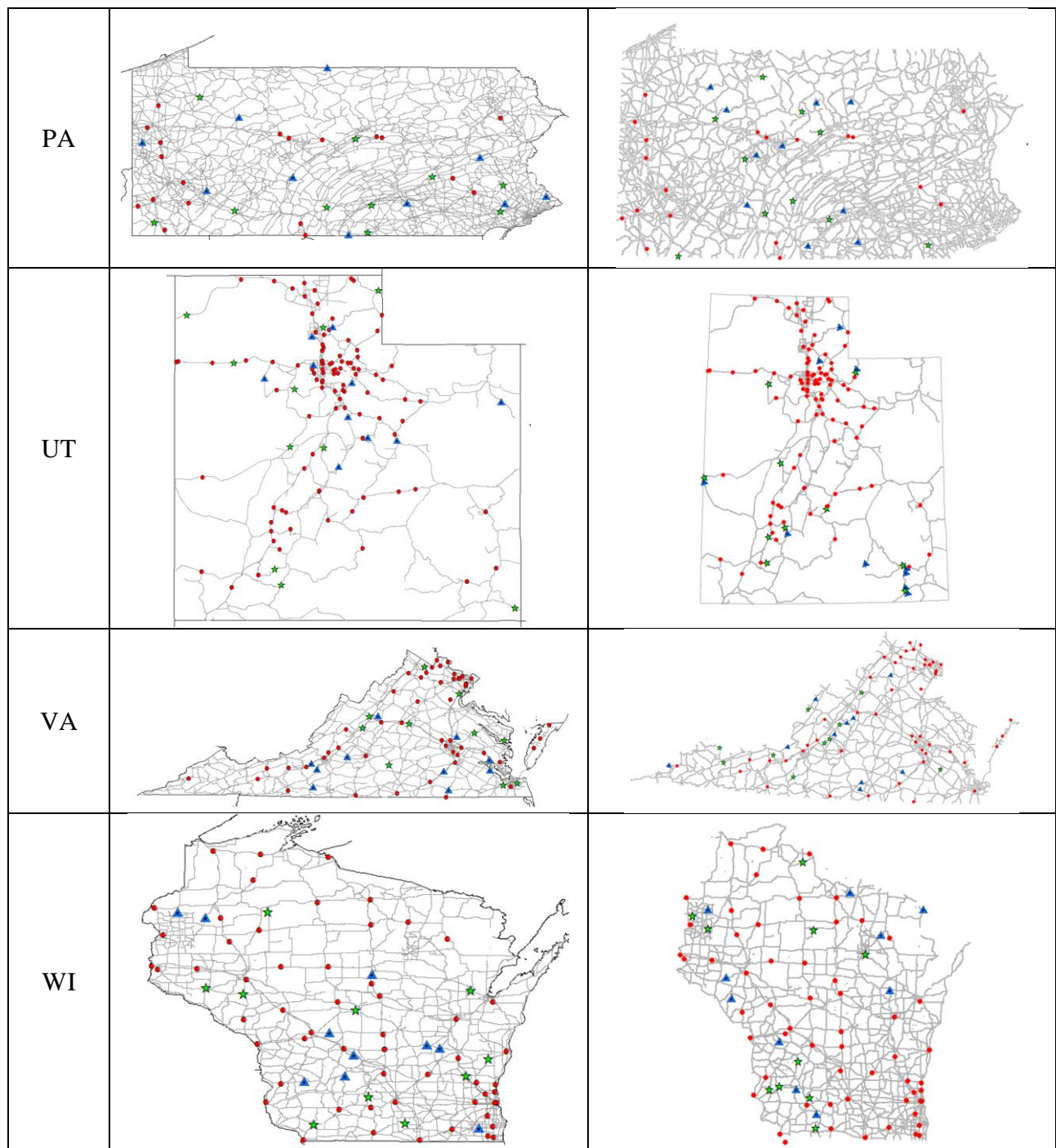
APPENDIX C. PLOTS OF EXISTING AND EXPANDED RWIS LOCATIONS FOR THE EXPANSION STRATEGY

In the figure, the existing stations are shown in red, the first addition of 10 new stations are shown in green, and the second additional 10 (for a total of 20) new stations are shown in blue.

State	Criteria 1 (Weather only)	Criteria 2 (Dual criteria)
CA		
CO		
DE		







● Existing Stations
 ★ Add First 10
 ▲ Add Second 10

APPENDIX D. LOCATION PLAN FOR ADDING NEW STATIONS TO EXISTING RWIS NETWORK

Note that in the following tables include the proposed addition of 20 new RWIS stations (which may be added 10 at a time as explained in Chapter 4) considering weather data only and dual criteria (considering both weather and traffic data).

Table D.1. Potential additional locations for RWIS stations in California

Station number	Weather only		Dual criteria	
	Longitude	Latitude	Longitude	Latitude
1	-120.04	35.35	-119.81	37.75
2	-122.43	40.23	-117.23	34.34
3	-121.98	37.32	-119.86	37.26
4	-117.35	34.01	-122.86	39.73
5	-116.99	32.68	-118.2	36.03
6	-121.4	39.82	-121.58	40.33
7	-117.39	36.34	-121.59	37.36
8	-120.56	37.33	-122.69	41.27
9	-117.65	33.98	-122.93	39.79
10	-121.47	36.52	-120.27	36.95
11	-121.95	38.42	-121.67	38.23
12	-118.29	33.82	-115.44	33.84
13	-116.40	33.65	-119.67	37.85
14	-121.23	36.63	-122.81	39.68
15	-121.73	39.66	-119.38	37.34
16	-119.41	34.34	-122.42	39.8
17	-118.00	34.70	-119.45	37.15
18	-117.63	34.14	-119.64	37.53
19	-116.51	33.12	-118.78	36.54
20	-122.50	37.70	-119.49	37.81

Table D.2. Potential additional locations for RWIS stations in Colorado

Station number	Weather only		Dual criteria	
	Longitude	Latitude	Longitude	Latitude
1	-104.73	40.58	-107.55	38.56
2	-104.50	40.12	-108.48	38.95
3	-107.30	38.08	-103.78	40.61
4	-108.76	37.59	-106.32	37.1
5	-108.53	37.46	-105.61	40.39
6	-104.73	38.23	-103.18	38.45
7	-107.89	38.47	-104.26	40.08
8	-104.79	39.59	-102.23	40.91
9	-105.48	38.14	-103.89	37.05
10	-105.72	39.76	-103.83	37.78
11	-106.83	39.66	-102.87	39.25
12	-102.07	40.59	-104.62	37.69
13	-105.90	40.17	-105.6	39.04
14	-107.69	37.75	-106.04	37.28
15	-105.49	39.41	-106.2	40.66
16	-102.30	40.55	-105.43	38.55
17	-105.14	37.56	-105.53	37.15
18	-103.72	40.61	-104.55	40.62
19	-102.30	40.68	-102.13	40.58
20	-105.60	39.67	-108.95	37.9

Table D.3. Potential additional locations for RWIS stations in Delaware

Station number	Weather only		Dual criteria	
	Longitude	Latitude	Longitude	Latitude
1	-75.65	39.24	-75.3	38.65
2	-75.54	39.20	-75.65	39.24
3	-75.65	39.15	-75.47	38.7
4	-75.30	38.61	-75.65	39.15
5	-75.36	38.70	-75.36	38.52
6	-75.59	38.74	-75.65	38.79
7	-75.60	39.64	-75.77	39.42
8	-75.66	38.83	-75.71	38.97
9	-75.36	38.52	-75.19	38.52
10	-75.59	38.61	-75.6	39.06
11	-75.47	38.61	-75.59	38.61
12	-75.47	38.48	-75.37	38.92
13	-75.77	39.41	-75.19	38.65
14	-75.59	39.10	-75.47	38.88
15	-75.42	38.92	-75.36	38.7
16	-75.65	38.52	-75.47	38.61
17	-75.19	38.74	-75.71	38.83
18	-75.72	39.51	-75.54	39.34
19	-75.66	39.73	-75.76	39.2
20	-75.18	38.52	-75.65	38.52

Table D.4. Potential additional locations for RWIS stations in Iowa

Station number	Weather only		Dual criteria	
	Longitude	Latitude	Longitude	Latitude
1	-92.53	41.75	-95.68	42.27
2	-94.98	41.38	-92.06	40.85
3	-95.70	41.23	-90.85	41.69
4	-91.19	42.24	-91.13	42.42
5	-94.23	42.74	-95.38	40.88
6	-91.09	41.43	-92.16	42.61
7	-91.92	42.47	-95.53	41.64
8	-93.80	42.30	-94.01	40.72
9	-93.43	41.67	-92.03	43.06
10	-92.83	41.04	-93.37	41.89
11	-95.47	41.50	-91.01	42.15
12	-95.06	41.52	-95.85	42.13
13	-91.01	42.29	-95.04	41.38
14	-92.03	43.06	-91.76	41.17
15	-95.83	42.98	-93.25	41.76
16	-91.63	41.48	-92.16	41.76
17	-96.14	42.85	-91.54	42.88
18	-93.39	43.15	-91.28	43.36
19	-95.37	42.01	-95.94	41.68
20	-91.92	41.80	-94.31	40.71

Table D.5. Potential additional locations for RWIS stations in Illinois

Station number	Weather only		Dual criteria	
	Longitude	Latitude	Longitude	Latitude
1	-90.67	40.69	-89.11	37.15
2	-91.13	39.92	-89.18	40.05
3	-88.68	37.43	-88.46	40.57
4	-89.72	38.31	-88.21	40.8
5	-88.45	40.11	-88.21	40.93
6	-88.29	37.46	-90.62	39.33
7	-88.62	41.51	-88.27	37.48
8	-89.05	41.51	-90.4	40.79
9	-90.11	42.03	-90.54	40.73
10	-89.47	37.56	-90.01	41
11	-88.34	39.05	-89.33	37.62
12	-87.69	41.61	-90.06	41.56
13	-90.98	40.67	-88.59	40.48
14	-87.73	41.04	-88.82	40.51
15	-89.88	38.53	-89.24	38.39
16	-87.93	38.39	-88.48	37.63
17	-89.23	38.32	-90.71	40.23
18	-89.11	38.62	-89.87	40.93
19	-89.61	40.81	-90.87	40.97
20	-90.18	38.59	-89.71	41.56

Table D.6. Potential additional locations for RWIS stations in Kansas

Station number	Weather only		Dual criteria	
	Longitude	Latitude	Longitude	Latitude
1	-96.90	38.81	-99.76	37.44
2	-96.87	39.84	-96.33	39.7
3	-95.68	37.69	-97.36	38.68
4	-95.21	39.22	-97.93	39.68
5	-94.95	38.62	-101.18	38.99
6	-95.13	39.57	-96.97	39.63
7	-100.12	38.64	-101.72	39.61
8	-97.64	39.00	-101.27	38.13
9	-98.74	38.15	-98.47	37.47
10	-94.95	37.72	-101.76	37.49
11	-100.49	39.58	-97.58	39.11
12	-95.36	38.55	-94.83	37.6
13	-95.69	38.64	-101.23	38.9
14	-98.86	38.87	-101.3	39.03
15	-95.76	37.20	-101.69	37.26
16	-96.96	38.67	-100.7	38.05
17	-96.26	38.88	-101.27	38.27
18	-101.76	39.33	-101.85	39.83
19	-97.33	37.51	-95.31	39.68
20	-100.83	39.44	-95.27	39.81

Table D.7. Potential additional locations for RWIS stations in Michigan

Station number	Weather only		Dual criteria	
	Longitude	Latitude	Longitude	Latitude
1	-84.93	43.41	-87.49	45.88
2	-86.25	43.24	-85.09	43.31
3	-83.75	42.50	-85	42.57
4	-85.72	43.61	-87.22	46.16
5	-85.65	43.02	-88.06	47.47
6	-84.60	43.39	-89.57	46.71
7	-85.23	42.36	-85.85	43.79
8	-84.73	45.45	-83.77	43.48
9	-85.41	41.98	-83.84	45.99
10	-83.36	42.04	-84.16	45.08
11	-84.22	42.29	-86.77	46.34
12	-84.11	44.38	-83.68	43.23
13	-85.34	43.43	-84.04	42.22
14	-83.33	43.34	-84.24	42.84
15	-83.75	42.35	-85.8	43.62
16	-84.50	46.27	-85.32	42.38
17	-84.36	45.36	-86.05	42.3
18	-83.87	43.59	-84.21	45.22
19	-84.26	43.66	-84.61	44.13
20	-85.53	43.68	-86.22	44.69

Table D.8. Potential additional locations for RWIS stations in Minnesota

Station number	Weather only		Dual criteria	
	Longitude	Latitude	Longitude	Latitude
1	-91.75	46.98	-92.53	47.51
2	-93.65	44.67	-93.46	44.94
3	-94.76	47.60	-93.29	44.8
4	-94.84	46.33	-93.45	45.1
5	-95.17	43.81	-93.06	45.04
6	-94.30	44.85	-93.09	44.97
7	-96.49	46.50	-93.07	44.88
8	-92.90	44.07	-92.89	47.45
9	-95.65	45.31	-93.28	43.92
10	-95.28	45.50	-96.76	46.84
11	-95.88	46.77	-95.74	45.11
12	-94.61	43.64	-96.18	45.23
13	-95.53	44.80	-95.00	45.89
14	-93.91	46.48	-95.94	44.12
15	-96.46	48.60	-91.82	43.79
16	-93.90	45.59	-95.51	45.7
17	-94.22	45.50	-95.97	44.79
18	-95.03	45.12	-95.47	46.33
19	-94.74	43.69	-96.42	46.13
20	-93.45	45.00	-95.48	45.03

Table D.9. Potential additional locations for RWIS stations in North Dakota

Station number	Weather only		Dual criteria	
	Longitude	Latitude	Longitude	Latitude
1	-98.34	48.03	-99.22	47.15
2	-98.69	46.63	-103.89	48.03
3	-99.74	47.44	-97.94	46.11
4	-100.96	48.06	-104	47.16
5	-100.01	47.44	-103.59	48.58
6	-99.63	48.52	-103.16	46.52
7	-97.20	48.15	-97.84	46.63
8	-100.25	46.27	-103.46	48.58
9	-97.13	46.26	-99.62	48.69
10	-98.94	48.79	-98.7	47.23
11	-102.28	46.86	-99.33	46.53
12	-100.88	47.84	-103.62	48.8
13	-100.72	46.71	-99.35	46.38
14	-100.50	46.31	-100.91	47.61
15	-103.62	48.57	-103.65	46.23
16	-98.87	48.16	-101.54	47.86
17	-99.41	47.49	-102.87	46.13
18	-99.94	47.76	-103.14	48.05
19	-98.35	47.80	-99.62	48.47
20	-101.72	48.46	-103.87	48.61

Table D.10. Potential additional locations for RWIS stations in Ohio

Station number	Weather only		Dual criteria	
	Longitude	Latitude	Longitude	Latitude
1	-84.12	40.06	-83.58	41.28
2	-82.79	40.80	-82.02	40.54
3	-84.61	41.57	-83.72	38.81
4	-83.07	40.35	-80.77	41.58
5	-82.06	39.96	-82.35	39.41
6	-83.45	39.22	-81.36	39.74
7	-82.84	40.67	-84.72	41.52
8	-81.85	41.13	-83.72	40.25
9	-82.02	40.68	-81.19	41.49
10	-84.10	40.82	-80.96	41.41
11	-81.61	40.86	-83.56	40.79
12	-81.37	40.73	-81.01	40.01
13	-82.14	40.68	-84.43	40.41
14	-83.07	40.26	-81.65	39.73
15	-81.90	40.77	-82.92	41.12
16	-82.65	39.95	-83.92	40.96
17	-83.91	40.42	-81.77	39.69
18	-83.65	40.11	-80.95	41.63
19	-82.67	40.85	-81.42	39.82
20	-80.59	41.04	-81.95	39.6

Table D.11. Potential additional locations for RWIS stations in Pennsylvania

Station number	Weather only		Dual criteria	
	Longitude	Latitude	Longitude	Latitude
1	-79.13	40.06	-73.14	41.24
2	-77.28	40.13	-73.63	39.72
3	-79.60	41.60	-72.7	40.8
4	-80.22	39.90	-71.89	41.33
5	-77.50	41.03	-70.09	39.86
6	-76.46	40.52	-71.61	41.11
7	-75.54	40.05	-71.49	40.15
8	-75.51	40.41	-72.46	41.71
9	-77.89	40.10	-72.01	40.35
10	-77.33	39.76	-72.4	40.21
11	-76.80	40.16	-72.67	40.3
12	-80.38	40.98	-73.22	41.59
13	-77.60	39.73	-72.17	40.96
14	-75.82	40.78	-71.68	41.43
15	-78.35	40.51	-71.79	39.86
16	-75.49	40.15	-71.28	40.25
17	-74.92	40.25	-72.98	41.34
18	-79.07	41.33	-71.17	41.44
19	-79.51	40.33	-71.08	39.91
20	-77.88	42.00	-72.54	40.86

Table D.12. Potential additional locations for RWIS stations in Utah

Station number	Weather only		Dual criteria	
	Longitude	Latitude	Longitude	Latitude
1	-111.89	41.25	-109.92	37.18
2	-113.86	41.42	-110.89	40.76
3	-112.31	40.35	-109.94	37.6
4	-112.59	37.75	-111.51	38.54
5	-113.18	40.73	-114.03	39.02
6	-112.50	37.51	-112.45	39.28
7	-112.37	39.52	-112.73	40.56
8	-109.12	37.18	-112.69	38.08
9	-111.09	41.78	-112.36	38.24
10	-111.88	39.50	-112.72	37.66
11	-109.32	40.17	-109.91	37.24
12	-111.25	39.65	-112.31	38.14
13	-112.74	40.51	-114.03	38.96
14	-111.76	41.25	-110.86	40.83
15	-112.06	41.12	-111.23	41.51
16	-111.53	39.95	-111.67	40.96
17	-111.67	39.23	-110.71	37.64
18	-112.03	40.70	-109.9	37.48
19	-110.83	39.61	-109.87	37.15
20	-111.48	40.44	-109.89	37.54

Table D.13. Potential additional locations for RWIS stations in Virginia

Station number	Weather only		Dual criteria	
	Longitude	Latitude	Longitude	Latitude
1	-79.09	38.15	-78.79	38.38
2	-76.43	36.78	-79.24	37.82
3	-78.69	37.18	-80.63	37.23
4	-77.01	37.82	-81.69	37.04
5	-79.22	37.91	-81.79	37.29
6	-78.00	39.12	-80.17	36.88
7	-77.31	38.59	-77.03	37.12
8	-76.16	36.82	-79.43	37.56
9	-76.42	37.67	-79.93	38.05
10	-78.29	38.00	-79.54	37.49
11	-76.70	37.07	-79.07	37.86
12	-77.36	37.74	-78.72	36.73
13	-78.92	38.15	-77.83	37.06
14	-77.61	37.06	-78.94	37.94
15	-77.52	36.68	-79.77	38.24
16	-80.13	37.10	-79.33	37.65
17	-76.71	37.28	-80.33	37.39
18	-79.52	37.34	-78.17	38.71
19	-80.24	37.21	-82.85	36.92
20	-80.21	36.74	-78.7	36.85

Table D.14. Potential additional locations for RWIS stations in Wisconsin

Station number	Weather only		Dual criteria	
	Longitude	Latitude	Longitude	Latitude
1	-89.70	43.12	-89.94	42.62
2	-91.46	44.57	-90.33	43.56
3	-88.33	43.42	-90.67	43.19
4	-89.18	42.75	-89.07	45.1
5	-90.47	42.74	-90.86	43.14
6	-88.01	43.66	-92.56	45.53
7	-91.98	44.66	-90.39	46.37
8	-88.26	44.62	-90.07	43.05
9	-91.11	45.72	-92.24	45.36
10	-89.88	44.34	-90.12	45.42
11	-89.65	44.84	-91.81	44.69
12	-90.25	44.02	-92.27	45.64
13	-88.70	43.81	-90.71	43.83
14	-88.88	43.86	-90.34	43.17
15	-90.61	43.34	-88.57	44.6
16	-90.04	43.42	-89.94	42.83
17	-89.91	43.71	-87.92	45.75
18	-92.00	45.64	-91.68	44.41
19	-88.15	42.69	-88.77	45.38
20	-92.38	45.72	-89.41	45.97

**THE INSTITUTE FOR TRANSPORTATION IS THE FOCAL POINT FOR TRANSPORTATION
AT IOWA STATE UNIVERSITY.**

InTrans centers and programs perform transportation research and provide technology transfer services for government agencies and private companies;

InTrans contributes to Iowa State University and the College of Engineering's educational programs for transportation students and provides K–12 outreach; and

InTrans conducts local, regional, and national transportation services and continuing education programs.



**IOWA STATE
UNIVERSITY**

Visit InTrans.iastate.edu for color pdfs of this and other research reports.